NTNU
Det skapende universitet

Eksperimentell undersøkelse av faseinversjon for olje-vann systemer.

Anders Nilsen Tysnes

Master i produktutvikling og produksjon
Oppgaven levert: Juni 2010
Hovedveileder: Ole Jørgen Nydal, EPT

Norges teknisk-naturvitenskapelige universitet
Institutt for energi- og prosessteknikk

Oppgavetekst

Bakgrunn og mål

En større andel av fremtidens olje produksjon vil bestå av tungolje. Utvinning av tungolje medfører nye utfordringer, inkludert transport. Rør strøm med tungolje kan føre til veldig høye trykkfall. Når vann også produseres, kan trykkfallet forårsaket av den strømmende vann-i-olje blandingen øke til veldig høy verdier, spesiellt opp til inversjons punktet hvor blandingen blir transformert til en olje-i-vann blanding. Etter dette punktet kan trykkfallet bli dramatisk redusert.

En transport metode foreslått er å frakte tungolje som en olje-i-vann emulsjon. Det er ikke noe referance i litteraturen om stabilitet for disse systemene under rør strøm, men det finnes store mengder arbeid som har blitt utført ved å studere systemene i batch prosesser.

Målet med dette arbeidet vil være å eksperimentelt studere faktorene som styrer stabiliteten av slike ustabile olje-i-vann emulsjoner under rør strøm.

Oppgaven bør inneholde de følgene punktene:

Arbeidet vil bestå av:
1 Et studie av relevant litteratur om fase inversjon fenomenet.
2 Et eksperimentelt fase inversjon studie av utvalgte fluider i batch prosesser.
3 Studere fase inversjon i rør strøm, ved å bruke de samme utvalgte fluidene.
4 Data vil bli analysert basert på eksisterende teorier i litteraturen.

Det eksperimentelle arbeidet vil bli utført laboratoriene ved Statoil s Forsknings Senter i Trondheim, hvor olje-vann strømings sløyfer og fluid kategorisering er tilgjengelig.

Oppgaven gitt: 26. januar 2010
Hovedveileder: Ole Jørgen Nydal, EPT

Master thesis

Experimental investigation of phase inversion for oil-water systems

Anders Nilssen Tysnes and Håvard Lamberg

Spring 2010

NTNU
Norwegian University of
Science and Technology

Preface

This master thesis is the result of conducting experimental work with oil-water mixtures at Statoil's research center at Rotvoll, spring 2010. The report marks the end of our engineering education at NTNU, and is therefore completed with mixed feelings.

Experimental work has proved to be a demanding and time-consuming process, with no guarantees of success. We have learned a lot about the effort, discipline and persistence needed, in order to achieve the desired results. We have also learned to appreciate having a solid and supporting company to aid us through the frequent unforeseen problems encountered.

We would like to thank Robert Orr, Ole Jørgen Nydal, Bjørnar Hauknes Pettersen, Tony Boassen and Jose Luis Plasencia for guidance and support. A special thanks to Robert Orr for all the time and effort he put in helping us with the experimental work.

Anders Nilssen Tysnes

Håvard Lamberg

II. Summary

This report focuses on an experimental investigation of phase inversion for oil-water mixtures. The investigation has been carried out through batch experiments and direct flow experiments (fixed concentrations), using both crude oil and model oil. When using model oil, hydrophobic surfactants have been used, in order to make the oil behave like crude oil and attempt to control the inversion process. Special emphasis has been placed on the formation of multiple emulsions (w/O/W), and how this can lead to phase inversion. Visual evidence is presented.

The first part of the report is theoretical, involving the necessary theory needed to interpret the experimental results. It also contains a description of the experimental setup used, and the experiments conducted.

The last part of the report contains a section with results from the experiments. This section contains pressure drop curves, chord length readings, visual evidence, and a collection of relations discovered, or confirmed, from conducting batch experiments.

The results are discussed and it is concluded that phase inversion can occur during direct flow experiments with crude oil (from the Grane field) as a result of multiple emulsions forming over time. Given the correct surfactant concentration, this can also occur when using model oil (Primol 352).

It is also concluded that Cryo ESEM technology can be used to document the formation of multiple emulsions with more certainty than the techniques used in previous research, known to the authors.

III. Sammendrag

Denne rapporten fokuserer på en eksperimentell undersøkelse av fase inversjon for olje-vann blandinger. Undersøkelsen har blitt utført ved batch forsøk og direkte strømnings forsøk (uten å øke den dispergerte fasen), og både rå-olje og modell-olje har blitt brukt. Når modell-olje har blitt brukt, har også hydrofobe surfaktanter blitt brukt for å prøve å få oljen til å oppføre seg som en rå-olje og forsøke å kontrollere inversjons prosessen. Spesiell fokus har blitt rettet mot formasjon av multiple emulsjoner (w/O/W), og hvordan dette kan føre til fase inversjon. Visuelle bevis er presentert.

Den første delen av denne rapporten er teoretisk, og inneholder den nødvendige teorien for å kunne tolke de eksperimentelle resultatene. Den inneholder også en beskrivelse av det eksperimentelle oppsettet som er brukt, og hvilke forsøk som er utført.

Den siste delen av rapporten inneholder en seksjon med resultatene fra forsøkene. Denne delen inneholder trykkfall kurver, korde lengde målinger, visuelle bevis, og en samling av oppdagede, eller bekreftede relasjoner fra de utførte batch forsøkene. Resultatene er diskutert og konklusjoner er gjort, basert på det eksperimentelle arbeidet og eksisterende teorier.

Resultatene er drøftet og det er konkludert med at fase inversjon kan skje i direkte strømnings forsøk med råolje (fra Grane feltet) som et resultat av at det dannes multiple emulsjoner over tid. Ved å bruke en korrekt mengde surfactant kan dette også skje når man bruker modell olje (Primol 352).

Det blir også konkludert med at Cryo ESEM tekonologi kan bli brukt til å dokumentere formasjonen av multiple emulsjoner med større sikkerhet enn ved metoder brukt i tidligere arbeid forfatterne kjenner til.

IV. Table of content

Preface 2
II. Summary 3
III. Sammendrag 4
IV. Table of content 5
V. Table of figures 7
VI. Nomenclature 9
1 Introduction 10
1.1 Motivation 10
1.2 Previous work 10
1.3 Project definition 11
2 Theory 12
2.1 Phase inversion point 12
2.2 Emulsions 12
2.2.1 Standard emulsions 12
2.2.2 Multiple emulsions 13
2.3 Phase inversion processes 14
2.4 Surface active agents (surfactants) 15
2.5 Batch experiments 16
2.6 Pipe flow experiments 17
3 Experiments 19
3.1 Batch experiments 20
3.1.1 Experimental setup 20
3.1.2 Experimental procedure 20
3.2 Flow experiments 22
3.2.1 Experimental setup 22
3.2.2 Experimental procedure 24
3.3 Experimental reproducibility 27
3.4 Visual documentation on phase inversion 27
3.4.1 Microscopic documentation 27
3.4.2 Cryo ESEM Analysis 28
4 Results 30
4.1 Batch experiments 30

4.1.1 Primol 352 experiments (first series) 30
4.1.2 Exxsol D60 experiments 31
4.1.3 Grane experiments 32
4.1.4 Primol 352 experiments (second series) 34
4.1.5 Summary of the results from batch experiments 36
4.2 Flow experiments 36
4.2.1 Primol 352 experiments 36
4.2.2 Grane experiments 46
4.2.3 Summary of the results from flow experiments 51
4.3 Visual comparison of droplet development 52
4.3.1 Pictures taken with a microscope 52
4.3.2 Images generated from Cryo ESEM analysis 57
5 Discussion 61
5.1 Effect of surfactants 61
5.2 Crude oil vs. model oil behavior 62
5.3 Visual evidence of multiple emulsion formation 63
5.4 Chord length readings and inversion mechanics 63
5.5 Experimental problems 65
5.5.1 Resistance readings 65
5.5.2 Torque readings 66
5.5.3 Microscopic observations 66
5.5.4 Pump capacity 66
6 Conclusion and suggestions for further work 67
6.1 Conclusion 67
6.2 Further work suggestions 67
References 68
Appendix A – Flow experiment readings 70
Apendix B – Chord length readings 88

V. Table of figures

Figure 2.2-1 Standard inversion 13
Figure 2.2-2 Inversion by multiple emulsion 13
Figure 2.4-1 Surfactant molecule 15
Figure 2.4-2 Formulation/composition map 16
Figure 2.6-1 Stratified oil-water flow 17
Figure 2.6-2 Dispersed oil-water flow 18
Figure 3.1-1 Schematic diagram of batch setup 20
Figure 3.2-1 : Schematic diagram of the flow loop 23
Figure 3.2-2 Cutaway illustration of the FBRM probe 24
Figure 3.2-3 Example of chord length measured by FBRM® 24
Figure 3.2-4 Friction factor evaluation 26
Figure 3.4-1- Cross section of an emulsion sample surface 29
Figure 4.1-1 Inversion time vs. surfactant concentration for Primol 352 at 60% oil fraction 30
Figure 4.1-2 Conductivity vs. time for Exxsol D60 using Arlacel P135 31
Figure 4.1-3 Conductivity vs. time for Exxsol D60 using Croda Atsurf 5000 31
Figure 4.1-4 Resistance vs. time with 60% Grane at 1500 rpm 32
Figure 4.1-5 Torque vs. time with 60% Grane at 1500 rpm 32
Figure 4.1-6 Inversion time vs. stirring intensity at 40% oil fraction 33
Figure 4.1-7 Inversion time vs. surfactant concentration at 60% oil fraction 34
Figure 4.1-8 Inversion time vs. stirring intensity at 60% oil fraction 35
Figure 4.2-1 Pressure drop vs. time for 69% Primol 352 with 1 g/L Arlacel P135 37
Figure 4.2-2 Chord length readings for 69% Primol 352 with 1 g/L Arlacel P135 38
Figure 4.2-3 Pressure drop vs. time for 69% Primol 352 with 4 g/L Arlacel P135 39
Figure 4.2-4 Chord length readings for 69% Primol 352 with 4 g/L Arlacel P135 40
Figure 4.2-5 Pressure drop vs. time for 69% Primol with 4 g/L Croda Atsurf 5000 41
Figure 4.2-6 Chord length readings for 69% Primol 352 with 4 g/L Croda Atsurf 5000 42
Figure 4.2-7 Pressure drop vs. time for 69% Primol 352 with 7.3 g/L Croda Atsurf 5000 43
Figure 4.2-8 Chord length readings for 69% Primol 352 with 7.3 g/L Croda Atsurf 5000 44
Figure 4.2-9 Pressure drop vs. time for 69% Primol 352 with 2.5 g/L Croda Atsurf 5000 45
Figure 4.2-10 Pressure drop vs. time for 69% Grane oil 46
Figure 4.2-11 Chord length readings for 69% Grane oil 47
Figure 4.2-12 Pressure drop vs. time for 62.5% Grane oil 48
Figure 4.2-13 Chord length readings for 62.5% Grane oil 49
Figure 4.2-14 Pressure drop vs. time for 50% Grane oil 50
Figure 4.2-15 Chord length readings for 50% Grane oil 51
Figure 5.4-1 Multiple emulsion effect on chord length measurements 64
Figure 5.4-2 Chord length measurements around phase inversion 65

Table 3-1 Physical properties 20
Table 3-2 Friction factor calculations 26
Table 4-1 Average time and variation (40% Grane oil) 33
Table 4-2 Average time and variation (60% Primol 352) 35

Micrograph 4.3-1 Dispersed phase - Batch experiment after 2 minutes 52
Micrograph 4.3-2 Dispersed phase - Batch experiment after 30 minutes 53
Micrograph 4.3-3 Dispersed phase - Batch experiment after 65 minutes 53
Micrograph 4.3-4 Continuous phase - Batch experiment after phase inversion 54
Micrograph 4.3-5 Dispersed phase - Flow experiment after 2 minutes 55
Micrograph 4.3-6 Dispersed phase - Flow experiment after 20 minutes 55
Micrograph 4.3-7 Dispersed phase - Flow experiment after 40 minutes 56
Micrograph 4.3-8 Continuous phase - Flow experiment after inversion 56
Picture 4.3-9 Sample surface-early stage 57
Picture 4.3-10 Fractured oil drop 1 - after 3 minutes 58
Picture 4.3-11 Fractured oil drop 2 - after 3 minutes 58
Picture 4.3-12 Sample surface after 17 minutes 59
Picture 4.3-13 Fractured oil drop after 17 minutes 60
Picture 4.3-14 Overview after phase inversion 60

VI. Nomenclature

A	Area [m^2]
L_e	Entry length [m]
D	Diameter [m]
$\in$	Pipe wall roughness
f	Friction factor
Re	Reynolds number
p	Pressure [Pa]
V	Velocity [m/s]
$\dot{m}$	Mass flow rate
Δ	Change
rpm	Rounds per minute
PIP	Phase inversion point
HLB	Hydrophilic- Lipophilic Balance
HLD	Hydrophilic -Lipophilic Deviation
$FBRM$	Focused Beam Reflectance Measurement
EDS	Energy Dispersive X-ray Spectroscopy
$ESEM$	Environmental Scanning Electron Microscope
RMS	Root mean squared

Greek letters

μ	Dynamic viscosity [Pa s]
ρ	Density [kg/m^3]

Subscripts

O	Oil
W	Water
O/W	Oil in water
W/O	Water in oil
$w/O/W$	Water in oil in water

1 Introduction

1.1 Motivation

The world's reserves of conventional oil are slowly running out. This means the production of heavy oil will become more relevant in the years to come. This type of oil is more viscous than the conventional type and will therefore result in higher pressure drop in pipeline transportation, during production. This pressure drop increases as water production increases together with the heavy oil, in a W/O dispersion, and continues to rise until phase inversion has occurred. After phase inversion, the mixture flows as an O/W emulsion, and the pressure drop will be greatly reduced. Hence, knowledge on phase inversion for oil-water systems is of great importance, since reduced pressure drop means higher oil production at less cost. However, the O/W emulsion is unstable, and may easily invert back to the more stable W/O emulsion. To ensure an energy efficient heavy oil recovery, it is important to have and maintain an O/W emulsion flowing through the pipes.

In the future, the development of oil fields in the Arctic area is very likely. Extremely long pipelines may be required, and the pressure drop in these lines will be critical. Optimizing the fraction of oil in an O/W emulsion with respect to high oil fraction and a stable emulsion, represent a significant economic potential by transporting a higher quantity of oil at a given pipeline pressure drop.

Upstream, oil wells with low reservoir pressures (a common problem), might also benefit from of this. O/W ratio could be controlled by producing from different reservoir zones, and surfactants could be injected through a SPM (Side Pocket Mandrel) downhole. This could reduce the pressure drop in the production tubing, and be an alternative to conventional gas lift system.

The main motivation for this paper is therefore to investigate the stability of O/W emulsions and study the factors of influence. To be able to do this, knowledge on phase inversion and how to delay/accelerate it, is important.

1.2 Previous work

The knowledge on phase inversion is mostly based on experiments carried out in batch. A term introduced by Salager [1] is "catastrophic phase inversion", which indicates an inversion induced by increasing the volume fraction of the dispersed phase. At higher volume fractions, a phase will always be continuous, while it is dispersed at lower fractions. The range between these fractions was defined by Selker and Sleicher [2] as the ambivalent region, and in this region, either phase can be continuous. They showed that this region is primarily a function of the viscosity ratio, and shifts towards higher fraction values as the ratio increases. Other factors were also observed influencing the ambivalent region, like density, stirring intensity and wettability. All these factors influence the location of the phase inversion point (PIP) inside the ambivalent region. Several correlations between the PIP and water cut were suggested by numerous researchers like Arirachakaran [3], Nädler and Mewes [4]. Arashmid and Jeffreys [5] assumed that phase inversion occurred when every drop-collision resulted in coalescence, and derived a model from this assumption. Coalescence proved to be dependent on drop size and stirring intensities, but most of all surface tension, influenced by surfactant concentration. This was shown by investigating the influence surfactants

had on the morphological development and in turn, the boundaries of the ambivalent region. Salager made numerous contributions in his analysis [6]. He distinguished between a standard inversion frontier given by a specific phase fraction, and a dynamic inversion. The dynamic inversion changes the PIP as the emulsion alters its morphology [7].

Most of the phase inversion experiments conducted during pipe flow have been continuous flow experiments, performed by adding to the dispersed phase. While in batch experiments, the breakage of drops is caused by the impeller, it is the viscous and turbulent shear in the flow that causes the breakage of drop in pipe flows [8]. Interfacial shear stress and surface tension causes the two phases to distribute themselves in a number of ways. The mapping of these configurations, depending on velocities and phase-fractions has been well documented [9], [10]. However, most of these documentations have limitations, in the sense that they do not include the investigation of multiple emulsions. Many researchers have explored the dynamics around drop coalescence and break-up, with interest in phase inversion during pipe flow, but their research has been carried out in batch experiments. Limited tests on phase inversion have been carried out in pipe flow, due to the required amounts of oil.

1.3 Project definition

A lot of the previous work, regarding phase inversion, is based on dynamic experiments and inversion related to a given phase fraction. The aim of this report is to achieve a better understanding of the phase inversion phenomena by approaching the problem from a different angle.

First, an attempt to predict when phase inversion occurs during batch experiments is made, by regulating the surfactant concentration in model oil, and stirring intensity for both model oil and crude oil. The natural surfactant concentration in crude oil cannot be controlled, so focus is placed on finding a surfactant concentration that makes mode oil behave like crude oil.

Second, the knowledge and relations obtained from the batch experiments will be used to attempt direct flow experiments, and achieve phase inversion during pipe flow, through the formation of multiple emulsions (w/O/W). An understanding of the development in droplet distribution is attempted by measuring the chord lengths, in order to help compare the experimental results up against this theory.

Emphasis is placed on gaining solid visual evidence of the formation on multiple emulsions, and explain the mechanics and factors which lead to, or influence phase inversion.

2 Theory

2.1 Phase inversion point

The PIP is known as the oil-water fraction where, for instance, a flowing oil-water mixture, switches from a dispersion of oil drops in water, to a dispersion of water drops in oil, or vice versa. In other words; the PIP is the critical volume fraction of oil/water where one of the phases changes from being the dispersed phase, into being the continuous phase. The PIP depends on fluid properties like density, viscosity, interfacial tension and pipe wettability. Phase inversion leads to a sudden change in the rate of momentum, heat transfer between flow and pipe walls, and the heat transfer between the continuous and dispersed phase. At this point, the effective viscosity of the mixture becomes very high, and this leads to a sudden change in pressure drop at, or near the PIP. The pipe corrosion is also very dependent on the characteristics of the fluid that wets it, and at the PIP, the corrosion level may change significantly.

2.2 Emulsions

2.2.1 Standard emulsions

An emulsion is defined as a mixture of two or more immiscible liquids where one is dispersed in the other. When considering an emulsion consisting of oil and water, there is usually a dominant phase called the continuous phase, and a non-dominant phase called the dispersed phase. Crude oil and water has different physical properties like viscosity, density and surface tension, and the emulsion tends to act more like one of them, rather than a fraction- based combination of the two. This is because the continuous phase is connected throughout the emulsion, while the dispersed phase is present as isolated drops in the continuous phase. Since the drops are separated, they are carried by the continuous phase, and the emulsion is therefore less affected by the physical properties of the dispersed phase. The viscosity of the continuous phase controls the behavior of the emulsion. The emulsions conductivity is also based on the continuous phase, since the dispersed phase is present as isolated drops.

Figure2.2-1 illustrates the transition from a W/O emulsion to an O/W emulsion by addition of water. When phase inversion occurs, the emulsion changes from being oil continuous to water continuous and the physical properties of the emulsion changes to values closer to the new continuous phase. The phase inversion is in this case identified at a given water and oil fraction. At any given point the emulsion consist of a continuous phase and a dispersed phase. This is not the case for multiple emulsions.

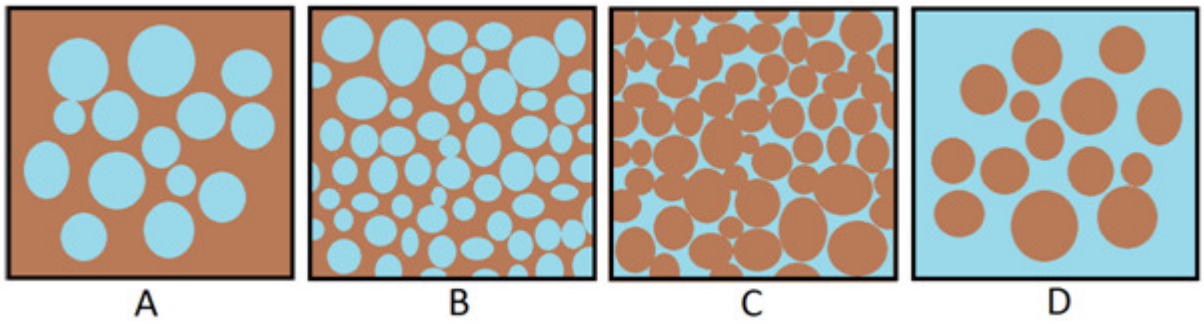

Figure 2.2-1 Standard inversion

A-Water is dispersed in oil. B- The addition of water has increased the dispersed fraction. C- Phase inversion occurs and water becomes the continuous phase. D- The addition of water has further reduced the dispersed oil phase.

2.2.2 Multiple emulsions

In a multiple emulsion, droplets of the continuous phase are trapped inside the dispersed phase. This increases the effective fraction of the dispersed phase, without any addition.

Figure 2.2-2 illustrates the coalescence of oil drops, capturing parts of the continuous water phase. As water droplets are captured in the oil, the effective fraction of the dispersed phase increases. The O/W emulsion turns into a w/O/W emulsion, where the small "w" denotes the droplets forming inside the dispersed phase. Even though the actual phase fractions remains constant, the effective fractions changes as the captured droplets of the continuous phase contribute to the dispersed phase volume.

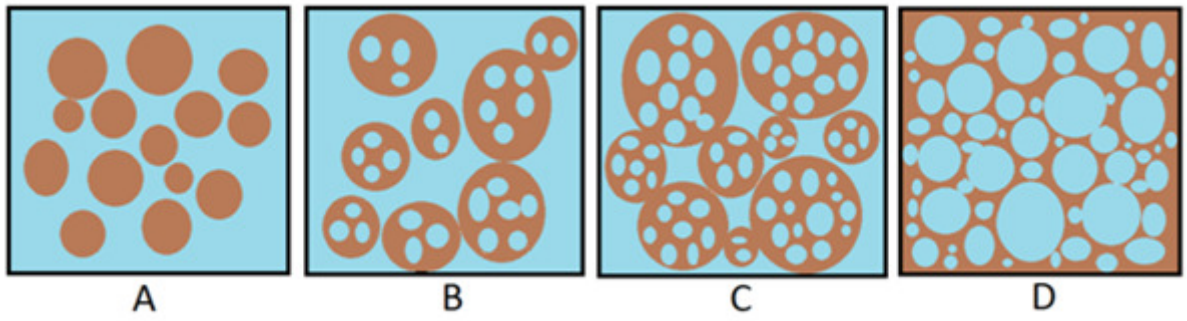

Figure 2.2-2 Inversion by multiple emulsion

A - Oil is dispersed in water. B – Multiple emulsions start to form as small droplets of water are captured in the oil phase. C- The effective oil fraction increases as more and more water is captured. D – Phase inversion occurs and oil becomes the new continuous phase.

2.3 Phase inversion processes

An emulsion is dynamically driven and balanced by two major processes [11]. One of these processes is the coalescence of drops. This is the rate of which separated drops unite and form larger drops. The coalescence between drops happens when they collide, and the force in this collision drains the film surrounding the droplets. If this force is large enough and the contact time is long enough, the film will ultimately rupture and the drops will unite.

The other process is the breakage of drops, which is the opposite of coalescence. It describes in what rate drops get crushed or disfigured to the point where the surrounding film is unable to resist the force. This causes the film to break and the drop to separate into smaller drops.

Phase inversion is caused by the dispersed phase forming a continuous phase by coalescing. The coalescence rate increases, as the fraction of the dispersed phase increases. If the coalescence occur at a higher rate than the breakup, the emulsion will eventually invert, but not if the breakup rate is higher or equal to the coalescence rate [12]. The dispersed fraction necessary to trigger an inversion is very dependent on the polydispersity of the drops. If the drops have exactly the same size, the required fraction is limited by the closest packing of spheres, proven by Gauss to be at a fraction of 0.74. The phase inversion will happen before this fraction is reached. When the drops consist of different sizes, the required fraction can exceed this limit value as the drops are closer packed [1].

In a multiple emulsion, two other mechanisms are introduced. One of these mechanisms is the encapsulation of continuous phase droplets inside the dispersed phase. The exact unfolding of this mechanism has, to the authors' knowledge, not yet been revealed, but the common conjecture is that it is closely connected to the coalescence of the dispersed phase. When drops of the dispersed phase are packed together, a small amount of water is trapped between the films. When this film is drained and ruptures, the drops coalesce, and the water is trapped as small droplets inside the newly formed drop [13].

The other mechanism is the escape rate of the captured droplets from the dispersed phase. It is suggested that this happens through coalescence between the internal droplet and the continuous phase through the surface film of the dispersed drop [13]. Escape can also occur when the dispersed drop is broken and releases the captured droplet.

If the encapsulation happens at a larger rate than the escape, the dispersed phase will increase in volume as it steals more from the continuous phase than it releases. This will, in contrast to a standard emulsion, enable phase inversion even when the breakage and coalescence of the dispersed drops is balanced. It will also, as previously mentioned, enable an effective volume increase of the dispersed phase, without adding to the emulsion.

2.4 Surface active agents (surfactants)

A surfactant can act as an emulsifier and stabilize an emulsion by increasing its kinetic stability. Surfaces and molecules are usually divided into two different categories; hydrophobic (lipophilic) and hydrophilic. Respectively, hydrophobic and hydrophilic means water-fearing and water-loving. Lipophilic means fat-loving, and is often used interchangeably with hydrophobic, although there are exceptions. Surfactants possess both these characteristics, meaning they have a hydrophilic head and a hydrophobic tail. Figure 2.4-1 shows an illustration of the surfactant molecule.

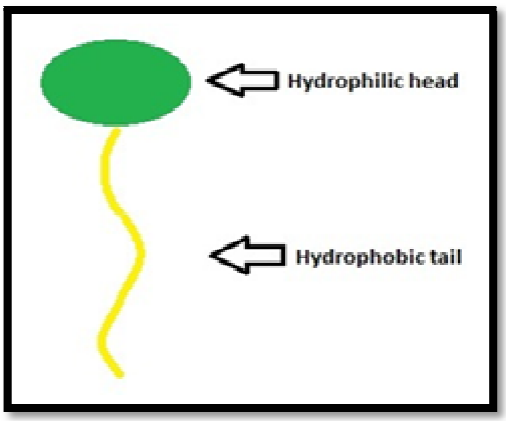

Figure 2.4-1 Surfactant molecule

Molecules inside a fluid share cohesive forces with all identical neighboring molecules. Molecules at the surface of a fluid have no neighboring molecules above, and will therefore experience larger attractive forces towards molecules at the inside of the fluid, and sideways at the surface. In order to increase the fluids surface area, molecules must move from the inside of the fluid to the surface, and attractive forces at the surface must be overcome. The fluids resistance to this increase in surface area is called surface tension. Fluids with high intermolecular attractive forces have higher surface tension.

Interfacial tension is similar to surface tension, but the main forces involved are adhesive forces. The adhesive forces are tension between a liquid and another substance (solid, liquid, or gas), and occurs at their interface.

Since surfactants have a water-loving and an oil-loving part, they will position themselves in the interface between oil and water. This will reduce the rejecting forces and in turn reduce the interfacial tension.

Salager [11] separated between a normal emulsion and an abnormal emulsion. The normal emulsion has a preferred morphology with the surfactant present in the continuous phase, and the abnormal emulsion has a non- preferred morphology with the surfactant present in the dispersed phase. Bancroft's rule [14] states that the continuous phase will be the phase in which the surfactant is most soluble. This balance of the surfactants solubility can be expressed by the hydrophilic-lipophilic balance (HLB) and is used as a scale to describe the surfactant. A HLB value of 0 indicates that the molecule is completely hydrophobic, and a value of 20 indicates a totally hydrophilic molecule. This value is often transformed into a hydrophilic-lipophilic deviation (HLD), where the 0

value indicates the perfect balance. The zero value of HLD is close to a HLB value of 10.5. A negative HLD has a hydrophilic tendency, and positive HLD has a lipophilic tendency.

Figure 2.4-2 shows the connection between composition and formulation for oil-water emulsions. The dashed line in the middle indicates the inversion line and separates the water continuous areas from the oil continuous. In the B- and C+ regions, the emulsions does not obey Bancroft's rule and are considered abnormal. These regions allow the formation of multiple emulsions.

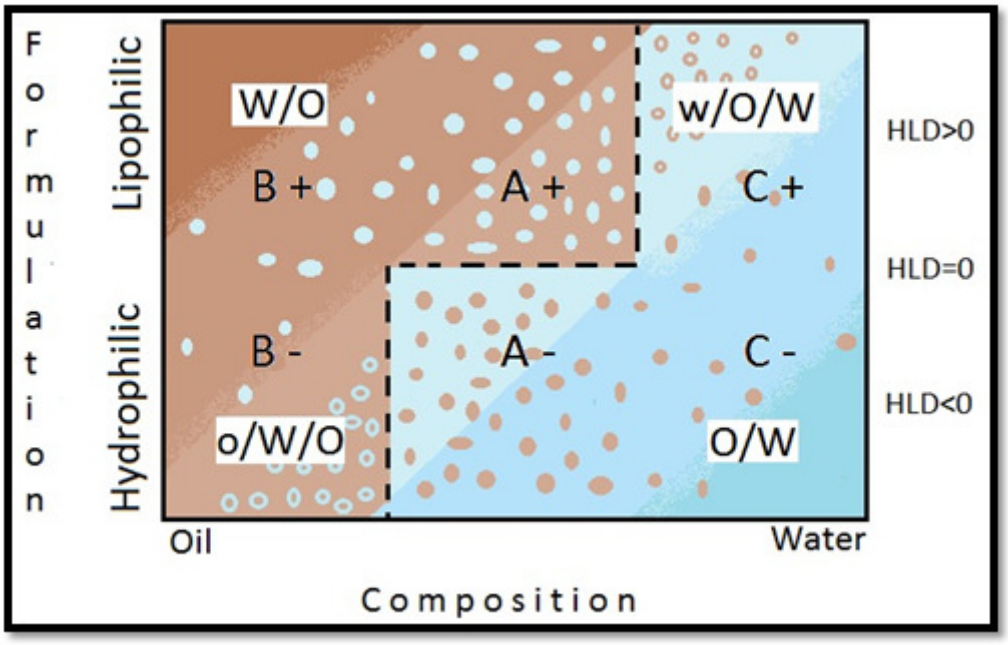

Figure 2.4-2 Formulation/composition map

The surfactants used in this paper are:

- Arlacel P135 – HLB 5.5
- Croda Atsurf 5000 – HLB from 4 to 6

Both surfactants are W/O emulsifiers with a positive HLD value. The experiments in this paper will be carried out from abnormal to normal emulsions (C+ → A+) [15].

2.5 Batch experiments

Phase inversion has been investigated by batch experiments. In these experiments, oil and water mixtures are stirred until a certain effective volume of the dispersed phase is reached, and inversion occurs. Some factors influencing the inversion are the addition rate of the dispersed phase, stirring intensity, container volume, and the physical properties of the fluids involved. The inversion can be achieved by three different methods; dynamic process, continuous stirring, or a combination of the two [7].

A dynamic process is associated with the continuous addition of the dispersed phase until phase inversion occurs. In these experiments the phase fractions and the addition rate of the dispersed phase becomes the most important variables.

During continuous stirring, no fluids are added to the mixture, and inversion happens by an increase in the effective volume fraction of the dispersed phase. The effective dispersed volume grows, as parts of the continuous phase are captured inside the dispersed phase. This mechanism is explained more detailed in chapter 2.3. The most important variables during these experiments are stirring intensity and surfactant concentration.

When using a combination of the two methods above, referred to as a standstill dynamic process, the dispersed phase is added up to a certain point. After this point is reached, the addition is stopped, while the stirring continues at the same intensity. In other words; the first part of the experiment is dynamic, while the last part is continuous stirring. The experiments conducted in this report are standstill dynamic processes.

2.6 Pipe flow experiments

A multiphase flow can be defined as a flow consisting of more than one phase/component and is, in contrast to a single phase flow, quite complex. While the single phase flow only has interaction between the component and the pipe, a multiphase flow also has interaction between the different components. The variation and parameters around these interactions complicate the flow.

Multiphase flows can consist of a number of different phase combinations, like gas-liquid, liquid-solid and liquid-liquid. This paper will focus on liquid-liquid flows, or to be more specific; oil-water flows. Although the morphology in a multiphase flow can have many forms, the two basic flow patterns are stratified and dispersed flow.

Stratified flow is found at very low superficial velocities. In this flow pattern, the gravity effects dominate, and the phases flow separately. The interfacial contact between the phases is only present as one single area, as can be seen in figure 2.6-1.

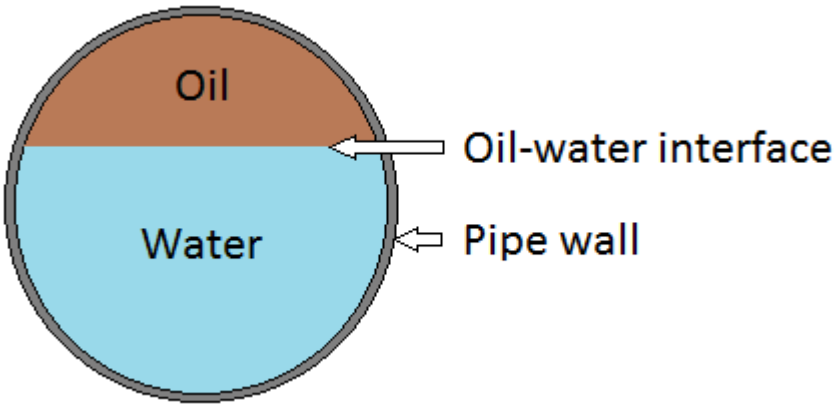

Figure 2.6-1 Stratified oil-water flow

At higher velocities the multiphase flow develops a pattern where one phase is dispersed as drops in the continuous phase. This is called a fully dispersed flow, and is illustrated in figure 2.6-2.

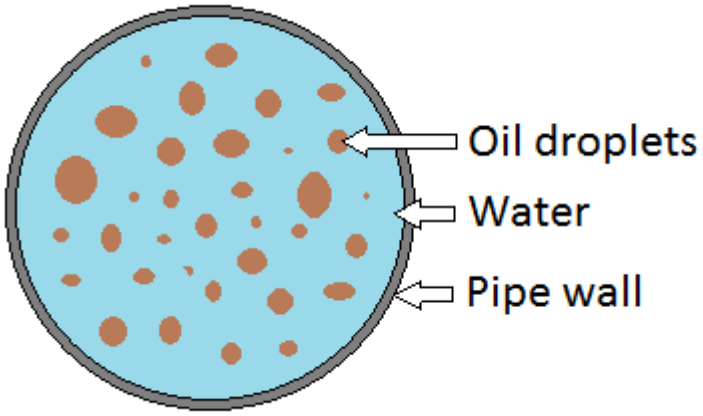

Figure 2.6-2 Dispersed oil-water flow

This pattern develops when the flow the flow is turbulent. The flow experiments in this paper are conducted under turbulent conditions. This is shown in section 3.2.2.4.

Under these conditions, it can be assumed that the mixture is homogenous, and that the dispersed drops flow at the same velocity as the continuous phase. The interface between the phases is now present around every drop, and since the size and count of drops constantly changes, the interface area changes as well. The interaction between the wall and the phases is also changing depending on numerous different parameters like pipe material, roughness, flow morphology and wettability. All these variables are codependent and make it very difficult to accurately predict and calculate the parameters of a multiphase flow, and experimental work has been done in an attempt to obtain an overview of different patterns in a pipe flow [9], [10].

The phase inversion phenomena can be investigated during multiphase pipe flow experiments. In these experiments, two or more fluids (in this case oil and water) flow through a pipe. In the experiments conducted in this report, these fluids flow as a mixture, where one phase is dispersed in the continuous phase in the form of drops. The study of phase inversion during pipe flow is complex and depends on many different parameters like fluid viscosities, surfactants, densities and the wetting properties of the pipe wall. There are mainly two different methods of conducting flow experiments; continuous flow experiments and direct flow experiments [16].

A continuous flow experiment is the most common method of conducting flow experiments. These experiments are associated with the continuous addition of the dispersed phase. At a certain point the dispersed phase fraction is high enough to form a continuous phase, and phase inversion occurs. In these kinds of experiments emphasis is usually placed on locating the critical fraction of which the phase inversion happens, while regulating parameters like flow velocity and the injection rate of the dispersed phase.

A direct flow experiment is a less common method of conducting flow experiments. In these experiments, the initial phase fractions are used throughout the entire experiment. This means no amount of fluid is added to the dispersed or continuous phase. There are two different methods of achieving phase inversion during a direct experiment. The first one is to start out with a large enough fraction of the dispersed phase, so that the inversion occurs within the first cycles, once the flow stabilizes. This kind of phase inversion is the result of having a sufficiently large initial dispersed phase fraction. The second method is when the dispersed phase fraction is small, and phase inversion does not occur during the first cycles. In this case, the experiment is kept under constant operational conditions, and phase inversion occurs as a result of an increase in the effective dispersed phase fraction. In these experiments emphasis is placed on regulating parameters like surfactant concentration, in order to increase/decrease the formation of multiple emulsions, and by this controlling the phase inversion. The flow experiments conducted in this report are direct flow experiments.

3 Experiments

This chapter contains a description of the experimental setups used during the batch experiments and during the flow experiments. It also gives a detailed description of the different experiments conducted and experimental conditions.

Table 3-1 shows the physical properties of the fluids used during the experiments.

Oil	Density [kg/m^3]	Dynamic Viscosity [Pa·s]
Primol 352	866	(20˚C) 0.18000
Exxsol D60	712	(20˚C) 0.00131
Grane	897	(27˚C) 0.17700
Salt water (3,5 wt %)	1030	(20˚C) 0.00108

Table 3-1 Physical properties

3.1 Batch experiments

3.1.1 Experimental setup

The batch is cylinder shaped with an internal diameter of 5.6 cm and a height of 13 cm. A thin, hollow layer outside the cylinder is filled with a circulating fluid which allows the temperature during the experiments to be regulated from 0-80 °C. The 3.6 cm diameter impeller (and 3.8 cm high) is driven by an electric motor. This motor allows regulation of stirring intensity, and also displays the necessary torque to maintain constant rotational speed. An electrical resistance probe is lowered into the batch, measuring the resistance in the fluid. A more detailed overview is shown in Figure 3.1-1:

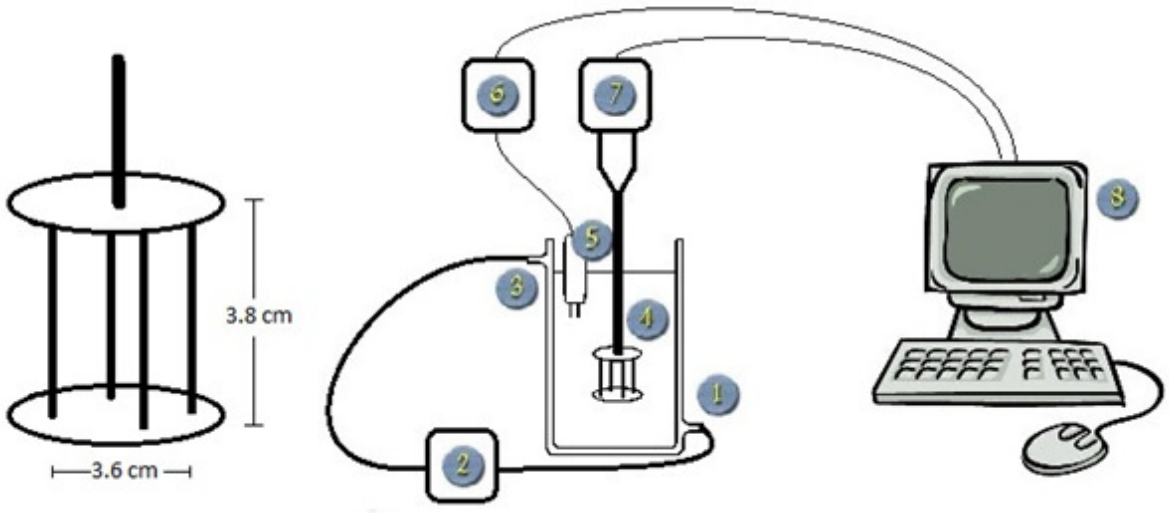

Figure 3.1-1 Schematic diagram of batch setup

1. Inlet 2. Temperature regulator 3. Outlet 4. Impeller 5. Conductivity probe 6. Conductivity reader 7. Electrical engine

3.1.2 Experimental procedure

Each batch experiment contained a total fluid amount of 0.2 liters. This amount included salt water, oil and surfactant. Since hydrophobic surfactants were used, the surfactant was dissolved into the oil phase. A specific, high concentrated oil-surfactant mixture was produced in large quantities and used as a base for all the experiments to ensure similar conditions. The consistency of the different surfactants varied, and in order to create a homogeneous mixture of oil and surfactant, the desirable amounts were placed into a small batch of oil. This batch was heated up to 60 C, while stirred at 1000 rpm for the required time, because the surfactants were easier to dissolve at higher temperatures. After the surfactant was completely dissolved in the oil, the content of the small batch was mixed with a desired amount of oil, depending on the surfactant concentration needed. This new mixture was again heated up to 60 °C and stirred until it was completely homogeneous.

The water was added to the batch, before the stirring started. While stirring at the desired intensity, the oil was gradually added to the continuous water, by using a funnel. The same funnel was used for all the experiments, ensuring a constant rate of addition.

After ending an experiment, emphasis was placed on cleaning the equipment thoroughly. The impeller, batch and conductivity probe were cleaned between all experiments. Toluene was used to dissolve the oil, and then Acetone was used to clean the remaining particles. High pressured air was used to dry the objects before the next experiment.

3.1.2.1 Primol 352 experiments (first series)

The first 6 experiments were conducted using the viscous model oil, Primol 352. The aim was to observe the effects of varying the phase fractions and surfactant concentration, while gaining the basic experience on how to perform batch experiments. The temperature and the stirring intensity were kept constant, at respectively 20 °C and 1500 rpm. Oil fractions of 50, 55 and 60% were used (i.e water fractions of 50, 45 and 40%). The hydrophobic surfactant, Arlacel P135, was mixed into the oil and the surfactant concentration ranged from 2.5-10 g/L.

3.1.2.2 Exxsol D60 experiments

10 experiments were conducted, using the low viscosity oil, Exxsol D60. The aim was to get an impression of what effects the two different surfactants (Arlacel P135 and Croda Atsurf 5000) has on the inversion time. Oil fractions of 30, 40, 50 and 60 % were used, while keeping the surfactant concentration and stirring intensity constant, at respectively 10 g/L and 1500 rpm.

3.1.2.3 Grane experiments

36 experiments were conducted, using crude oil from the Grane field. This oil is very viscous and dense. The crude oil was demulsifier free and contains natural surfactants, so no additional surfactant was added. Temperature was kept constant at 27 °C, and at this temperature, the crude oil viscosity is identical to Primol 352's viscosity at 20 ˚C. Oil fractions of 40, 50 and 60% where tested, but the main emphasis were placed on 40 and 60%, in order to identify the influence of different fractions more easily. The first experiments were conducted at a constant stirring intensity (1500 rpm), with the intention of testing the repeatability of the experiments, and study the effect of different oil fractions. In the next session, the stirring intensity ranged from 750-2000 rpm, while the oil fraction was kept constant at 40%. With an oil fraction of 60%, the phase inversion occurred too quickly to be accurately measured, at stirring intensities higher than 1500 rpm.

3.1.2.4 Primol 352 experiments (second series)

After the Grane experiments, 28 new experiments were conducted, using Primol 352. The aim was to find a surfactant concentration that made the model oil behave like crude oil. As in the first series of Primol experiments, the temperature was kept constant at 20° C. Both surfactants were tested, but primarily Arlacel P135 was used. By considering the results from the first series of Primol 352 experiments, which indicated that Primol 352 takes a long time inverting at low oil fractions, a 60% fraction was chosen.

3.2 Flow experiments

3.2.1 Experimental setup

The flow loop consists of a 20 meter long SS316 pipe, with an internal diameter of 2.21 cm. The liquid is pumped through the loop by a low shear Lobe pump, and is being directed by a series of valves. The valves detain the fluid inside the loop, or lead it to the outlets.

The liquid is injected into the loop through an open tank, which is the same tank the flow passes through after completing a cycle. The pipe contains 7.5 liters of liquid, so any excess fluid is stored in the tank, up to the maximum volume of 20 liters. Two different pressure drops are recorded. The pressure drop over the pipe is measured by two pressure taps, placed over a 3 m section. Pressure taps are also installed at each side of the pump, so that the pressure drop over the pump can be monitored. The pump was not capable of maintaining an oil continuous flow, due to the increased pressure drop over the pump, so the experiments were terminated shortly after the inversion.

Figure 3.2-1 shows the experimental setup for the flow experiments.

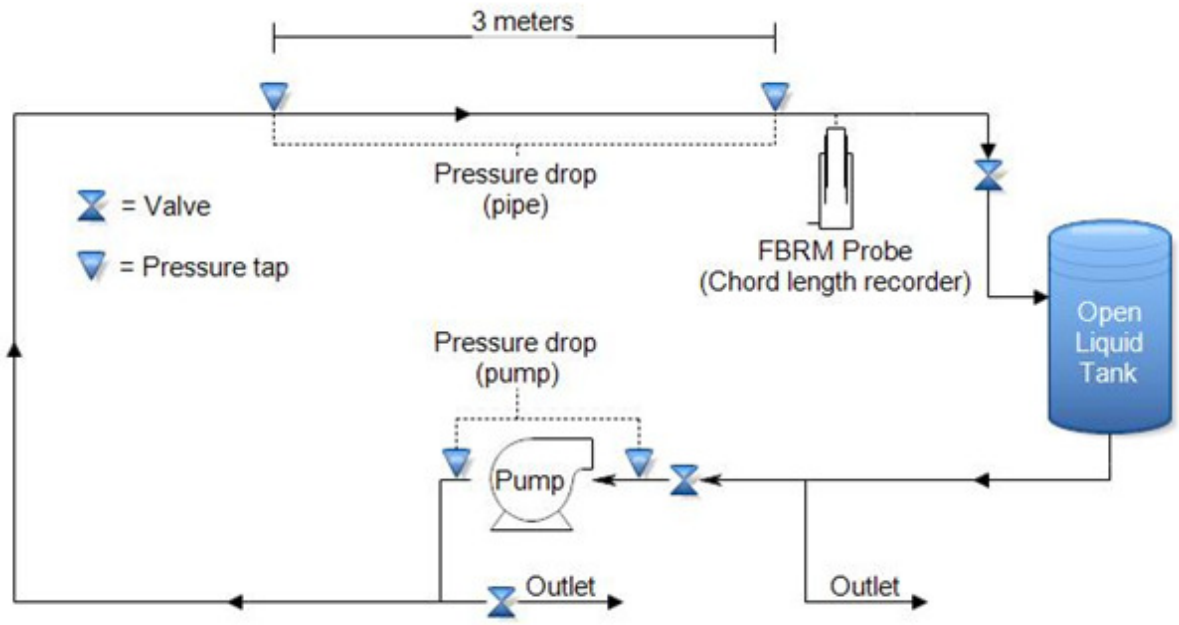

Figure 3.2-1 : Schematic diagram of the flow loop

An optical laser is installed at the end of the cycle to record the cord length distribution throughout the flow. This can aid in understanding the morphological development around the phase inversion. The chord length measurements were done with FBRM® technology, using a Lasentec® D600 probe mounted through the pipe wall. FBRM® stands for Focused Beam Reflectance Measurement, and was developed by Lasentec. It tracks the rate and degree of change of particles or droplets in real-time, and in process. The apparatus uses a laser which is carefully focused on a point right outside the probe window.

Figure 3.2-2 illustrates a cutaway of the probe, showing the internal workings of the optic mechanism. The laser circulates the focus area at constant speed, and as the laser hits new particles or substances, the light is backscattered into the probe. This is interpreted into chord length, based on scanning speed and backscatter time. The mechanism is illustrated in figure 3.2-3.

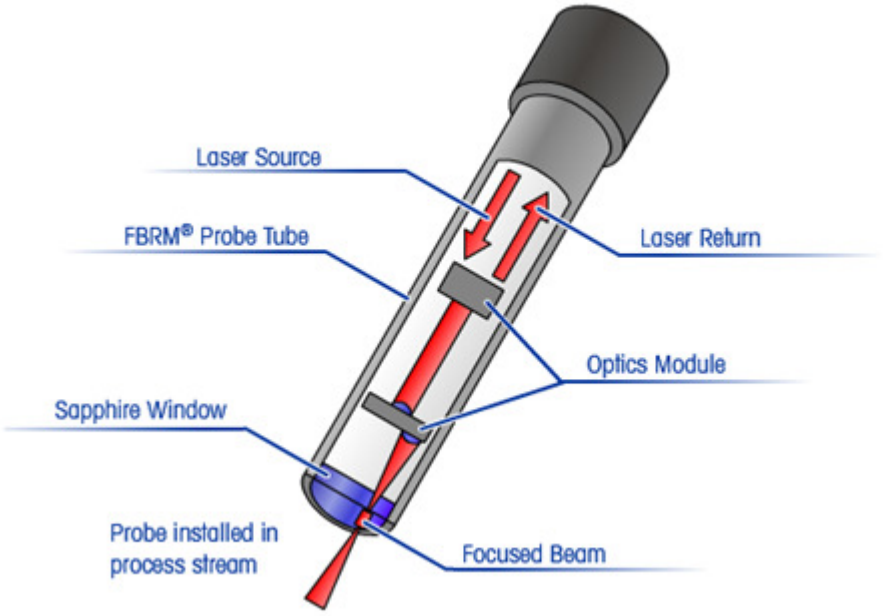

Figure 3.2-2 Cutaway illustration of the FBRM probe

Figure 3.2-3 shows an example of how the presence of a droplet can be measured and interpreted into a chord length by the FBRM®. The mechanism can register a chord length ranging from 0.5 microns to 2.5 mm.

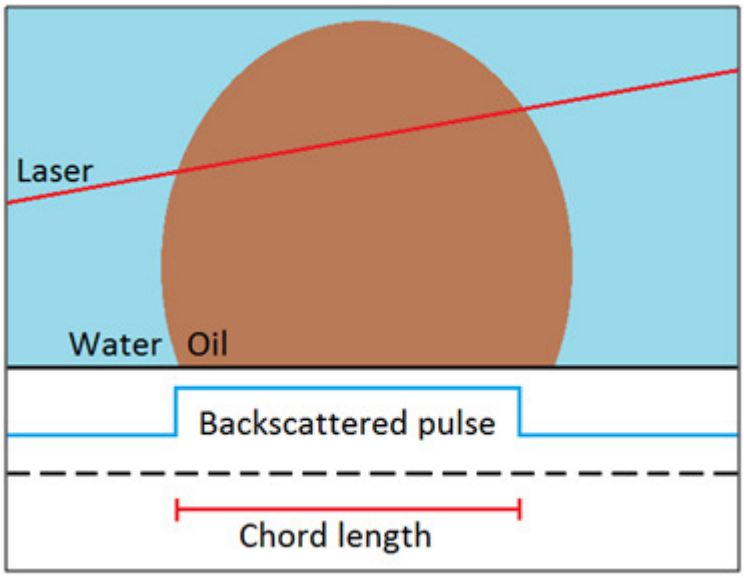

Figure 3.2-3 Example of chord length measured by FBRM®

3.2.2 Experimental procedure

Dissolving the surfactant into the oil phase was done in the same way as for the batch experiments. The only difference was that the amount of oil was greatly increased. This meant that when the small batch mixture had been heated and stirred, its content was added to the desired amount of oil. The container size made it hard to heat the mixture, so it was shaken vigorously until the mixture was homogeneous.

A total fluid amount of 8 liters was used for each flow experiment, which provided a buffer of 0.5 liters in the open liquid tank. This ensured that a continuous flow was maintained throughout the entire pipe length, without risking any separation in the tank.

The pipe had to be cleaned after each experiment to ensure similar experimental conditions. The structure of the flow loop made it difficult to drain completely. After the pump was shut down, the outlet valves were opened so that most of the content in the pipe was emptied. High pressure air was blown into the pipe to clear out the remaining emulsion. After this, single phase distilled water was used, and the same draining procedure was repeated until clear water exited the pipe and the next experiment could begin.

3.2.2.1 Primol 352 experiments

The 9 first experiments were conducted using Primol 352, Aracel P135 and Croda Atsurf 5000. All experiments were direct experiments, and the aim was to obtain phase inversion from O/W to W/O, while keeping the oil and salt water fractions constant. Emphasis was placed on using different surfactant concentrations, different initial fractions and different mixture mass flow rates.

The surfactant Arlacel P135 was used for the first experiments, and once successful results were obtained, Croda Atsurf 5000 was tested. The motivation for these experiments was to obtain a better understanding of different surfactants influence on phase inversion, during pipe flow with constant phase fractions.

3.2.2.2 Grane experiments

Grane oil was used for the last three experiments. These were also direct experiments, with no addition of any phase after the experiment started. The aim was to compare these experiments with the Primol 352 results, to see if the addition of surfactants makes the oils behavior similar. No surfactants were added to the Grane oil, and the mixture mass flow rate was kept constant during all three experiments. The only variable was the initial fractions of oil and salt water.

3.2.2.3 Flow loop calibration test

The accuracy of the pressure drop, and mixture mass flow rate readings had to be tested before starting the flow experiments. In order to achieve this, single phase salt water was flowed through the pipe, and the measured data was compared against theoretical values.

The pressure drop at four different mixture mass flow rates was used for the evaluation. The flow velocity could be calculated from the mixture mass flow rate ($\dot{m}$), by using $V = \frac{\dot{m}}{\rho \cdot A}$, where A is the flow area, and ρ is the density of salt water. The Reynolds number could then be calculated from the velocity, by using $Re = \frac{\rho \cdot V \cdot D}{\mu}$, where μ is the viscosity of salt water. The formula for pressure drop over a pipe was used to calculate a friction factor, based on the pressure drop (ΔP) readings: $f = \frac{2 \cdot \Delta P \cdot D}{\rho \cdot V^2 \cdot L}$, where D is the pipe diameter and L is the length between the pressure taps. Finally, a theoretical friction factor was calculated from Haalands formula, $\frac{1}{\sqrt{f}} = -1.8 log\left[\left(\frac{\epsilon/D}{3.7}\right)^{1.11} + \frac{6.9}{Re}\right]$, where ϵ is the pipe wall roughness.

Table 3-2 shows the calculated values, which resulted in two different friction factors; one based on the measured pressure drop and mixture mass flow rate (f), and one based on only the mixture mass flow rate (f Haaland). Since mixture mass flow rate is a common factor used, the two friction factors are presented as a function of flow velocity.

$\dot{m}$ [kg/s]	ΔP [Pa/m]	V [m/s]	Re [-]	f [-]	f Haaland [-]
0,31	470,00	0,78	17687,08	0,033	0,029
0,28	410,00	0,71	16189,15	0,035	0,030
0,25	350,00	0,64	14489,58	0,037	0,030
0,22	286,67	0,56	12818,81	0,039	0,031

Table 3-2 Friction factor calculations

Figure 3.2-4 shows the two friction factors as a function of flow velocity. The difference between the curves is not significant and this indicates precise reading equipment. This meant the experiments could be initiated.

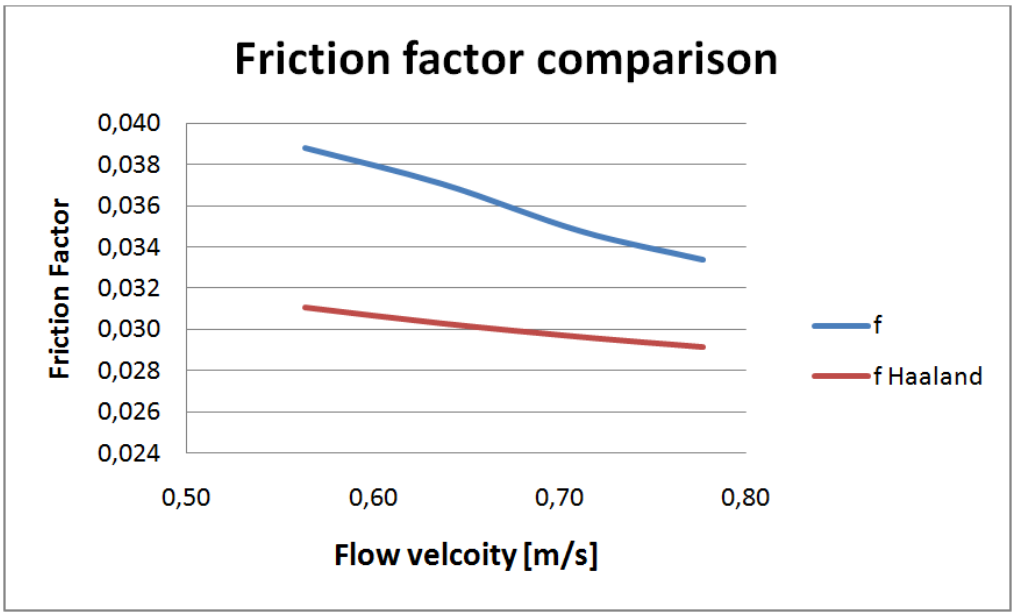

Figure 3.2-4 Friction factor evaluation

3.2.2.4 Turbulent vs. laminar flow

As mentioned earlier, the continuous phase affects the Reynolds number, since the dispersed phase is only present as isolated drops. All the experiments in this paper are water continuous flows, and were stopped immediately after phase inversion occurred. To ensure fully dispersed and turbulent flow, the lowest Reynolds number, based on the experiments, should be calculated. The lowest mixture velocity during the experiments is 0.48 m/s and can be seen in figure 4.2.8. The Reynolds number at this velocity and water continuous flow is $Re = \frac{\rho \cdot V \cdot D}{\mu} = \frac{1030 \cdot 0.48 \cdot 0.0221}{0.001} = 10926$. A flow is defined as turbulent for Re > 4000 and it can therefore safely be assumed that all the experiments conducted in this paper are under turbulent conditions.

3.3 Experimental reproducibility

To make sure that the experimental results could be used to investigate the mechanisms of phase inversion, the reproducibility of the conducted experiments was thoroughly tested through batch experiments.

7 experiments were conducted with Grane oil, under the same experimental conditions. The inversion times ranged from 13 to 17 minutes, with an average of 15.1 minutes. This meant that the maximum deviation from the average was 14%, which indicated a good reproducibility for the experiments conducted with Grane oil.

Since Primol 352 was used for a large fraction of the conducted experiments, reproducibility was also tested for this oil. 6 experiments were conducted, under the same experimental conditions and with the same surfactant concentration. The inversion times ranged from 14.5 to 18.5 minutes, with an average of 16.7 minutes. This gave a maximum deviation of 13% from the average, which also indicated a good reproducibility.

The reproducibility of the conducted flow experiments was difficult to confirm, due to insufficient amounts of Grane oil and surfactant. Emphasis was placed on achieving a phase inversion in a direct flow experiment, by using the model oil Primol 352 and regulating surfactant concentration.

3.4 Visual documentation on phase inversion

3.4.1 Microscopic documentation

Samples were taken from both batch and flow experiments and placed under a microscope for analysis. The samples were obtained with a hydrophobic plastic pipette. This made it possible to extract the internal oil phase exclusively, as this was the only phase attaching to the pipette. A droplet from this pipette was placed on a microscopic viewing plate and photographed. The equipment used was a Leica Wild M10 microscope with an 80x magnifier, and a PixeLINK 3.0Megapixel USB2.0 CMOS Camera.

3.4.2 Cryo ESEM Analysis

3.4.2.1 Cryogenics

Cryogenics is defined as "*-the branch of physics which deals with the production of very low temperatures, and their effect on matter*" [17]. Very low temperatures are here defined as below -150 °C, and cryogenic fluids with very low boiling points are used to obtain this temperature. Natural gases present in the atmosphere have a very low boiling point, and these gases liquidized are often used in the application of cryogenics. In this paper, liquid nitrogen was used to obtain cryogenic conditions.

3.4.2.2 Environmental Scanning Electron Microscopy (ESEM)

The ESEM is actually a modification of the regular Scanning electron Microscope (SEM). An electron microscope is a device which uses electrons to scan the surface of a given sample. The electrons are reflected with a certain intensity, energy and angle, depending on the molecular composition and the topography of the surface. This returning data is interpreted by a computer into a visual representation of the sample surface. By performing an elemental analysis with an Energy Dispersive X-ray Spectroscopy (EDS), the x-rays emitted by the sample matter, can be analyzed to accurately define the material composition of the sample [18]. This emitting is the result of the sample matter being hit by charged particles.

The SEM technology needs to operate under a vacuum, and this is where the ESEM differs from regular SEM. Water at lower pressure than 609 Pa is unable to maintain a liquid phase, and would therefore evaporate in the vacuum conditions of SEM. The pressured environment in ESEM avoids this evaporation, and allows the analysis of wet samples.

The ESEM operates with an ionic gas in the sample chamber which, in difference to SEM, avoids the formation of a negative electrical charge on/at the sample surface. This electrical charge comes from the electron beam used to analyze the sample. The beam also releases ions from the surrounding gas, which has a neutralizing effect [19].

Using a modified ESEM, (developed in the laboratory at Statoil Rotvoll, Trondheim), capable of operating under cryogenic conditions, opens the possibility of instantly freezing a sample from an unstable emulsion, and analyze the structural composition under static conditions.

3.4.2.3 Experimental procedure – Cryo ESEM analysis

In this paper, an experimental method for observing emulsion morphology has been attempted. As previously mentioned, an O/W emulsion is fairly unstable, and changes its morphology quite rapidly after being extruded from a stirred batch. In order to stop this rapid change, the samples had to be quickly introduced to a cryogenic environment. Immediately after being extracted from the batch by a wide pipette, the pipette was lowered into in a liquid nitrogen container at 77 K (-196 ˚C). The sample was then inserted into an electron microscope, designed for operating under cryogenic conditions.

Inside the microscope, the pipette was cut in half, revealing a surface of the sample. This surface, which was quite rough, was then subjected to an ESEM analysis. An attempt to polish the surface would most likely generate heat and damage the surface structure. This limitation makes it a bit more difficult to interpret the rendered image.

Figure 3.4-1 illustrates that only some of the drops are revealing a cross section. The other drops remain intact or completely fall out of their socket. This makes it difficult to accurately evaluate the phase areas on the sample surface, since a rough surface gives an inaccurate portrayal of the samples cross section.

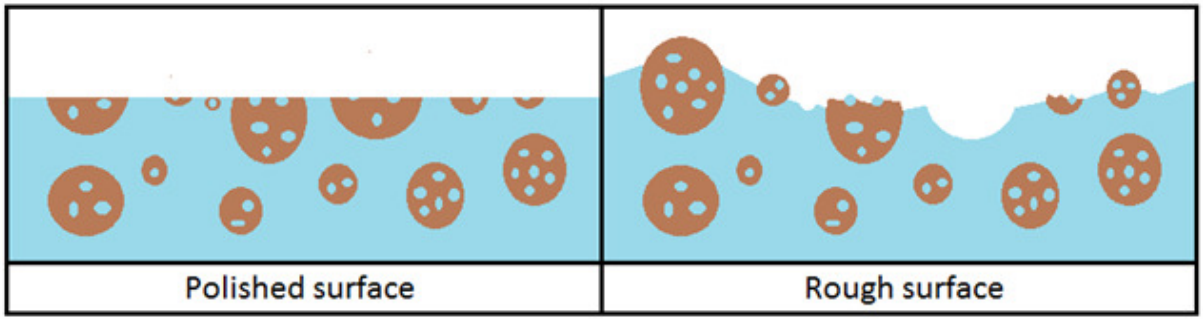

Figure 3.4-1- Cross section of an emulsion sample surface

The EDS elemental analysis will identify each phase and mark them with a color impression on the rendered image. This eliminates any risk of misinterpreting the emulsions phases.

4 Results

This chapter contains the obtained results from the experiments described in chapter 3. The first section describes the results from all the batch experiments, and the last section describes the results from the flow experiments. A brief summary is given at the end of each section.

4.1 Batch experiments

The batch experiments are divided into four different sections; the first series of Primol 352 experiments, the Exxsol D60 experiments, the Grane experiments, and the last series of Primol 352 experiments. This is the same order of which the experiments were conducted.

4.1.1 Primol 352 experiments (first series)

This section illustrates how the variation of surfactant (Arlacel P135) concentration influences the inversion time (the stirring time until phase inversion occurs). Stirring intensity was kept constant at 1500 rpm during all experiments.

Figure 4.1-1 shows the inversion times at 60 % oil fraction. The inversion times increase as the surfactant concentrations increases. Experiment 1-3 contains longer inversion times than experiment 4-6, but the influence of surfactant concentration is similar for all 6 experiments. Experiment 1-3 and 4-6 were conducted with oil-surfactant mixes from two different batches, which may help to explain the constant different between the two sets of experiments.

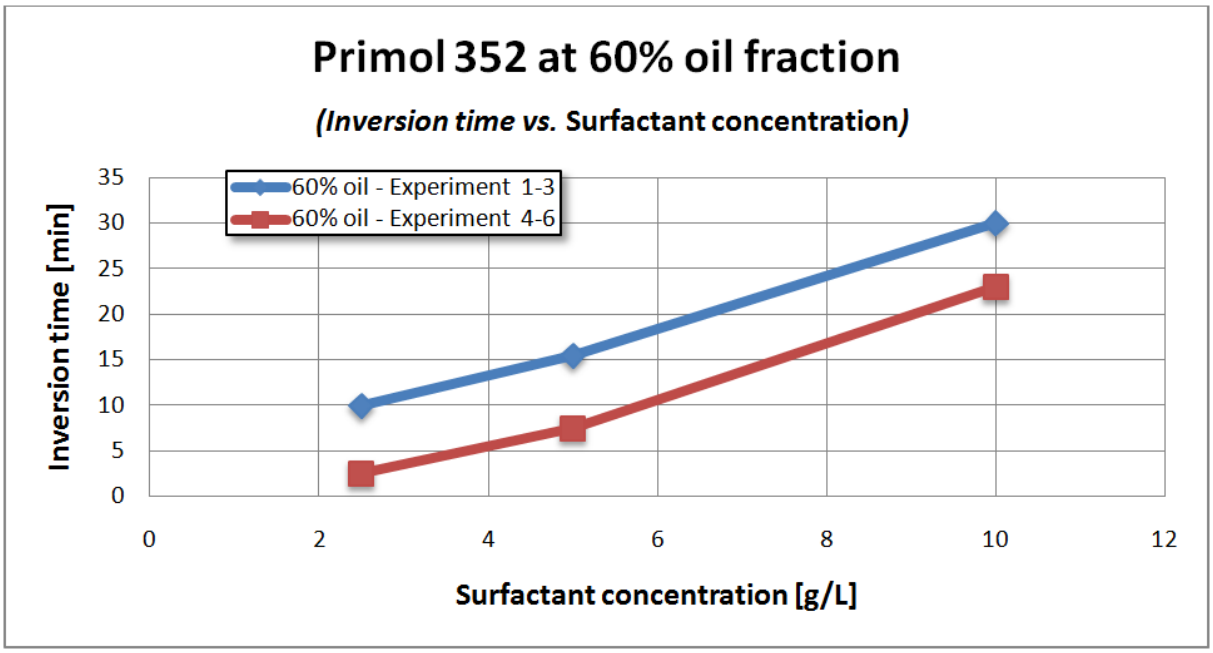

Figure 4.1-1 Inversion time vs. surfactant concentration for Primol 352 at 60% oil fraction

4.1.2 Exxsol D60 experiments

The Exxsol D60 experiments reveal the difference between the two surfactants used. Since the conductivity of oil is close to zero, the inversion times were determined when the conductivity readings drop to zero.

Figure 4.1-2 shows the inversion times at different oil fractions, using Arlacel P135 as a surfactant. As oil fraction increases, then inversion time decreases.

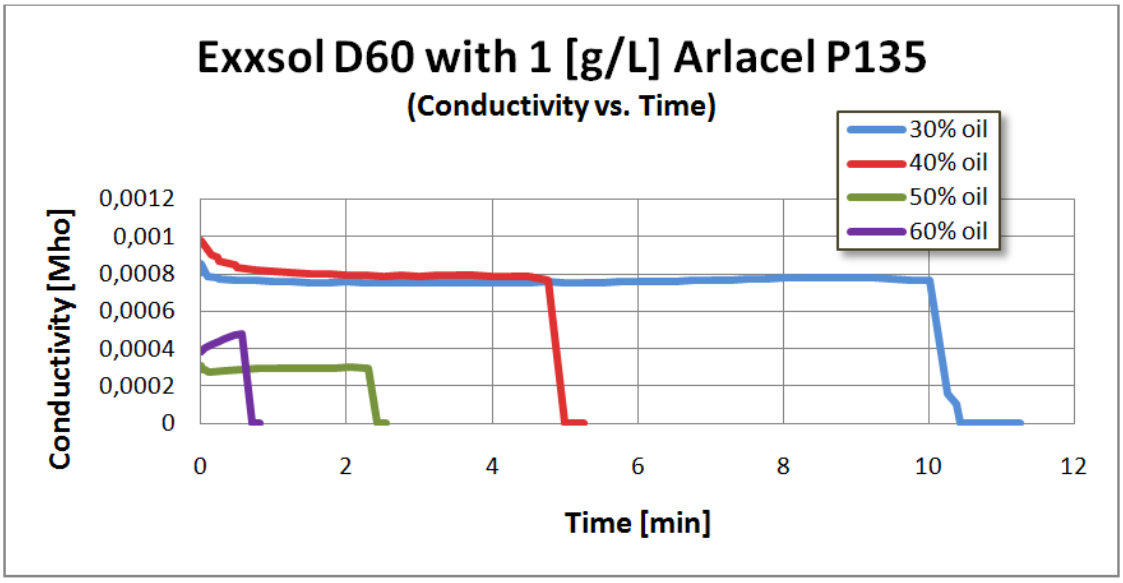

Figure 4.1-2 Conductivity vs. time for Exxsol D60 using Arlacel P135

Figure 4.1-3 shows the inversion times at different oil fractions, using Croda Atsurf 5000 as a surfactant. The trend is the same as with Arlacel P135; an increase in oil fraction leads to a decrease in inversion time. However, it is clear that for the same surfactant concentration, the inversion times are much longer when using Croda Atsurf 5000. At a 30 % oil fraction, phase inversion did not occur.

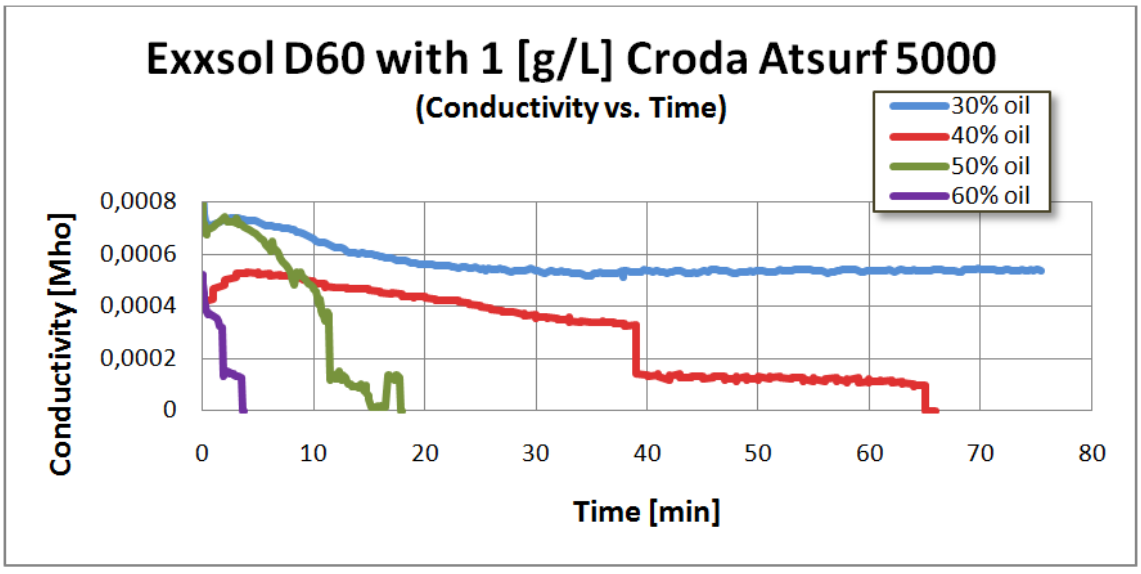

Figure 4.1-3 Conductivity vs. time for Exxsol D60 using Croda Atsurf 5000

4.1.3 Grane experiments

The results obtained from the Grane experiments give an impression of the behavior of crude oil. This section investigates the behavior of Grane oil at different phase factions.

Figure 4.1-4 shows the measured resistance in the batch as a function of time for 7 different experiments under the same conditions. The sudden jumps in resistance represent the occurrence of phase inversion. The results reveal a good reproducibility when Grane oil is used, and the variance in inversion time is low.

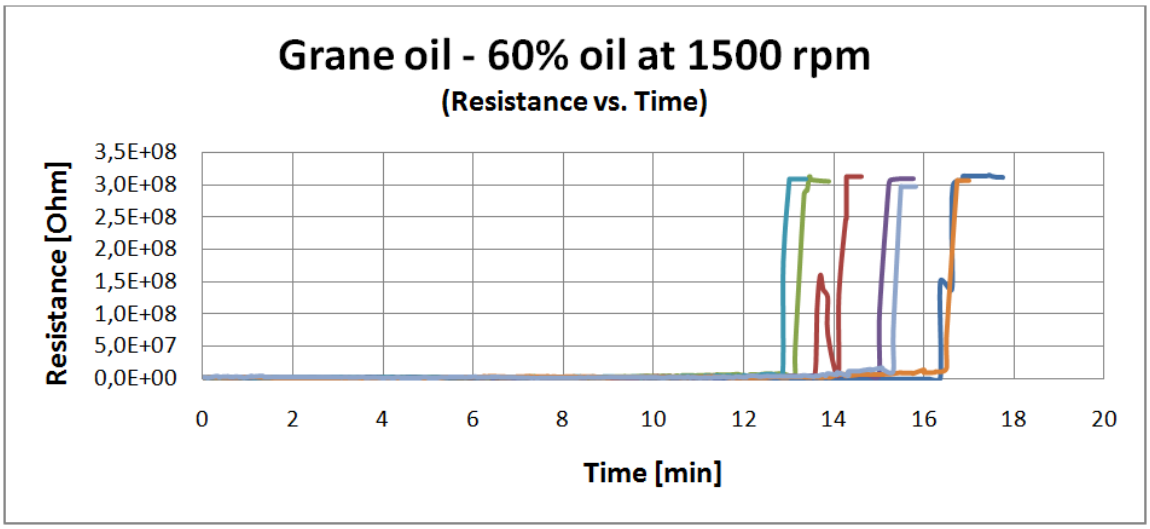

Figure 4.1-4 Resistance vs. time with 60% Grane at 1500 rpm

Figure4.1-5 shows the torque as a function of time. The inversion times are very coherent with the results from figure 4.1-4. However, it is worth noticing that the torque readings do not have the same initial value for all the experiments.

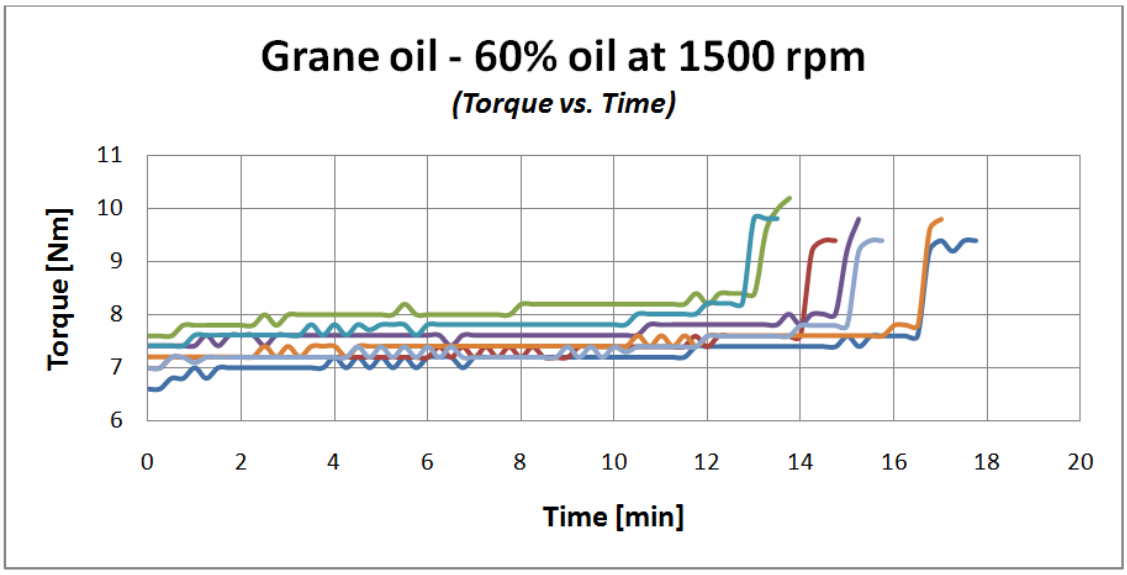

Figure 4.1-5 Torque vs. time with 60% Grane at 1500 rpm

Figure 4.1-6 shows the inversion time as a function of different stirring intensities. The curve illustrates a decrease in inversion time, as the stirring intensity increases. The experiments were repeated between 4 and 6 times for each condition.

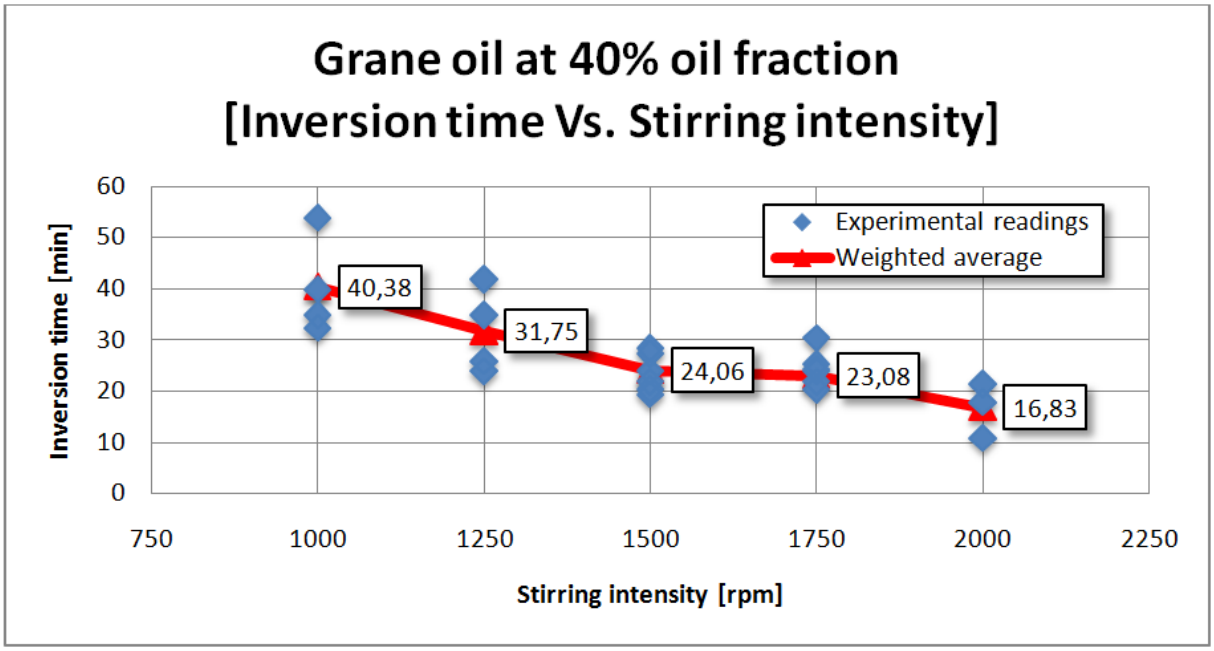

Figure 4.1-6 Inversion time vs. stirring intensity at 40% oil fraction

Table 4-1 shows the average inversion times at the different stirring intensities. It also shows the calculated maximum deviations from the average in percentage. The smallest deviations are found at 1500 and 1750 rpm. The average inversion time at these speeds are almost identical.

Stirring intensity [rpm]	Average time [min]	Maximum deviation below average [%]	Maximum deviation above average [%]
1000	40,38	13	34
1250	31,75	24	32
1500	24,06	15	18
1750	23,08	11	10
2000	16,83	35	28

Table 4-1 Average time and variation (40% Grane oil)

4.1.4 Primol 352 experiments (second series)

The inversion time results from the second series of Primol 352 experiments are presented as a function of surfactant (Arlacel P135) concentration and stirring intensity.

Figure 4.1-7 shows the inversion time as a function of surfactant concentration. The experiments were repeated between 3 and 6 times for each condition. As the surfactant concentration increases, the inversion time also increases.

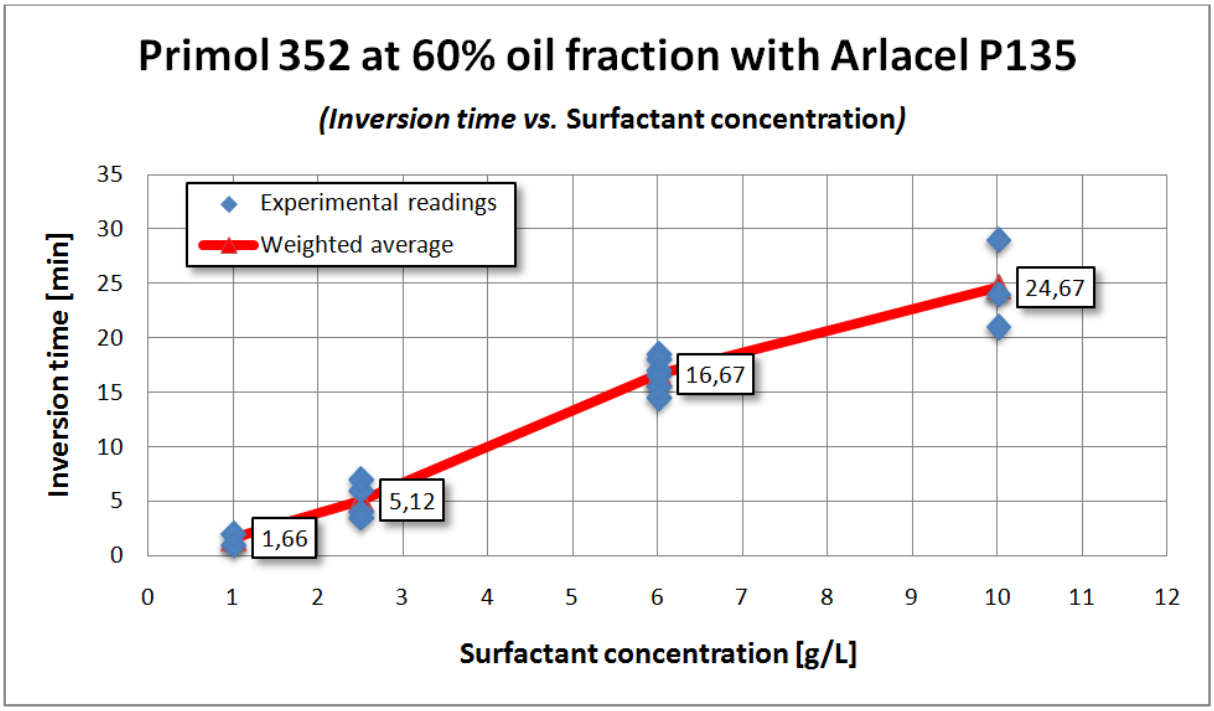

Figure 4.1-7 Inversion time vs. surfactant concentration at 60% oil fraction

Figure 4.1-8 shows the inversion time as a function of stirring intensity. As the stirring intensity increases, the inversion time decreases.

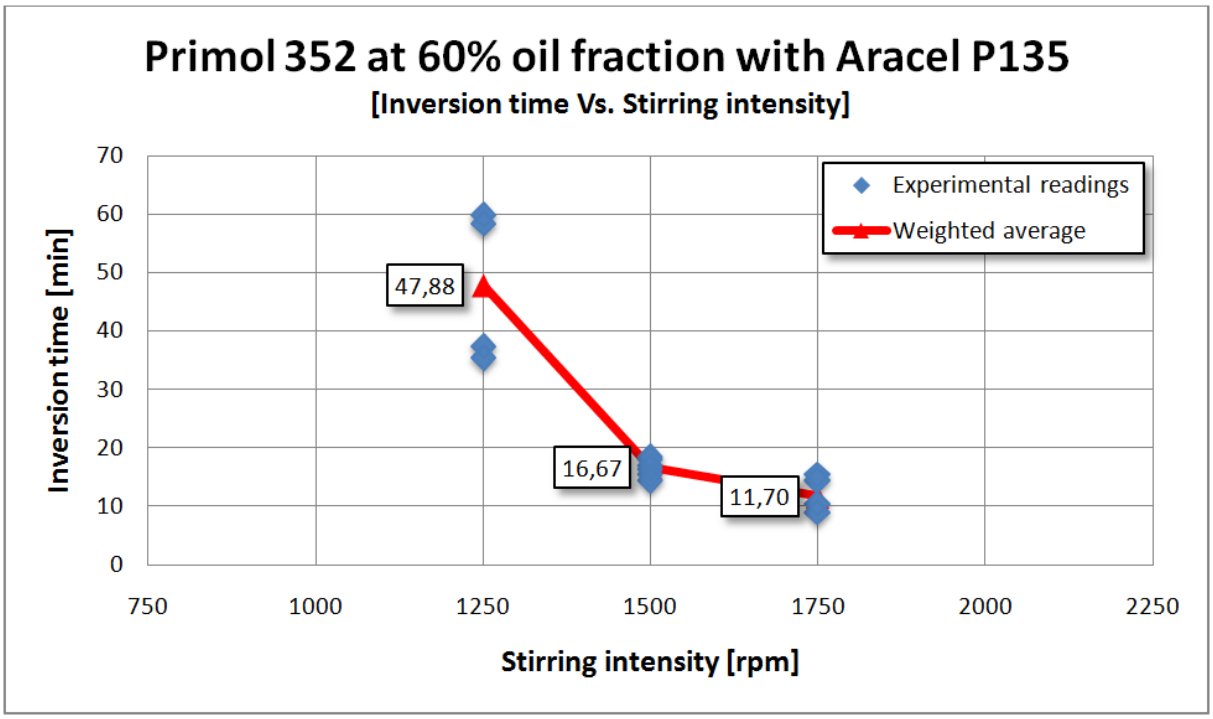

Figure 4.1-8 Inversion time vs. stirring intensity at 60% oil fraction

Table 4.1-2 shows the average inversion times at the different stirring intensities. The maximum deviations are also calculated in percentage from the average times. The largest deviations occur at the lowest stirring intensity (1250 rpm). The smallest deviations occur at a stirring intensity of 1500 rpm.

Stirring intensity [rpm]	Average time [min]	Maximum deviation below average [%]	Maximum deviation above average [%]
1250	47,88	34,87	25,31
1500	16,67	14,97	10,98
1750	11,70	30,00	32,48

Table 4-2 Average time and variation (60% Primol 352)

4.1.5 Summary of the results from batch experiments

The results from the first Primol 352 experiments show that, in general, increasing the surfactant concentration leads to a longer inversion time.

The Exxsol D60 experiments investigate the influence two different surfactants (Arlacel P135 and Croda Atsurf 5000) have on inversion time, at different oil fractions (30, 40, 50 and 60%). The concentrations of the two surfactants were held constant in all the experiments. The results reveal that the inversion time is longer at all oil fractions when using Croda Atsurf 5000 instead of Arlacel P135.

The Grane experiments investigate crude oil behavior at different oil fractions and stirring intensities. The inversion times are considerably shorter at 60% oil fraction than at 40% oil fraction. At 40% oil fraction the different stirring intensities reveal a clear pattern; the inversion time decrease as the stirring intensity increase. At 2000 rpm and 40% oil fraction, the inversion time is approximately the same as for 1500 rpm and 60% oil fraction.

The second Primol 352 experiments investigate the effect different surfactant concentrations (using Arlacel P135) and stirring intensities have on the inversion time. A 60% oil fraction was used during all the experiments. The results show that the inversion time increases as surfactant concentrations increases. They also show that the inversion time decreases as stirring intensity increases. At 1500 rpm and a surfactant concentration of 6 g/L the inversion time is approximately the same as for Grane oil, using the same stirring intensity and oil fraction.

4.2 Flow experiments

The results from the flow experiments will be presented in three different sections. The first section shows the results from experiments with Primol 352 and the surfactant Arlacel P135, while the second section shows the results using the surfactant Croda Atsurf 5000 in Primol 352. The last section shows the results from experiments conducted with Grane oil. The pressure drop curves are showed first in each section, followed by the corresponding chord length curves.

4.2.1 Primol 352 experiments

4.2.1.1 Arlacel P135

The first flow experiments were conducted based on the results from the batch experiments. It was evident from the batch experiments that phase inversion occurred faster at low surfactant concentrations, so this was also assumed in the initial flow experiments. The following curves show some of the result from the experiments with Arlacel P135.

Figure 4.2-1 shows an attempt to reach phase inversion with 1 g/L of surfactant. The left side axis shows the pressure drop over the pipe, while the right side axis shows the pressure drop over the pump. The initial fluctuations are the result of the oil and water mixing, before a water continuous phase is established. The sudden changes in pressure drop are the result of increased/decreased mixture mass flow rate and addition to the oil phase towards the end of the experiment (close to 80% oil when the experiment ended). The pump was initially working at 60% capacity, and with a 69% oil phase the mixture mass flow rate was approximately 0.28 kg/s, which gives a flow velocity of approximately 0.78 m/s. The experiment lasted for 330 minutes and no phase inversion occurred.

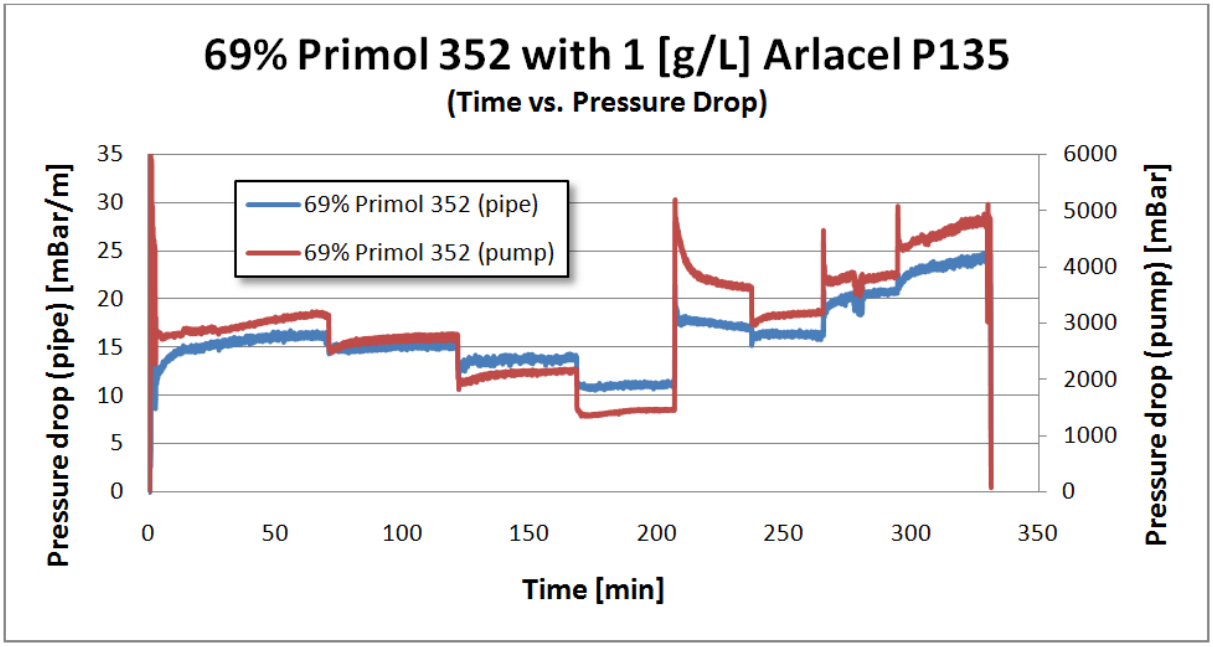

Figure 4.2-1 Pressure drop vs. time for 69% Primol 352 with 1 g/L Arlacel P135

The cord length distribution in the oil-water mixture was measured throughout the flow experiments, in an attempt to reach a better understanding of the morphology and structure in the flow leading up to the phase inversion. A large variety of chord lengths were monitored, but focus was placed on illustrating the changes in the root mean squared (RMS) chord length, and the count of small chord lengths (< 10 µm) per second, as these two readings gave the best indication on important changes in morphology. This will be further discussed in section 5.4. These readings were extracted from the log files, presented in appendix B, and they give a visual impression of changes in droplet distribution.

Figure 4.2-2 shows the cord length readings from the same experiment as figure 4.2-1. The left side axis shows the counts per second of small chord lengths (brown curves), while the right side axis shows the RMS chord length in microns (blue curves). The original readings had large fluctuations, so bold lines showing the moving average values were added, in order to easier identify the chord length development.

During the first 70 minutes the velocity is kept constant at 0.78 m/s, but still the RMS and small chord length count are unstable. Both readings experience a significant fall around 38 minutes, although there was no significant change in the operational conditions around that time.

After 70, 120, 166 and 236 minutes the flow velocities are reduced and the same pattern can be seen for the first three cases; the small chord length increases while the RMS chord length decreases, before receding after a few minutes. At 236 minutes, both curves increase before slowly receding.

After 205 minutes, the velocity is increased to 0.83 m/s, and the opposite trend can be seen as the small chord length count decrease, and the RMS chord length increase.

The decrease in both values which is apparent around 260 minutes is coherent with the addition of 1.5 liters extra oil, which happened at the same time.

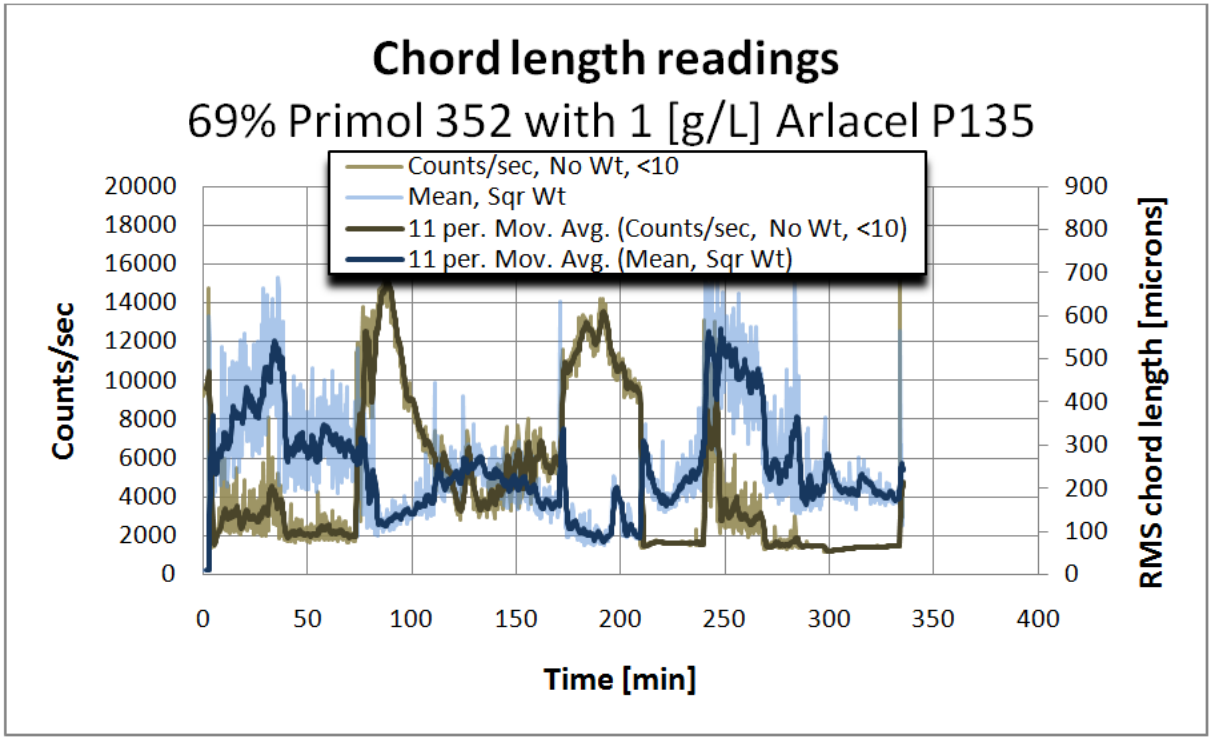

Figure 4.2-2 Chord length readings for 69% Primol 352 with 1 g/L Arlacel P135

Figure 4.2-3 shows an experiment with the same initial conditions as the one in Figure 4.2-1. Phase fractions, mixture mass flow rate and temperature were the same, but the surfactant concentration was increased to 4 g/L. After about 2 minutes of stable water continuous flow, phase inversion occurred. The figure indicates that the inversion occurred over the pump, and not inside the pipe. This is evident in the delay in pressure variations in the measured pressure over the pipe. The pump did not have the capacity to run an oil continuous flow, so it had to be shut down after the inversion, at 4.5 minutes.

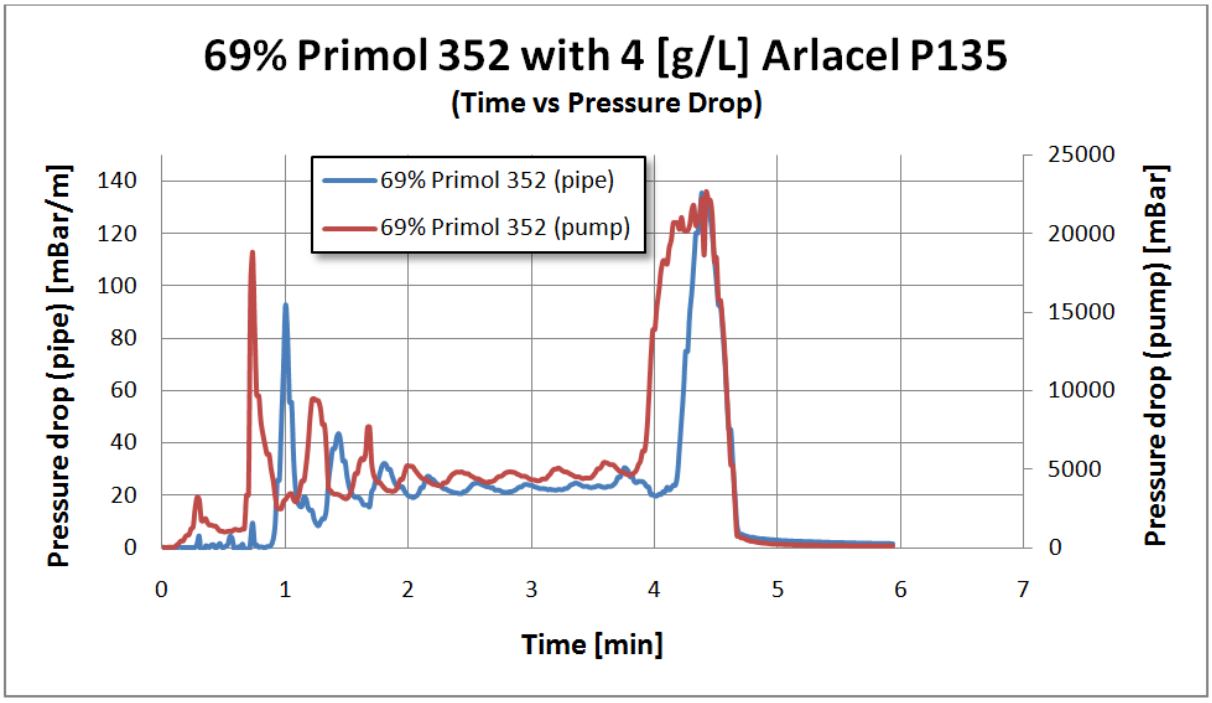

Figure 4.2-3 Pressure drop vs. time for 69% Primol 352 with 4 g/L Arlacel P135

Figure 4.2-4 shows the corresponding chord length curve. The pressure readings in figure 4.2-3 show that the phase inversion occurred after approximately 4 minutes, and the cord length distribution also clearly shows a change at this time. The small chord length count increases remarkably, and peaks at around 3 times its original value, and then drops down again. The RMS chord length shows a stable increase, not showing any signs of receding after the inversion.

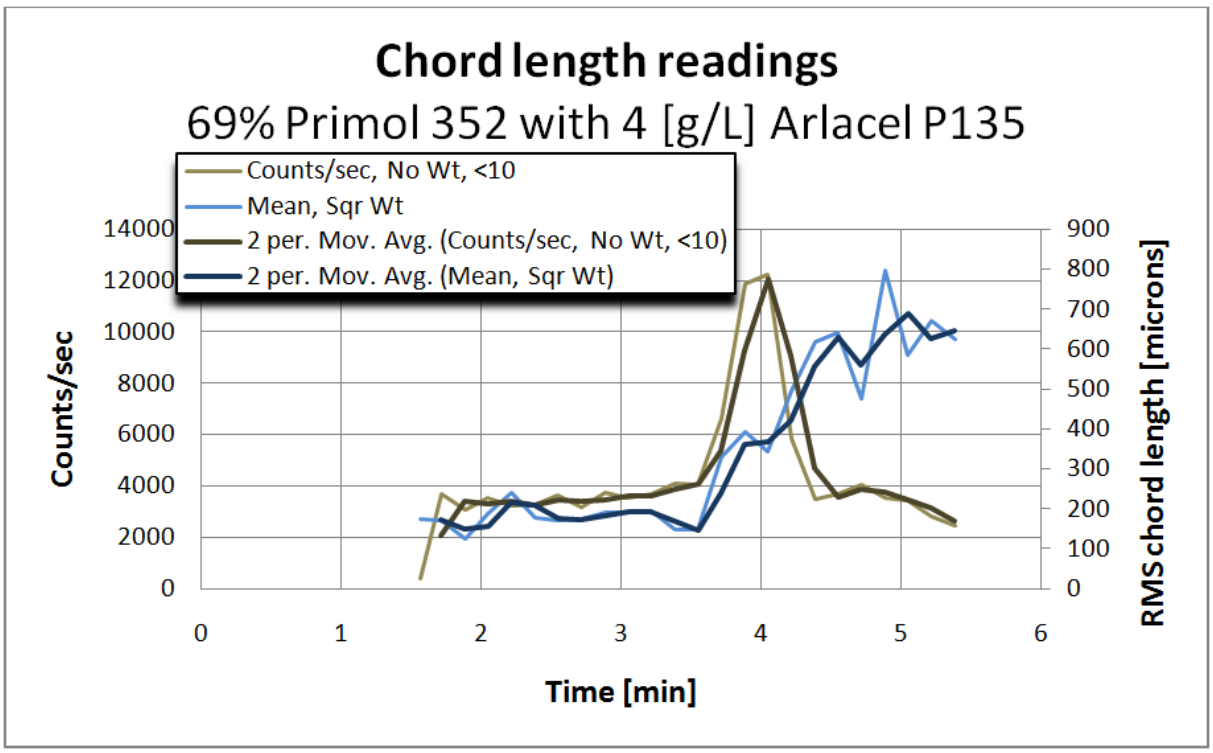

Figure 4.2-4 Chord length readings for 69% Primol 352 with 4 g/L Arlacel P135

4.2.1.2 With Croda Atsurf 5000

After phase inversion occurred, using Arlacel P135, experiments using Croda Atsurf 5000 were initiated. This section shows attempts of reaching phase inversion with the same phase fractions used in section 4.2.1.1, but this time at different surfactant concentrations.

Figure 4.2-5 shows the pressure drop curves for the first Croda Atsurf 5000 experiment. The sudden drop after 82 minutes was the result of a decrease the flow velocity from 0.63 m/s to 0.54 m/s which had to be done to stay within the allowed operational conditions of the pump. The same surfactant concentration at which phase inversion occurred with Arlacel P135 was used. No transition from O/W to W/O was observed. The gradual increase in pressure drop exceeded the pump capacity and the experiment had to be stopped after 160 minutes. It is possible to observe that the pressure drop was still increasing which might indicate that the inversion could have occurred. An increasing pressure drop indicates that the viscosity of the emulsion is increasing. This increase may be explained from oil drops coalescing to larger drops and encapsulating water from the continuous phase.

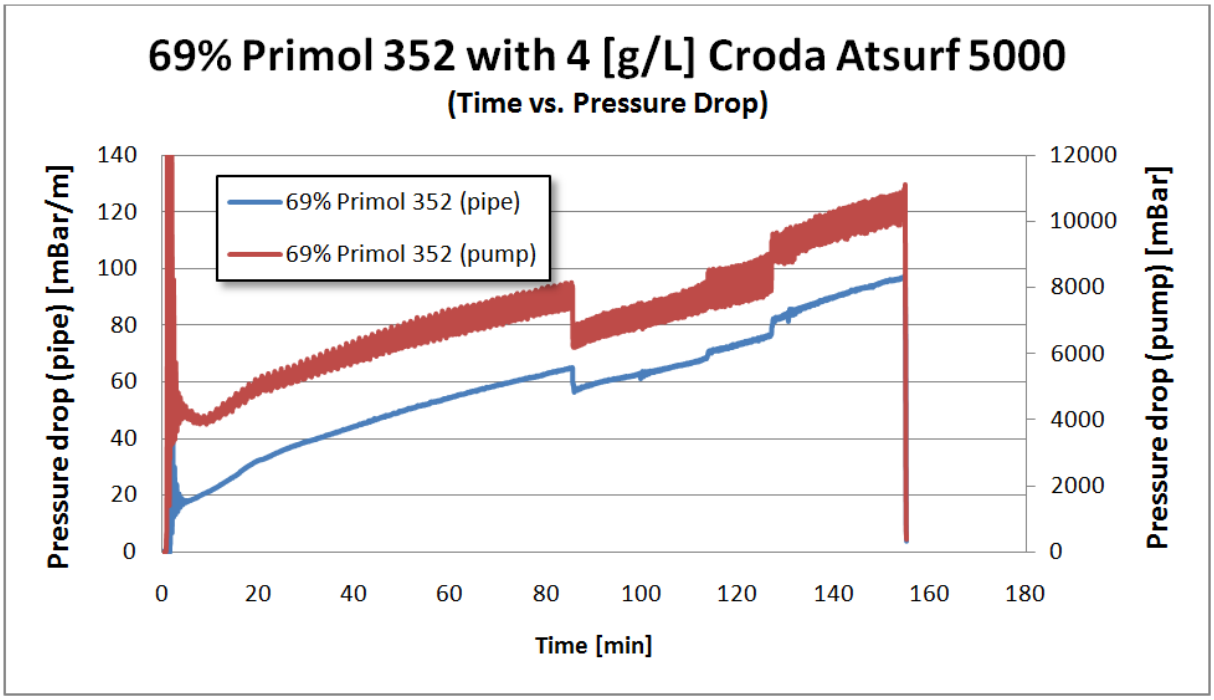

Figure 4.2-5 Pressure drop vs. time for 69% Primol with 4 g/L Croda Atsurf 5000

Figure 4.2-6 shows the corresponding chord length curve. In contrast to the results shown in figure 4.2-2, the decrease in velocity from 0.63 m/s to 0.54 m/s does not result in a sudden change in the cord length distribution around this time, even though a constant change in the pressure drop was experienced during this experiment (see figure 4.2-5).

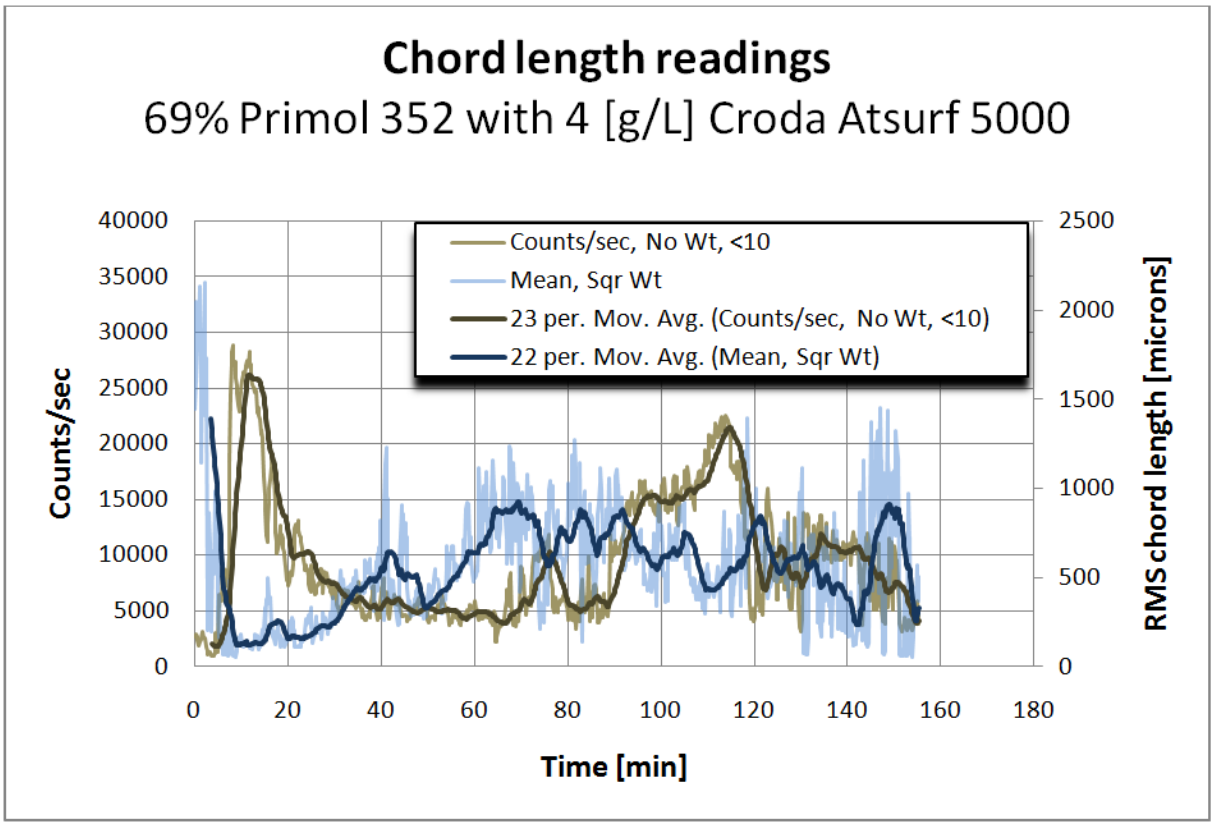

Figure 4.2-6 Chord length readings for 69% Primol 352 with 4 g/L Croda Atsurf 5000

Figure 4.2-7 shows the pressure drop curves for the second experiment using Croda Atsurf 5000. From the Arlacel P135 experiments, it was found that an increase in surfactant concentration leads to phase inversion. In this experiment, the surfactant concentration was almost doubled, but phase inversion did not occur. The sudden changes in the pressure drop curves are the result of changing mixture velocities.

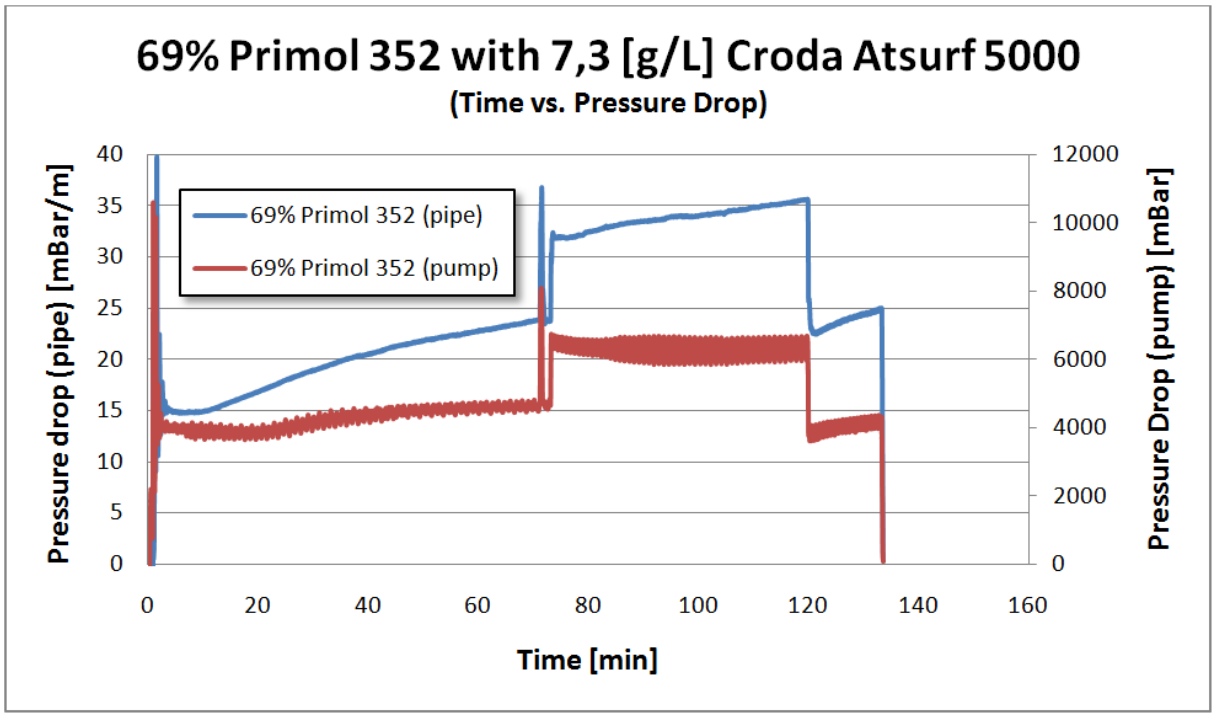

Figure 4.2-7 Pressure drop vs. time for 69% Primol 352 with 7.3 g/L Croda Atsurf 5000

Figure 4.2-8 shows the corresponding chord length distribution. With more surfactant distributed in the oil, the count of small chord lengths increase greatly and the mean count decreases. The readings seem to stabilize, and when the mixture velocity is increased from 0.54 m/s to 0.71 m/s after 72 minutes, the small chord length count decrease gradually, and the RMS chord length increases. The sudden drop in RMS chord length and the stabilizing of small chord length count around 100 minutes happens, without any changes in operational conditions. After 118 minutes, the mixture velocity is reduced to 0.48 m/s and the RMS chord length jumps, but immediately drops back down.

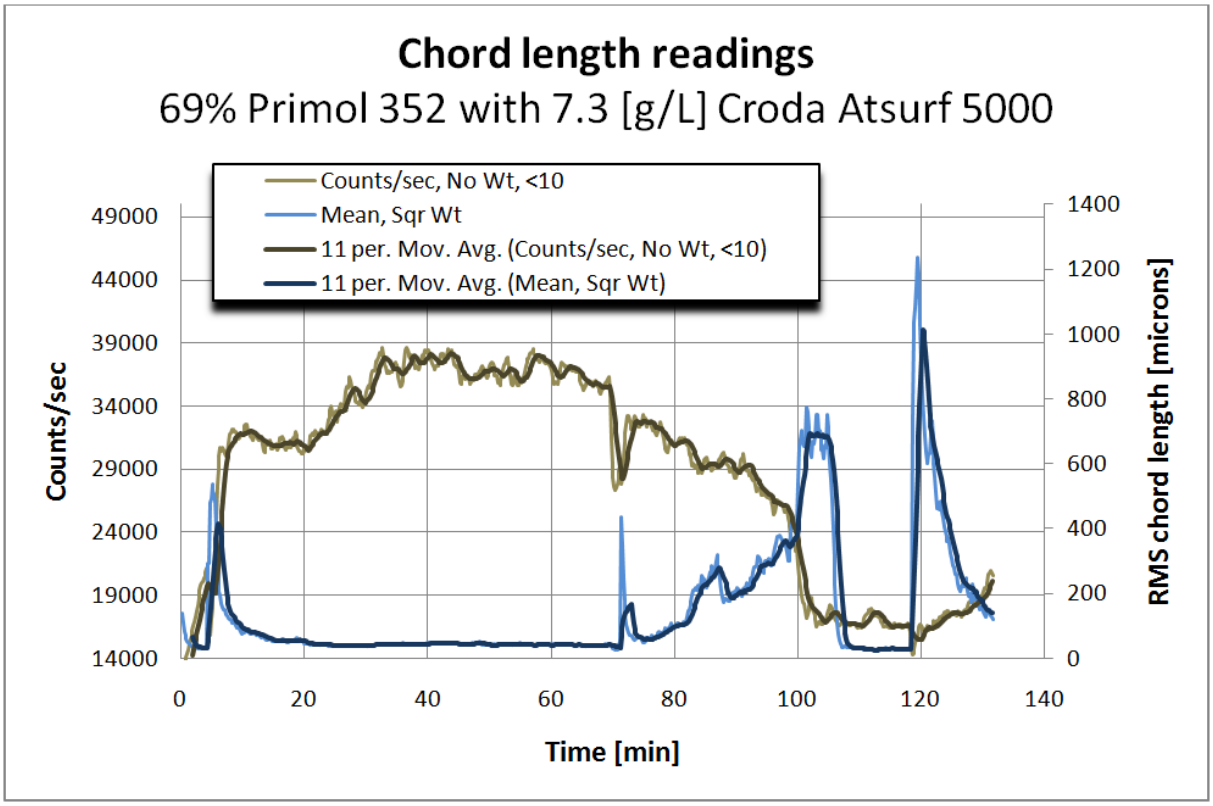

Figure 4.2-8 Chord length readings for 69% Primol 352 with 7.3 g/L Croda Atsurf 5000

Figure 4.2-9 shows the pressure drop curves for the third experiment using Croda Atsurf 5000. In this experiment the surfactant concentration was close to half the concentration used in the first experiment. Similar to when the concentration was doubled, phase inversion did not occur.

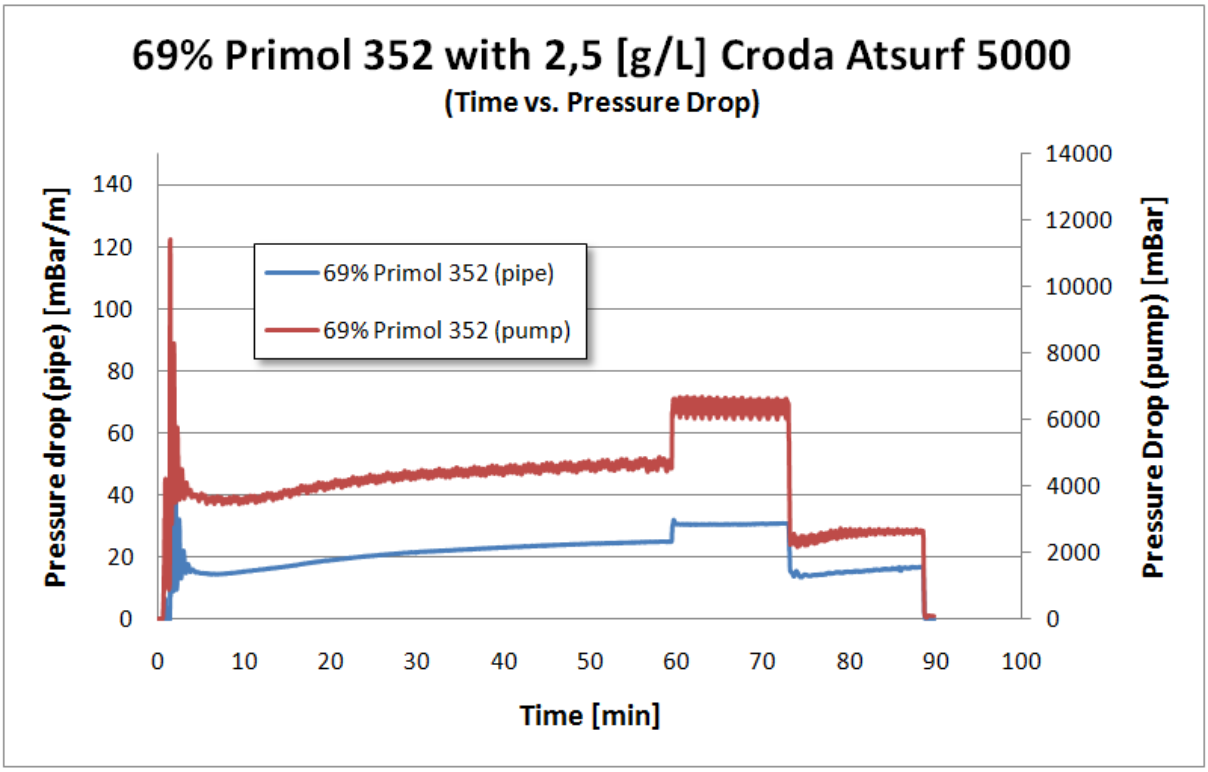

Figure 4.2-9 Pressure drop vs. time for 69% Primol 352 with 2.5 g/L Croda Atsurf 5000

4.2.2 Grane experiments

Three different experiments were conducted at a constant pump power using Grane oil with no surfactant added. The only changing parameter for these experiments was the phase fraction.

Figure 4.2-10 shows the pressure drop curves for the first Grane experiment. The phase fractions are identical to the fractions used when phase inversion occurred in the last Arlacel P135 experiment (69% oil and 31% salt water). After about 8 minutes, the flow inverted from O/W to W/O. It seems that phase inversion happens simultaneously in the pipe and over the pump, which can be seen from the figure. The flow stops fluctuating at a mixture velocity of 0.84 m/s and slowly decreases down to 0.72 m/s where the phase inversion occurs.

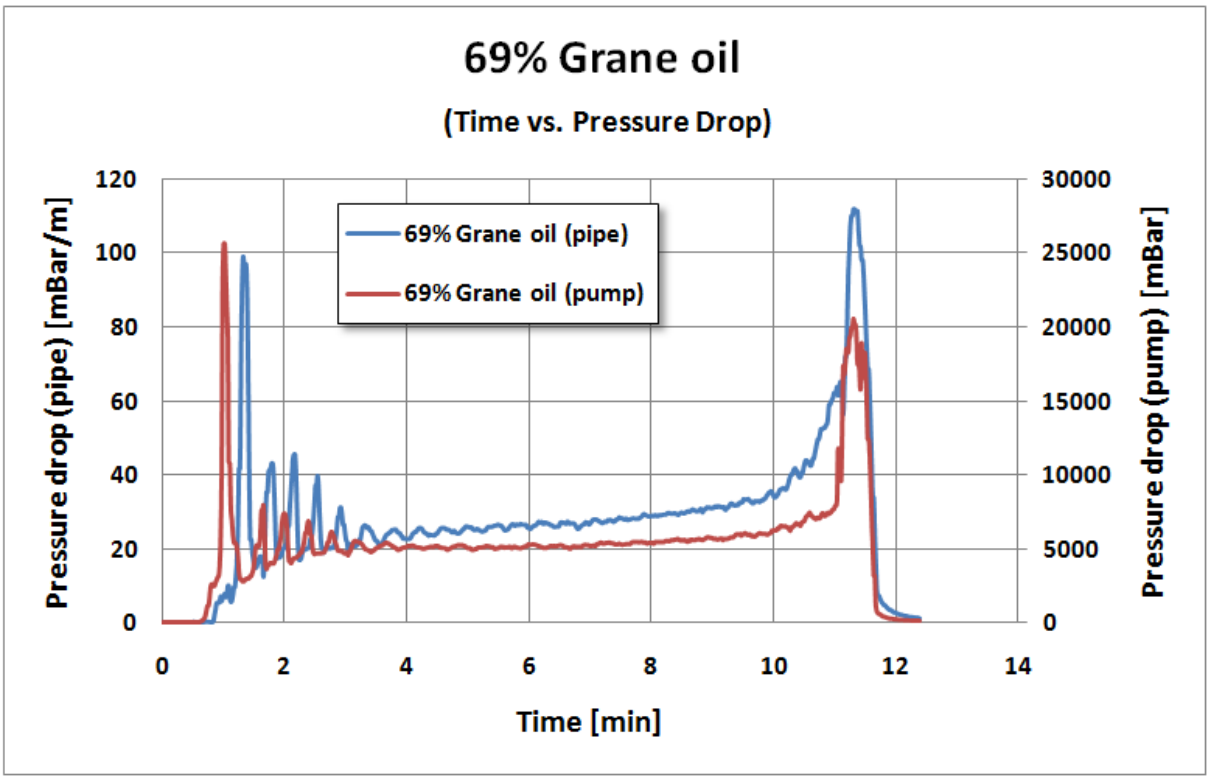

Figure 4.2-10 Pressure drop vs. time for 69% Grane oil

Figure 4.2-11 shows the chord length readings for the 69 % Grane experiment. It shows that the chord length count stabilizes after approximately 4 minutes, although minor fluctuations are present throughout the experiment. The RMS chord length increases around 10 minutes, and then suddenly drops around 11 minutes, before jumping up again at 12 minutes. The small chord length count starts a slight increase at 10 minutes. This increase continues up to 12 minutes and drops down simultaneously as the RMS chord length increases. Based on pressure drop readings from figure J, the inversion occurs around 11.5 minutes.

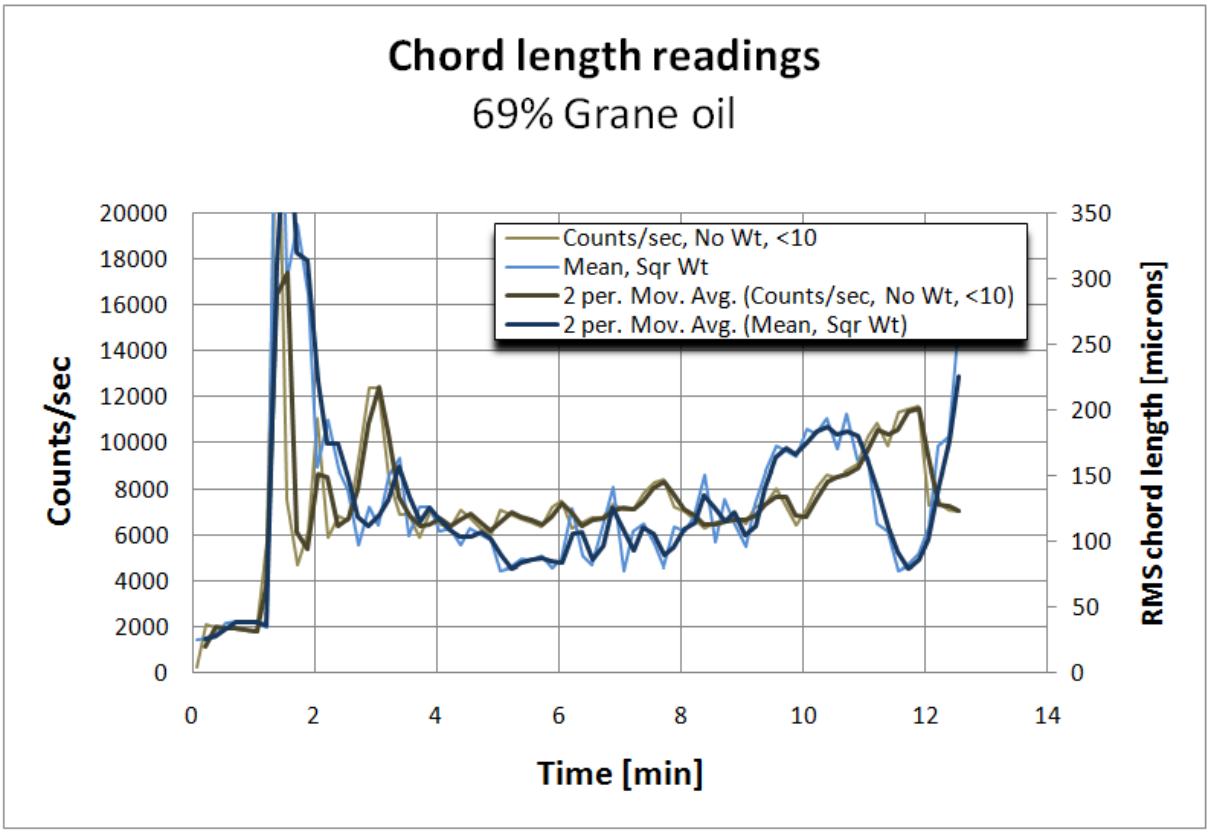

Figure 4.2-11 Chord length readings for 69% Grane oil

Figure 4.2-12 shows the pressure drop curves for the second Grane experiment. In this experiment, the oil fraction was reduced to 62.5 %, and the inversion occurred after 17 minutes of water continuous flow. From Figure 4.2-7 it appears that phase inversion happens simultaneously over the pump and in the pipe, but due to the long time interval, the log file has to be interpreted to obtain the exact result. The log file can be found in the appendix, and reveals that phase inversion occur over the pump first, then about 15 seconds later in the pipe. The mixture velocity begins at 0.81 m/s and slowly decreases until it reaches 0.74 m/s after approximately 5.5 minutes. This mixture velocity remains stable until phase inversion occurs.

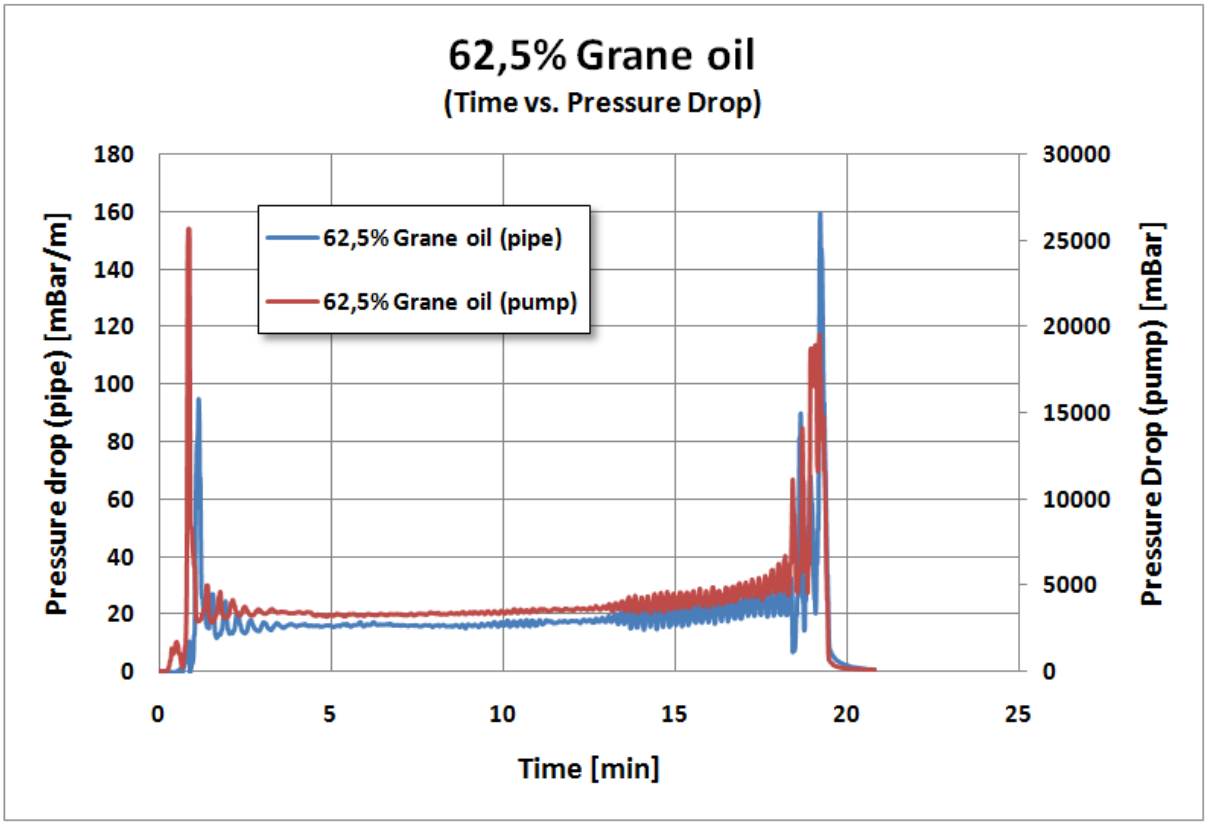

Figure 4.2-12 Pressure drop vs. time for 62.5% Grane oil

Figure 4.2-13 shows the chord length readings for the 62.5 % Grane experiment. The inversion time increased, as the oil cut was reduced. Both the RMS chord length and the small cord length count varied throughout the experiment, but when compared to the pressure drop changes shown in figure 4.2-12, it can be seen that the chord length distribution developed the same way around the inversion (at 18.5 minutes) as the previous Grane experiment. The small chord length count increased continuously from 10 minutes and then rapidly dropped down after 19.5 minutes. The RMS chord length was very unstable, but decreased in value around 18.5 min, and jumped simultaneously as the small chord length count fell.

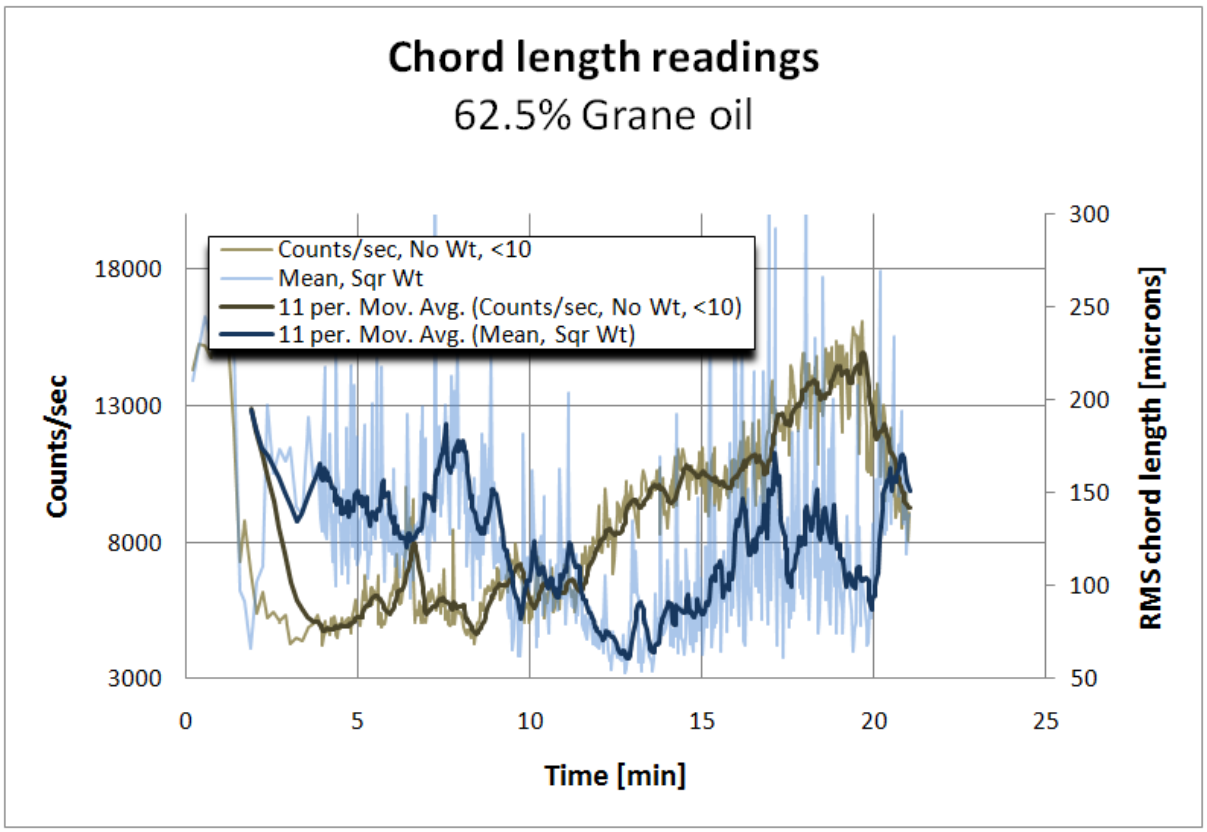

Figure 4.2-13 Chord length readings for 62.5% Grane oil

Figure 4.2-14 shows the pressure drop curves for the third Grane experiment. The oil fraction was reduced further down to 50 %. This resulted in a water continuous flow which lasted for about an hour before the inversion occurred. The log file in the appendix reveals that the inversion happened with only a few seconds in time difference. The mixture velocity starts at 0.79 m/s and decreases until it reaches 0.72 m/s after approximately 7.5 minutes. The mixture velocity remains stable at 0.72 m/s until phase inversion is reached.

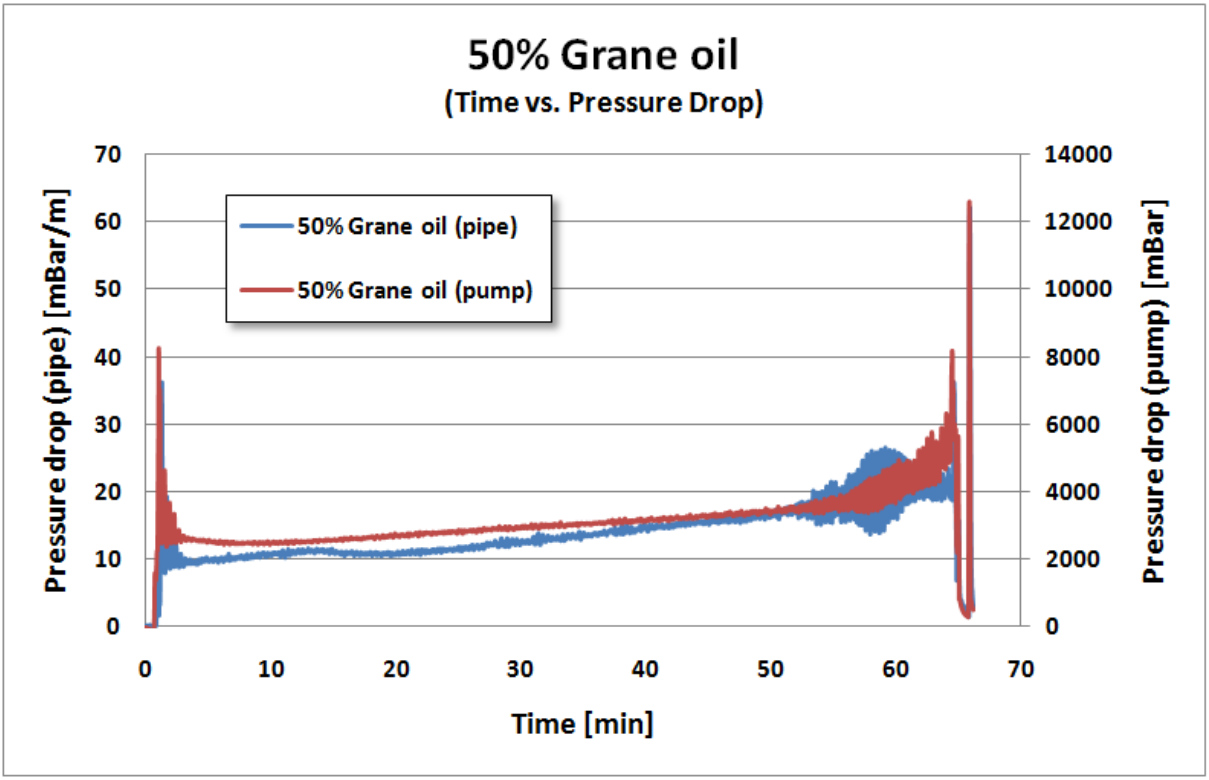

Figure 4.2-14 Pressure drop vs. time for 50% Grane oil

Figure 4.2-15 shows the chord length readings for the 50 % Grane experiment. The phase inversion occurs around 65 minutes, and the same development as in the two previous Grane experiments can be seen. The small chord length count decreased in value, while the RMS chord length increased.

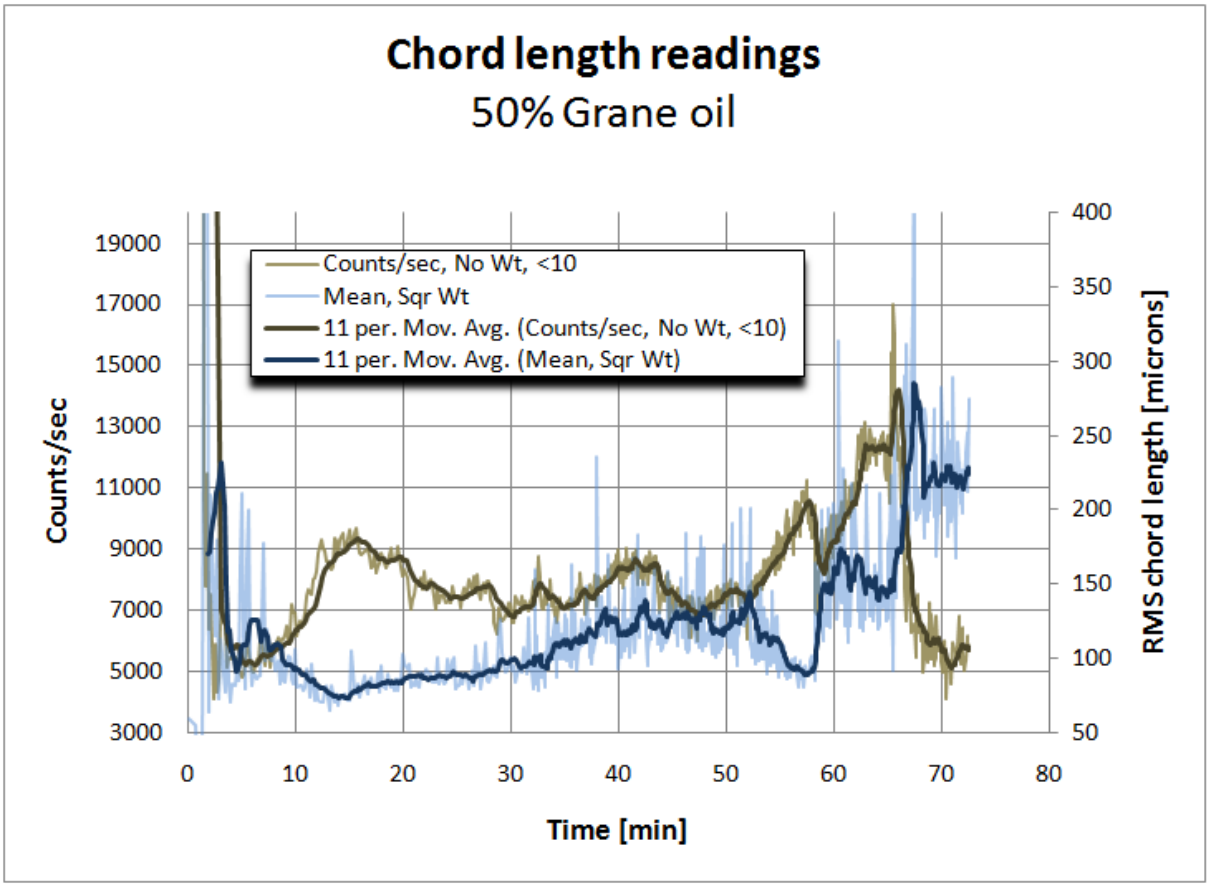

Figure 4.2-15 Chord length readings for 50% Grane oil

4.2.3 Summary of the results from flow experiments

The Primol 352 experiments were used to investigate the conditions needed for phase inversion to occur during direct flow experiments, using Arlacel P135 as a surfactant. The regulation of the mixture mass flow rate and oil fraction did not give the desired result, when using a surfactant concentration of 1 g/L. However, after increasing the surfactant concentration to 4 g/L, phase inversion occurred after about 2 minutes of stable water continuous flow. Interpretation of the pressure drop curve indicates that the inversion took place over the pump, and not inside the pipe. An oil fraction of 69% was used during all the experiments.

The Primol 352 experiments using Croda Atsurf 5000 were an attempt to obtain the same result as with Arlacel P135, at the same mixture mass flow rate and oil fraction. Surfactant concentrations of 2.5, 4 and 7.3 g/L were used, but phase inversion did not occur. The changes in pressure drop were much higher at 4 g/L than at the two other concentrations, but the experiment was stopped, due to insufficient pump capacity. This is the same surfactant concentration at which phase inversion occurred, using Arlacel P135.

The Grane experiments investigated phase inversion using crude oil with no added surfactant. Direct flow experiments were conducted at 50, 62.5, and 69% oil fractions, and at constant mixture mass flow rate. Phase inversion occurred at all three fractions after 62, 17 and 8 minutes respectively, of water continuous flow.

During the pressure drop increase right before the inversion, the count of small chord length (<10 µm) increases, while the RMS chord length decreases. As phase inversion occurs, this development also inverts, and the small chord length count falls down, simultaneously as the RMS chord length jumps up.

Increasing/decreasing the flow speed of the mixture has a temporarily effect on the chord length readings, but stabilizes after some time.

4.3 Visual comparison of droplet development

4.3.1 Pictures taken with a microscope

The pictures below were taken from samples obtained from both batch experiments and flow experiments, and show the morphological development in the dispersed oil phase. The pipette used to obtain the samples was hydrophobic. This made it possible to extract a sample from the dispersed oil phase alone. The oil attached itself to the pipette, while the water ran right off. The water present in these pictures is therefore droplets encapsulated by the dispersed oil.

The first four pictures are from samples taken from a batch experiment conducted with an oil (Grane) fraction of 0.4 and stirring intensity at 750 rpm. Phase inversion occurred after 111 minutes.

Micrograph 4.3-1 was taken of a sample obtained at the beginning (2 minutes) of the experiment, and shows that only a small amount of water has been encapsulated by the oil. Only a few droplets are visible, and the oil is almost single phase.

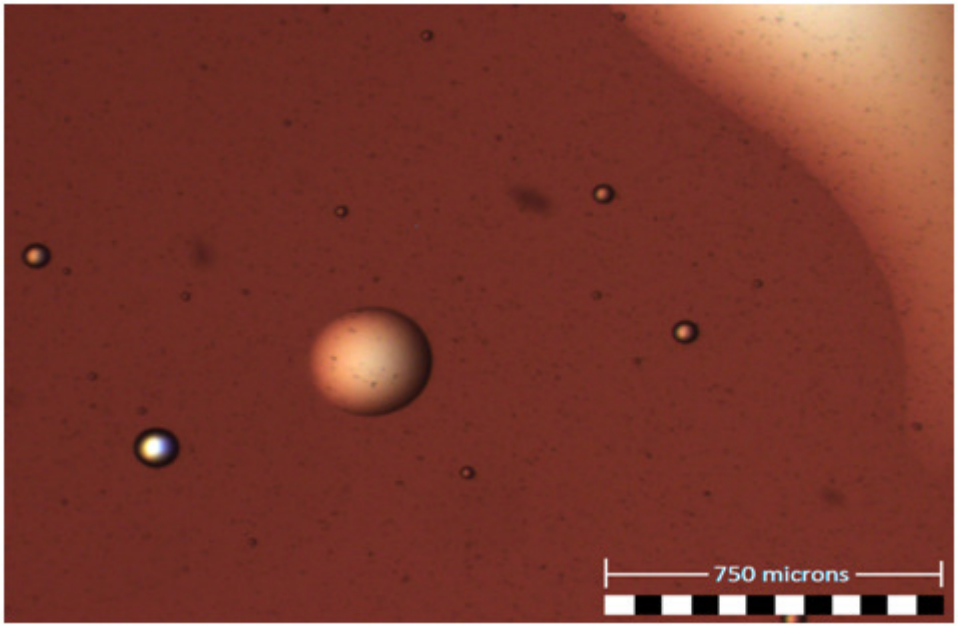

Micrograph 4.3-1 Dispersed phase - Batch experiment after 2 minutes

Micrograph 4.3-2 was taken approximately 30 minutes into the experiment. The oil has encapsulated a larger fraction of water, and the amount of droplets has increased. The droplets vary in size from the smallest being only a few microns in diameter to the largest being around 200 microns in diameter.

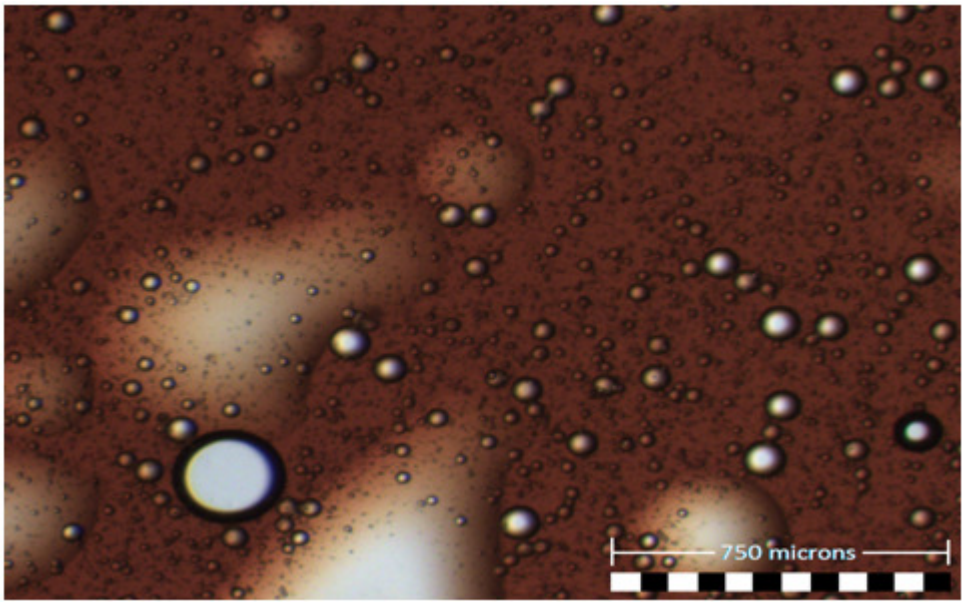

Micrograph 4.3-2 Dispersed phase - Batch experiment after 30 minutes

Micrograph 4.3-3 shows a sample taken 65 minutes into the experiment. The sample got darker as the amount of captured droplets increased. It appears as if the distribution in droplet size is similar to the one observed in micrograph 4.3-2.

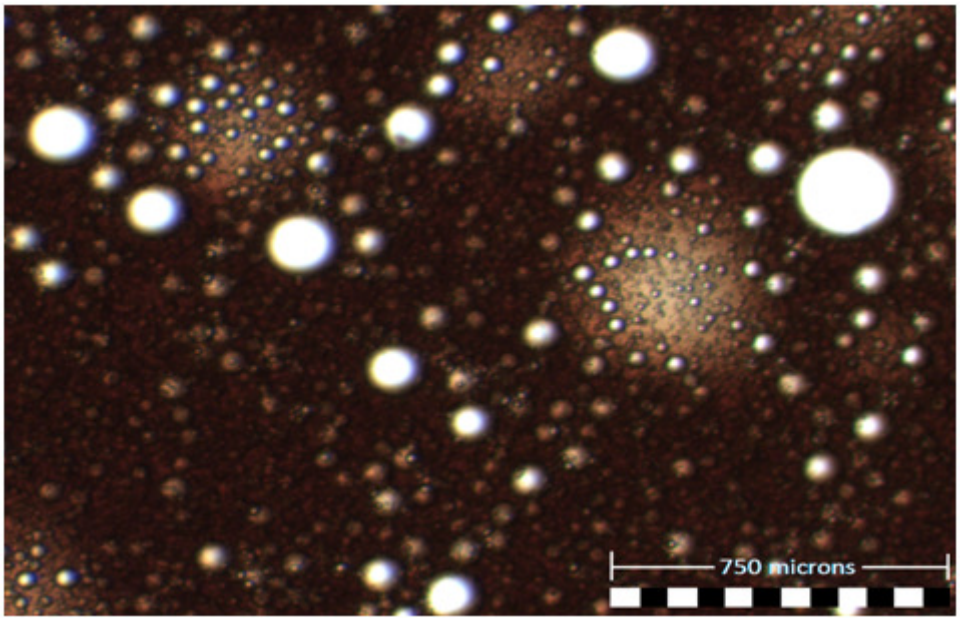

Micrograph 4.3-3 Dispersed phase - Batch experiment after 65 minutes

Micrograph 4.3-4 shows the last sample, taken after the phase inversion. The amount of encapsulated water has now darkened the sample further and increased the effective oil fraction enough for oil to form the continuous phase. The emulsion has changed to W/O, and the picture is now representative for the entire emulsion.

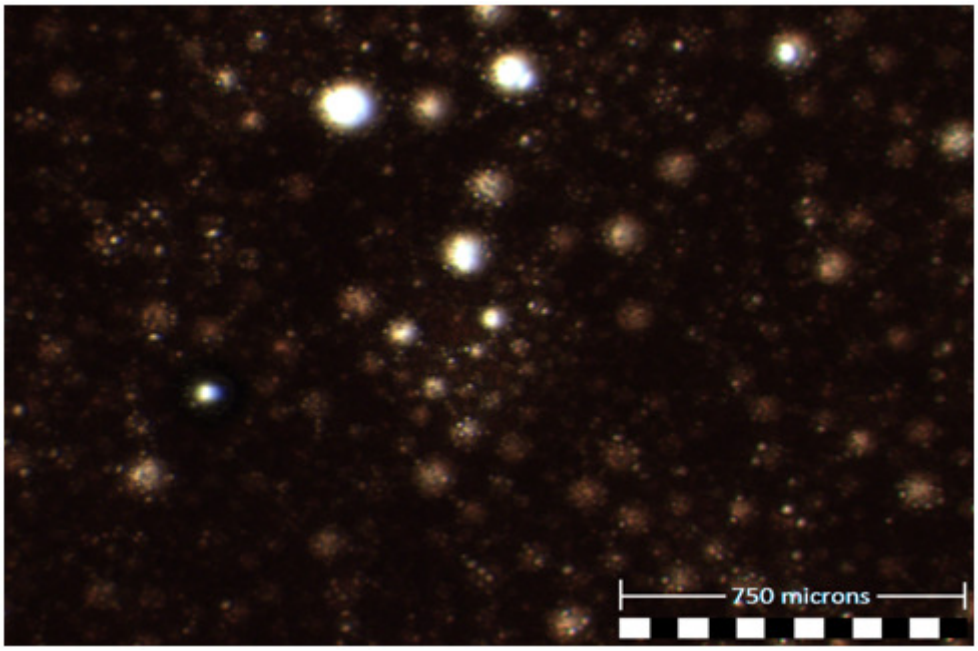

Micrograph 4.3-4 Continuous phase - Batch experiment after phase inversion

The next four pictures show the morphological development in the dispersed oil phase during a flow experiment. The experiment was conducted with an oil (Grane) fraction of 0.5 and phase inversion occurred after 68 minutes. The samples taken from the flow experiment was (in contrast to the batch samples), not photographed until approximately 1.5 hours after they were taken, so small pockets of air developed throughout the samples. These air pockets must not be confused with water. They can be identified by having an outward blend at the edges while the water droplets have an inward blend. Almost all the grey areas in these pictures are air pockets, and are fairly constant throughout the samples.

Micrograph 4.3- 5 shows a sample taken after 2 minutes, where almost no water has been encapsulated by the oil.

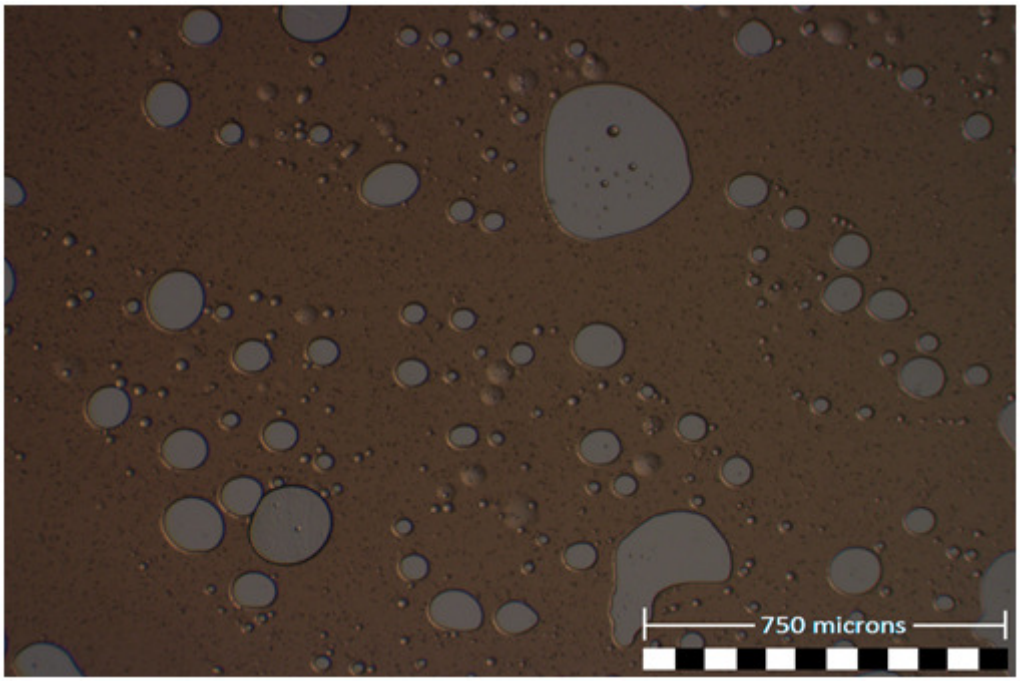

Micrograph 4.3-5 Dispersed phase - Flow experiment after 2 minutes

Micrograph 4.3-6 shows a sample taken after 20 minutes, where the changes in morphology can be seen clearly. Encapsulated water droplets with a diameter of only a few microns are present throughout the sample, and gives it a darker appearance.

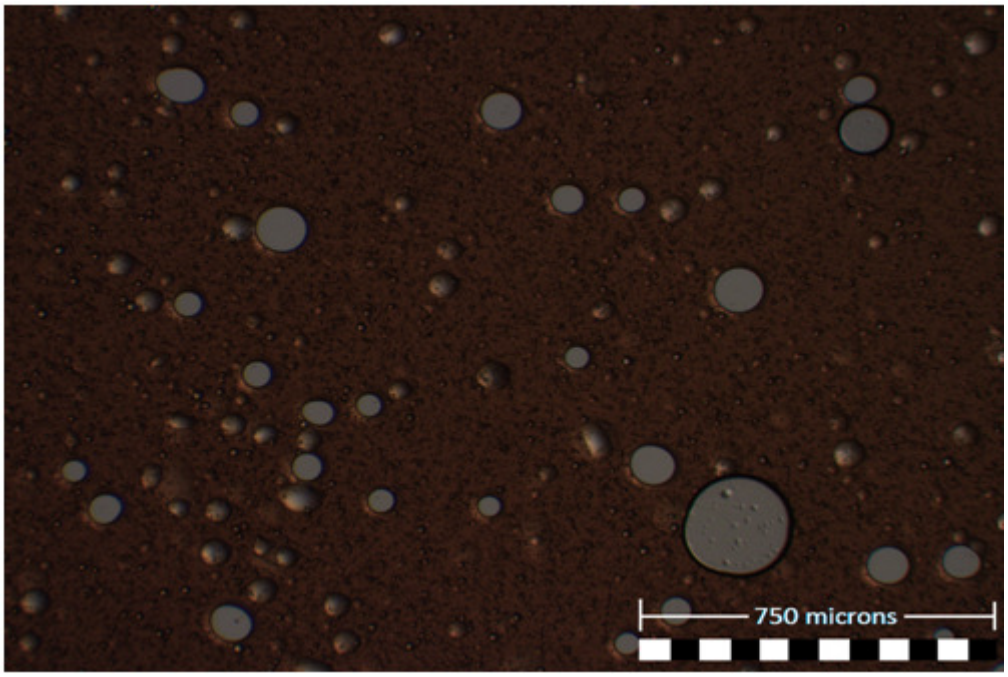

Micrograph 4.3-6 Dispersed phase - Flow experiment after 20 minutes

Micrograph 4.3-7 shows a sample taken after 40 minutes. The concentration of smaller water droplets has increased even further. As in the previous sample, most of the encapsulated water droplets remain very small in size.

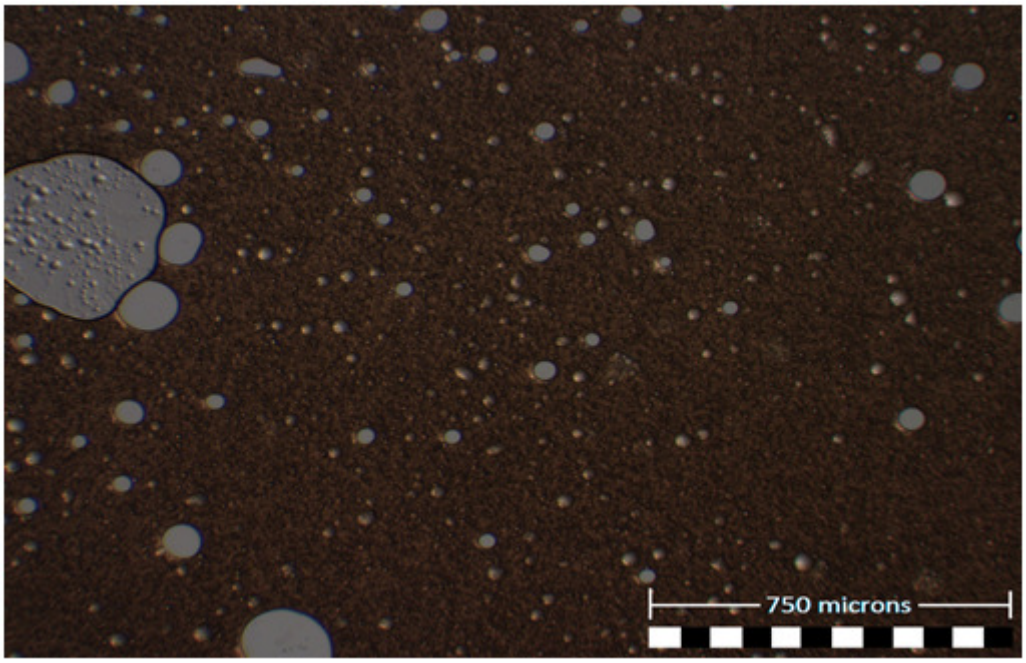

Micrograph 4.3-7 Dispersed phase - Flow experiment after 40 minutes

Micrograph 4.3-8 shows a sample taken after the inversion occurred. The concentration of water droplets has now increased the effective oil fraction enough to form the continuous phase. As in micrograph 4.3-4 from the batch experiment, the sample now represents the entire emulsion.

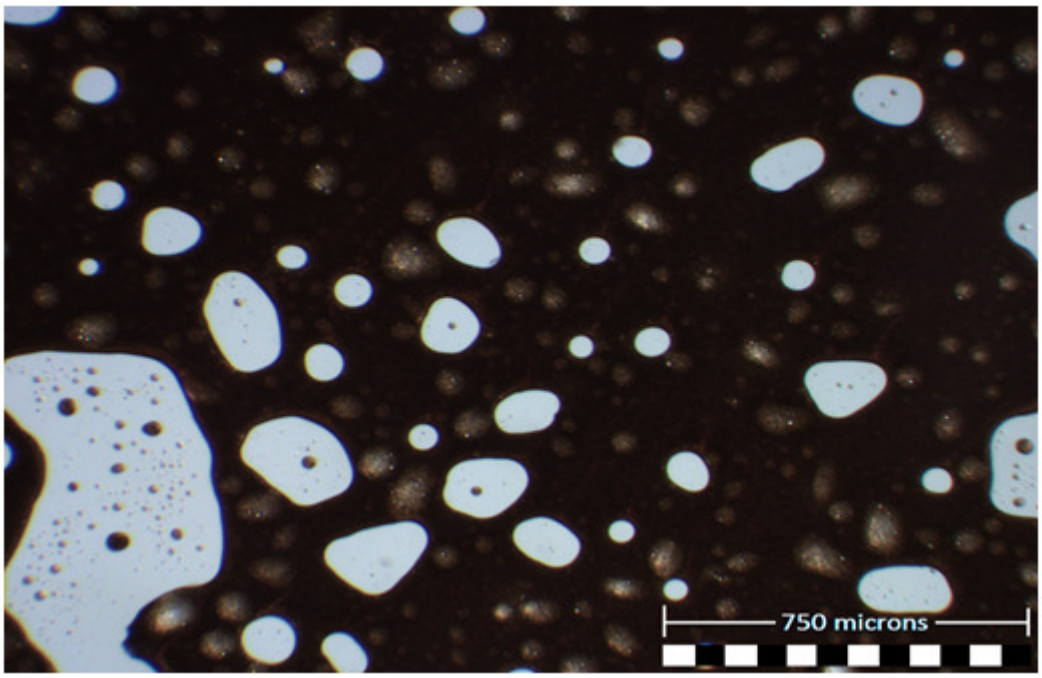

Micrograph 4.3-8 Continuous phase - Flow experiment after inversion

4.3.2 Images generated from Cryo ESEM analysis

This section contains the visual images generated from Cryo ESEM analysis. The images show the morphological development from an O/W emulsion, to a w/O/W emulsion, and finally a W/O emulsion. The samples were taken from a batch experiment with a 60% oil cut (Primol 352), containing 10 g/L of surfactant (Arlacel P135). The experiment was conducted at room temperature (23°C) without any temperature regulation in the batch and with a stirring intensity of 1500 rpm. The phase inversion occurred after 20 minutes.

Picture 4.3-9 shows the coarse surface of a sample taken 3 minutes after the experiment started. The different phases have been revealed by EDS and marked with color for easy identification. Carbon (oil) is marked with red and oxygen (water) is marked with blue. The grey areas in the image are due to topographical limitations, outside of the EDS rays scattering. Since most of the oil drops are whole and unfractured, the large scale image makes it difficult to identify any water droplets inside the oil drops. The average size of the oil drops seems to range from 250 to 300 microns.

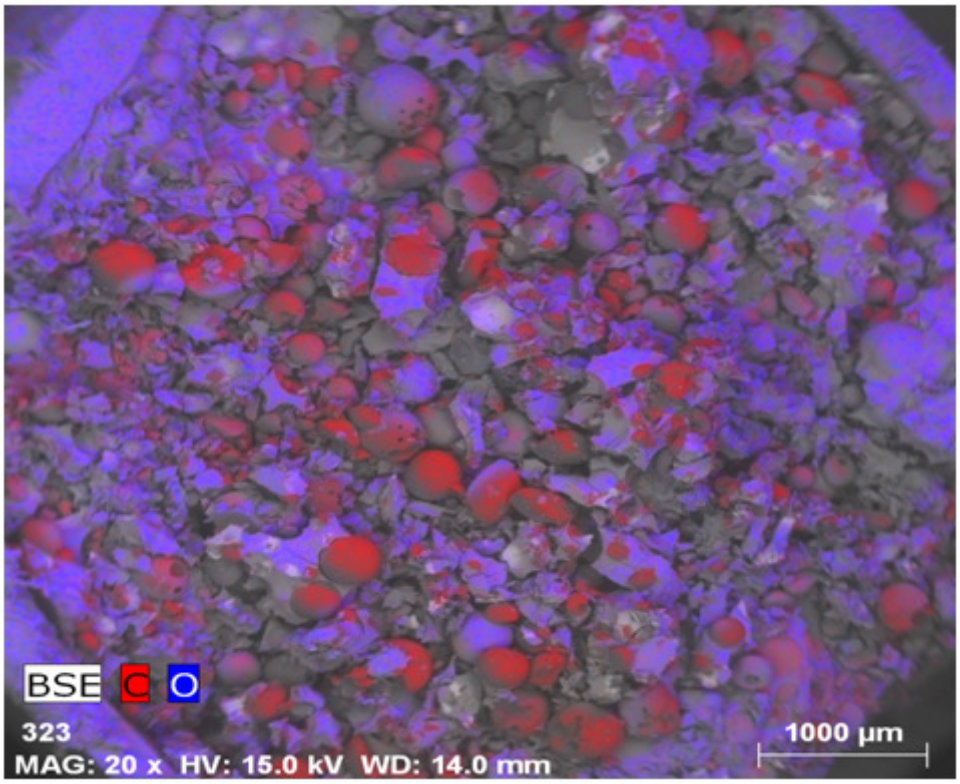

Picture 4.3-9 Sample surface-early stage

Picture 4.3-10 and 4.3-11 show two fractured oil drops identified after a closer look at the sample surface from picture 4.3-9. They clearly show how the oil has encapsulated water droplets. This proves that the initial emulsion has become a multiple w/O/W emulsion, after only 3 minutes of stirring.

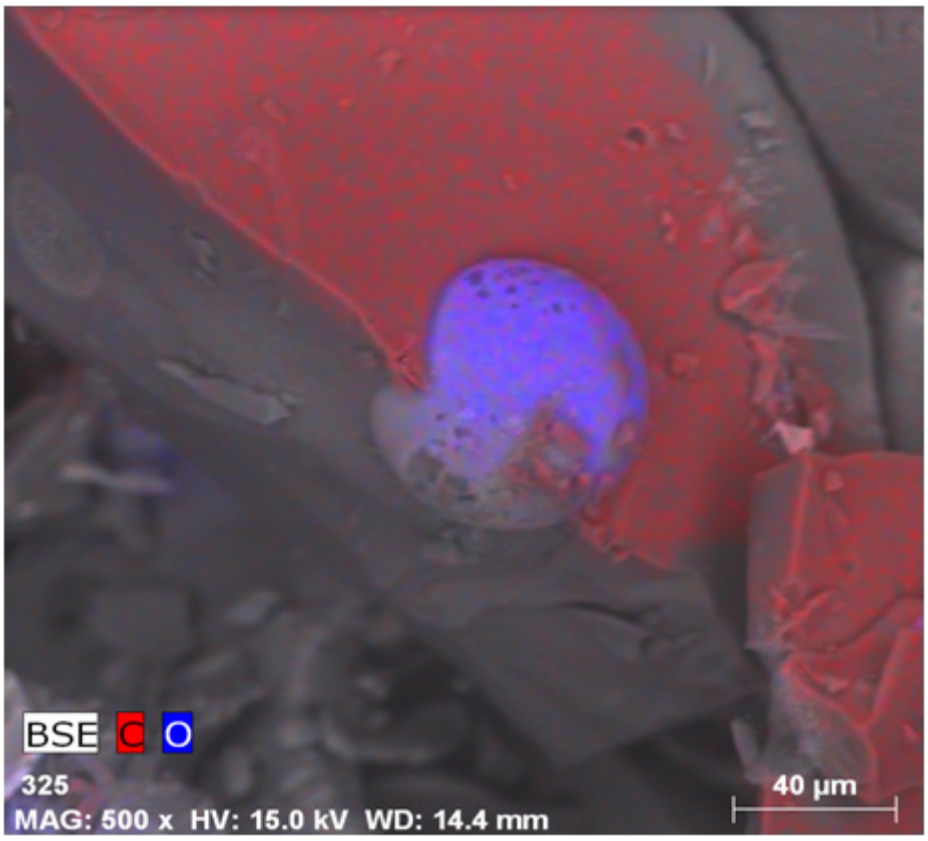

Picture 4.3-10 Fractured oil drop 1 - after 3 minutes

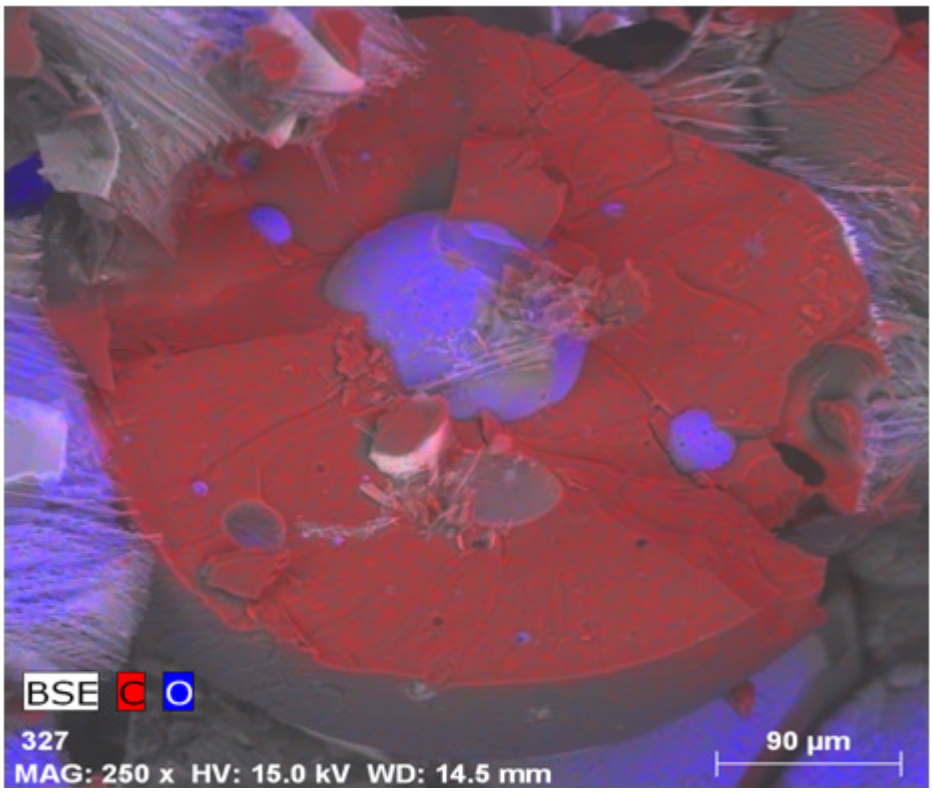

Picture 4.3-11 Fractured oil drop 2 - after 3 minutes

Picture 4.3-12 shows the surface of a sample taken 17 minutes after the experiment started, which is about 4 minutes before phase inversion occurred. The average size of the oil drops appears to have increased, ranging from 350 to 500 microns. Water is still the continuous phase, but the fractured oil drops reveal that a considerable amount of water has been captured inside the oil.

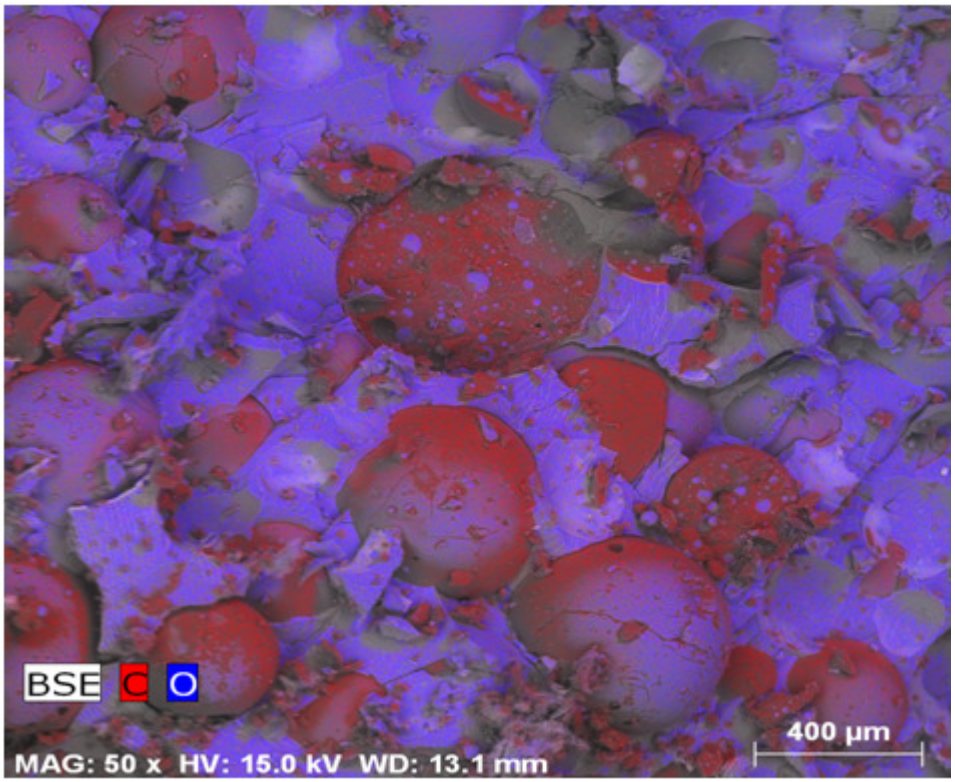

Picture 4.3-12 Sample surface after 17 minutes

Picture 4.3-13 shows a close-up of the fractured oil drop, found in the sample taken after 17 minutes. The amount of water captured has increased significantly, when compared to the sample taken after 3 minutes.

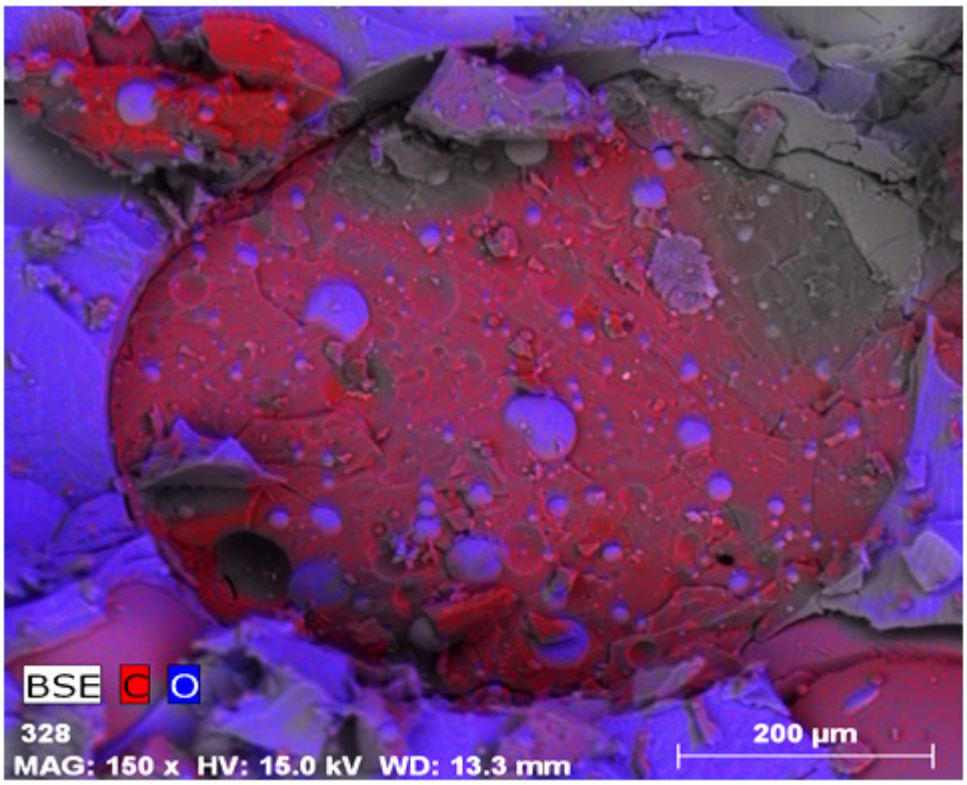

Picture 4.3-13 Fractured oil drop after 17 minutes

Picture 4.3-14 shows the surface of a sample taken after phase inversion. The emulsion is no longer a multiple emulsion and oil is now the continuous phase. The dispersed water seems to be present as either larger drops, or smaller droplets.

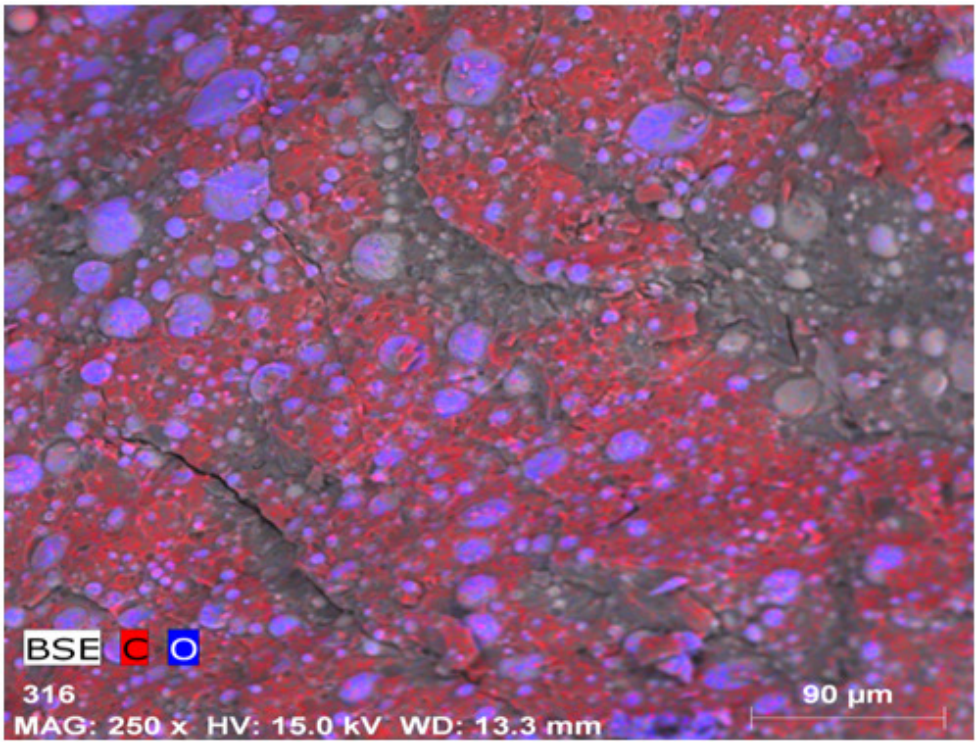

Picture 4.3-14 Overview after phase inversion

5 Discussion

5.1 Effect of surfactants

Based on the experimental results presented in this report, the effect of surfactants has to be looked at in two different sections; the effect during batch experiments and the effect during flow experiments.

Two different hydrophobic surfactants were used (Aralcel P135 and Croda Atsurf 5000). All the results indicate that the inversion time is longer when using Croda Atsurf 5000. This means that if the aim is to induce phase inversion for experimental reasons, Arlacel P135 should be used. This result is confirmed from both batch experiments and flow experiments.

For the batch experiments conducted, an increase in surfactant (Arlacel P135) concentration leads to an increase in inversion time. The concentration varied from 1-10 g/L of surfactant, and the shortest inversion times occurred at 1 g/L. This is unexpected, considering that phase inversion did not occur at all, without any surfactant present in the oil. This may indicate the existence of a specific concentration the authors were unable to identify, where both an increase and decrease of surfactant will increase the inversion time. This concentration will have to exist in the range between 0 and 1 [g/L].

The surfactant concentration showed an opposite effect during the flow experiments. Phase inversion did not occur when using a surfactant concentration of 1 g/L. However, it did occur when increasing the concentration to 4 g/L. This indicates that an increase in surfactant concentration leads to a shorter inversion time, when conducting flow experiments.

After closely inspecting the emulsion containing 1 g/L Arlacel P135, it was clear that from the 9.2 liters extracted, 3 liters was separated water, 1.8 liters stable emulsion, and 4.4 liters separated oil. The water content in the emulsion was measured to about 25%, and from this it can be calculated that approximately 23.5% of the total amount of oil was transformed into a stable W/O emulsion. When the surfactant concentration was increased to 4 g/L, phase inversion occurred and the mixture contained no separated water. 40% of the mixture consisted of separated oil, while the remaining 60% was a stable W/O emulsion.

The relationship between the drop breakup, coalescence, encapsulation and escape rate is obviously very different in a batch process than during pipe flow. An impeller rotating at 1500 rpm has a much larger impact on the emulsion than flowing through a pipe, at approximately 0.8 m/s. The shear stress is therefore much lower during pipe flow experiments. During batch experiments, phase inversion occurs faster when using small amounts of surfactants, so increasing the concentration leads to either a decrease of encapsulation, an increase of escape, or a combination of the two. The inversion time decreases as the stirring intensity increases. A possible explanation is that the impeller breaks the oil droplets in a way that leaves many small oil droplets at high velocities, which increases the collision rate, the coalescence and, in turn, the encapsulation. The emulsion receives a much lower energy contribution during pipe flow, and the drops are not subjected to the same crushing effect as during batch experiments. This means the different mechanics required to form multiple emulsions will work differently during pipe flow, considering the lowered breakup rate. It is likely that the most important factor is to use the correct amount of

surfactant, since once the coalescence rate is high enough, the breakup rate will be too low to prevent the formation of a continuous phase, resulting in phase inversion. It is also worth noticing that the inversion time depended on the surfactant used, even though these two surfactants had a very similar HLB value (as shown conclusively from the Exxsol D60 experiments). This indicates that HLB value is not the only factor influencing the effect of a surfactant.

5.2 Crude oil vs. model oil behavior

The experimental results presented in chapter 4.1.3 state that the inversion time of an oil-water mixture is less dependent on oil fraction when using crude oil from the Grane field, instead of model oil. The average inversion time for the batch experiments with Grane oil was 24.1 minutes at a 40% oil fraction, and 14.6 minutes at a 60% oil fraction. When Primol 352 was used with 10 g/L Arlacel P135, the inversion time was 29 minutes at 60%, 39 minutes at 55%, and too long to determine at a 50% oil fraction. The same trend could be observed from the flow experiments. The emulsions containing model oil never inverted at lower oil fractions than 69%, while the emulsions containing Grane oil inverted at a 50% oil fraction. It is also apparent from figure 4.1-7 and 4.1-9 that Grane oil is less sensitive to the different stirring intensities than the model oil. The variation in inversion time presented in table 4.1-1 and 4.1-2 does not differ enough to give any conclusive results, regarding the difference in reproducibility between model oil and crude oil.

The experiments show that emulsions containing Grane oil have a more stable development, leading towards phase inversion, compared to emulsions containing model oils. The contributing factors leading up to an inversion are far less sensitive to a change in shear forces or phase fraction when using Grane oil. Phase inversion occurs at 40 % oil fraction when using Grane oil, while 55 % is required when using Primol 352. A possible explanation is that the escape rate is much lower in crude oil than in model oil. The total amount of measured natural surfactants in the Grane oil was approximately 50 %, but the quality of these surfactants may vary. These surfactants are much better W/O stabilizers than the “artificial” surfactants used in Primol 352, so the ability to confine the water droplets inside Grane oil is much higher. The low escape rate will reduce the effect different stirring intensities has on the encapsulation-escape balance, and be less sensitive to this variation. This theory is a simplified view on escape rate, and does not include all four mechanisms involved. These mechanisms are dynamic and co dependent. It is safe to assume that the actual dynamics are far more complex, but the experimental results suggest higher stability in crude oil than in model oil.

This stability allows inversion at much lower oil fractions, since the encapsulation rate is larger than the escape rate, even at low fractions. As long as this is the case, inversion is to be expected over time. Perhaps a surfactant with a lower HLB value could be a better approximation towards adapting behavior more similar to crude oil, but this cannot be concluded without further investigation.

5.3 Visual evidence of multiple emulsion formation

Some of the experiments presented in this paper have gone from an abnormal to normal emulsions at constant and low dispersed oil fractions, which indicate the formation of multiple emulsions. The microscopic images presented in chapter 4.3.1 shows how the water droplets appear at higher and higher concentrations in the dispersed oil, as time increases. Since the oil drops coalesce when the sample is placed on the microscopic plate, it is difficult to observe the actual emulsion, as it exists in the experiment, and this creates an uncertainty towards the behavior and size of the oil drops. Another problem is that a microscopic image always will be open for interpretation, as it is hard to separate the phases with certainty.

The images generated with Cryo ESEM analysis are not open for the same interpretation, and provide firmer evidence of the formation of multiple emulsions, and how this leads to phase inversion. Picture 4.3-9 to 4.3-14 show how the morphology changes during a batch experiment. The amount of water droplets captured inside the oil drops increases over time. The samples taken at 3 minutes and 17 minutes also indicate that the average size of the oil drops increases over time. This reveals the mechanism that leads to phase inversion; the effective volume of the dispersed oil phase increases, by capturing water droplets, until it is large enough to form a continuous phase. Picture 4.3.14 shows the dispersion after the inversion, and it is interesting to see that the size of dispersed water drops seem to fall under two categories; either small, or significantly larger. A possible explanation for this can be that the small drops are the ones that were trapped inside the oil drops, while the larger ones formed the continuous water phase up until phase inversion. This theory is supported by Salager [20], who states that the two sizes of drops are produced by different mechanisms, and therefore exhibit different sizes. By different mechanisms, he means the drops locations before the inversion; inside the oil drops and in the continuous water phase.

These are the first images of multiple emulsions generated with the Cryo ESEM technology. They help confirm that the pictures taken with the regular microscope are, in fact, showing an increase in captured water droplets, inside the oil drops, leading to phase inversion for both standstill dynamic batch processes and direct flow experiments. However, further investigation using this technology should be conducted to verify these first results.

5.4 Chord length readings and inversion mechanics

As stated in section 4.2.3, the chord length readings for the four direct flow experiments that resulted in phase inversion indicate a clear pattern. Right before the inversion, there is a significant increase in the small chord length counts (wt < 10), while the RMS chord length decreases. At the PIP, this development changes and the small chord length counts decreases drastically, simultaneously as the RMS chord length increases. The chord length distribution shown in figure 4.2.4 (using Primol 352 and Aralcel P135) indicate a slightly different development than for the Grane experiments. The RMS chord length does not decrease right before the inversion, even though the small chord length count increases rapidly. However, the RMS chord length reading may not have had the necessary measurements required to update, considering how quickly this inversion happened, compared to the others.

The chord length readings do not provide the same information as monitoring the actual droplet distribution, but the two methods are still connected. To be able to make an accurate interpretation of the chord length readings, an understanding of the mechanics of the focused beam reflectance measurement (FBRM) is necessary.

Figure 5.4-1 illustrates the difference between chord length readings in an O/W emulsion and in a w/O/W emulsion. In part A of figure 5.4-1, 4 different chord lengths of oil are measured, while in part B, 8 different chord lengths of oil are measured, due to the encapsulated water droplets. The figure shows that the interpretation of chord length as droplet size will be inaccurate, especially when the formation of multiple emulsions is involved.

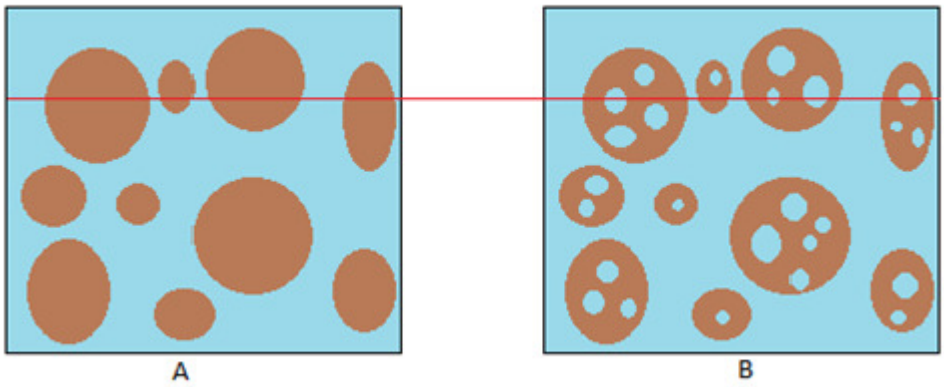

Figure 5.4-1 Multiple emulsion effect on chord length measurements

The capturing of water droplets would result in an increasing small chord length count, as the emulsion moves towards phase inversion, and the formation of multiple emulsions increases rapidly. This implies that the cord length development measured in the experiments from this report supports the formation of multiple emulsions as the cause of phase inversion. The sudden drop in small chord length count after the inversion also supports this theory, as the captured droplets are released when oil forms the continuous phase and the emulsion is no longer a multiple emulsion. As mentioned earlier, the water will be dispersed as either large drops, that used to form the continuous phase, or smaller drops, that were captured inside the oil. The larger drops form a considerable volume fraction of the emulsion, and contribute to a reduced count per second of small chord lengths.

Figure 5.4-2 illustrates the chord length readings just before, and right after phase inversion. Part C of the figure shows large oil drops containing a large amount of water droplets, right before the inversion. Part D shows the W/O emulsion after the inversion, and how the large water drops contribute to the reduced count of small chord lengths.

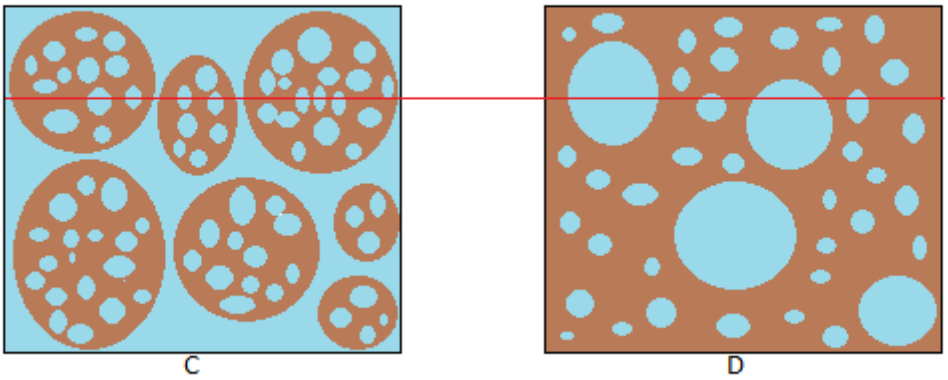

Figure 5.4-2 Chord length measurements around phase inversion

5.5 Experimental problems

This section contains a description of the different problems encountered while conducting the experiments, and if possible, solutions are suggested. Hopefully this can be helpful for later experiments, so that making the same mistakes can be avoided.

5.5.1 Resistance readings

The resistance readings during the batch experiments were a problem. The probe could not be lowered further down than just above the impeller, due to insufficient space inside the batch. When starting with small water fractions (< 50%), the probe was not initially in contact with the water, which meant it got coated with oil, as the dispersed phase was added to the batch. This lead to problems when trying to decide the initial resistance of the emulsion, as it varied for all the experiments, depending on the level of coating. The resistance readings were hard to interpret for the entire experiment, and no development pattern could be established for the experiment. The actual inversion point was the only solid data that could be obtained from the resistance readings, as the resistance made a considerable jump when moving from water continuous to oil continuous.

5.5.2 Torque readings

The torque readings presented in figure 4.1-5 show that the initial values vary from 6.5 Nm to 7.5 Nm. This slight change in value can be explained by a difference in the positioning of the impeller and the batch-lid between the experiments. If the impeller touches the side walls of the hole drilled in the lid, this friction can affect the torque, and result in a higher torque reading. The torque can also be affected if the impeller is mounted with eccentricity, and you get an unbalanced impeller rotation. This can affect the preset rpm, and change the operational conditions.

5.5.3 Microscopic observations

The W/O emulsions were stable, while the O/W emulsions were unstable, and more difficult to observe. The problem with observing a sample that represents the entire emulsion was that the oil drops coalesced as soon as the emulsion was placed on the viewing plate. A large oil drop formed in the middle of the sample while the water was forced to the edges of the sample. Any attempt to stop, or slow this process was unsuccessful, so the only successful microscopic observation of O/W emulsions was that of the dispersed phase presented in this paper.

5.5.4 Pump capacity

The limitations in pump capacity made it impossible to continue the experiment after phase inversion. This made it difficult to evaluate the behavior of a stable W/O emulsions, and record chord length distributions after the inversion.

6 Conclusion and suggestions for further work

6.1 Conclusion

Both batch and flow experiments have been conducted with oil-water mixtures in order to investigate the phase inversion phenomena. A thorough research on the effect of surfactants and stirring intensities has been conducted in the batch experiments. It has also been attempted to achieve phase inversion during direct flow experiments (fixed concentrations), by regulating the concentration of surfactant present in the abnormal emulsion. Special emphasis has been placed on studying how the formation of multiple emulsions can result in phase inversion, and collecting solid visual evidence to support this theory. These are the conclusions from the work conducted.

- Increasing the hydrophobic surfactant concentration in model oil, will result in longer inversion times during batch experiments. This is valid at 1500 rpm, and for surfactant concentrations ranging from 1-10 g/L.
- Increasing the stirring intensity during batch experiments, will result in shorter inversion times. This is valid from 750 to 2000 rpm.
- Phase inversion occurs with crude oil (from the Grane field) at low oil fractions without adding to the oil phase after the experiment has started (direct flow experiment).Phase inversion during pipe flow can therefore not be based solely on phase fractions. The required time depends on the initial fractions used. Lower oil fraction results in longer inversion time.
- Given the correct concentration of surfactant in model oil, phase inversion can occur during direct flow experiments. The experiments indicate an easier achieved phase inversion, when increasing the surfactant concentration.
- Phase inversion during direct flow experiments is the result of the formation of multiple emulsions.
- Cryo ESEM technology can be used to document the formation of multiple emulsions with more certainty than the techniques used in previous research, known to the authors´. The Cryo ESEM images in this report help confirm and better understand the mechanisms of phase inversion through multiple emulsion formation.

6.2 Further work suggestions

More work has to be done, both to verify the results from this paper, and to explore the areas this paper does not cover. This section contains some suggestions for further work.

- Direct flow experiments with lower crude oil fractions (<0.5) should be conducted.
- Direct flow experiments should be conducted using a pump with a higher capacity, allowing higher mixture velocities and single phase oil flow.
- The effect of using surfactants with different HLB values than the ones used in this report should be tested.
- Surfactant concentrations between 0 and 1 g/L should be tested through batch experiments.
- More images from multiple emulsion formation should be generated using Cryo ESEM analysis to further verify the results in this report.

References

1. "Emulsion Catastrophic Inversion from Abnormal to Normal Morphology.3." *Ind. Eng. Chem. Res.* **2003**, 42, 4311-4318 Tyrode, Mira, Zambeano, Marqués, Gonzales and Salager.

2. "Factors affecting which phase will disperse when immiscible liquids are stirred together" *Can .J. Chem. Eng.* **1965**, 43, 298-301 by Selker and Sleicher.

3. "An analysis of oil-water flow phenomena in horizontal pipes." *SPE Paper 18836, SP Prof.Prod. Operating Symp*. **1989** Oklahoma. By Arirachakaran, Oglesby, Malinowsky, Shoham and Brill.

4. "Flow induced emulsification in the flow of two immiscible liquids in horizontal pipes." *Int. J. Multiphase flow 23(1*), **1997**, 55-68, by Nädler and Mewes.

5. "Analysis of the phase inversion characteristic of liquid-liquid dispersions." AiChe J. **1980** 26, 51. By Arashmid and Jeffreys.

6. "Emulsion properties and related know how to attain them" *Pharmaceutical emulsions and suspensions vol 105 chapter 3* by Salager.

7. "Emulsion Catastrophic Inversion from Abnormal to Normal Morphology 4." *Ind. Eng Chem. Res. **2005,** 44, 67-74 by* Tyrode, Allouche, Choplin and Salager.

8. "Modeling of phase inversion phenomenon in two-phase pipe flows" *International journal of multiphase flow 28*. **2002,** 1177-1204 by Brauner and Ullman.

9. "Study on oil water two-phase flow in horizontal pipes" *Journal of Petroleum Science and Engineering*. **2007,** 59, 43–58 by Xu.

*10. "*Oil water flow through different diameter pipes-Similarities and Differences*"* *Trans IChemE, Part A*. **2007**, *Vol* 85 (A8) 1123–1128 by Mandal, Chakrabarti and Das.

11. "Predicting catastrophic phase inversion on the basis of droplet coalescence kinetics" *Langmuir.* **1996**, 12, 875-882 by Vaessen, Visschers and Stein.

12. "On the mechanism of the inversion of emulsions" *Trans IChemE, Vol 76, part A.* **1998** by Groeneweg, Agterof, Jaeger, Janssen, Wieringa and Klahn.

13. "On the escape process during phase inversion of an emulsion" *Colloids and Surfaces A: Physico chem. Aspects 210. **2002,** 167-181* by Klahn, Janssen, Vaesse, Swart, and Agterof.

14. *"*Microemulsions, macroemulsions and the Bancroft rule."
Langmuir Vol 12 no 26. **1996***, 12, 6351-6552 by Eli Ruckenstein.*

15. "Emulsion Catastrophic Inversion from Abnormal to Normal Morphology.1."
Ind. Eng. Chem. Res. **2003**, 42, 50-56 by Zambeano, Tyrode, Mira, Marqués, Rodriguez and Salager

16. "Infulence of a surfactant or salt on phase inversion in a water-oil pipe flow."
2009, by Piela, Djojorahardjo, Koper and Ooms.
17. Oxford English Dictionary, 2nd edition, Oxford University Press. **1989**.

18. "Foundations of environmental scanning electron microscopy"
Advances in Electronics and Electron Physics 71. **1988**, 109–250 by Danilatos.

19. "Environmental scanning electron microscope: A new tool for inspection and testing."
The 6th International MicroProcess Conference, Micoprocess. **1993,**102-103 by Danilatos.

20. "Emulsion catastrophic inversion from abnormal to normal morphology. 7."
Ind. Eng Chem. Res. ***2008,*** *47, 2314-2319 by Gonzáles, Sadtler, Choplin and Salager.*

Appendix A – Flow experiment readings

Appendix A presents the measured data from the four flow experiments where phase inversion occurred. Data from experiments where inversion did not occur is not shown, in order to limit the number of pages in the appendix, and to focus on the results that are important for for this paper.

The tables only show the area of interest, over the inversion.

Primol 352 experiments (from section 4.2.1.1)

69% oil fraction with 4 g/L of surfactant (Arlacel P135):

Time [min]	Temperature [C]	Mass flow [kg/s]	dP Pipe [mBar/m]	dP Pump [mBar]
3,00	23,44	0,26	23,95	4333,90
3,02	23,42	0,26	23,46	4328,48
3,03	23,39	0,26	23,21	4287,34
3,05	23,42	0,26	22,95	4253,73
3,07	23,63	0,26	22,62	4285,64
3,08	23,55	0,26	22,66	4366,00
3,10	23,63	0,26	22,66	4366,60
3,12	23,42	0,27	22,51	4394,70
3,13	23,47	0,27	22,20	4573,20
3,15	23,65	0,27	22,43	4684,17
3,17	23,69	0,27	22,12	4900,29
3,18	23,47	0,27	22,12	4999,33
3,20	23,49	0,27	22,07	4998,12
3,22	23,73	0,27	22,35	5084,91
3,23	23,73	0,27	22,26	4996,71
3,25	23,73	0,27	22,17	4902,80
3,27	23,68	0,27	22,68	4829,05
3,28	23,68	0,27	22,68	4828,65
3,30	23,69	0,27	23,31	4759,42
3,32	23,74	0,26	24,05	4673,93
3,33	23,55	0,26	24,28	4623,87
3,35	23,52	0,26	24,71	4534,57
3,37	23,73	0,26	24,71	4515,21
3,38	23,57	0,26	24,38	4515,21
3,40	23,58	0,26	23,98	4451,59
3,42	23,58	0,26	23,52	4399,52

3,43	23,53	0,26	23,54	4443,87
3,45	23,52	0,26	23,54	4438,45
3,47	23,60	0,26	23,16	4440,05
3,48	23,60	0,26	23,04	4463,63
3,50	23,79	0,27	23,19	4609,32
3,52	23,77	0,27	23,35	4780,79
3,53	23,76	0,27	23,71	5021,10
3,55	23,79	0,28	23,71	5022,10
3,57	23,61	0,28	23,37	5187,66
3,58	23,68	0,28	23,17	5423,35
3,60	23,77	0,28	23,13	5427,86
3,62	23,81	0,28	23,52	5384,02
3,63	23,84	0,28	23,52	5296,92
3,65	23,77	0,27	23,64	5296,92
3,67	23,81	0,27	24,24	5265,91
3,68	23,71	0,27	25,15	5108,09
3,70	23,68	0,27	26,96	4980,26
3,72	23,68	0,27	26,96	4847,21
3,73	23,63	0,27	28,53	4846,01
3,75	23,63	0,27	30,58	4788,32
3,77	23,69	0,27	30,30	4681,97
3,78	23,69	0,27	29,29	4643,84
3,80	23,69	0,26	27,14	4658,99
3,82	23,84	0,26	27,14	4658,79
3,83	23,87	0,27	25,39	4784,71
3,85	23,87	0,27	24,86	4939,62
3,87	23,89	0,27	25,44	5289,60
3,88	23,87	0,28	25,39	5528,50
3,90	23,89	0,28	25,39	6163,93
3,92	23,92	0,28	24,68	6163,93
3,93	23,89	0,28	23,44	7190,46
3,95	23,77	0,28	23,24	9361,04
3,97	23,77	0,27	20,44	11897,13
3,98	23,65	0,24	20,44	13874,35
4,00	23,42	0,23	19,79	13887,99
4,02	23,00	0,22	19,85	15354,90
4,03	22,88	0,21	20,53	16406,72
4,05	22,54	0,21	20,44	17621,90

4,07	22,36	0,21	21,53	18259,64
4,08	22,14	0,20	21,53	18260,45
4,10	21,88	0,20	23,21	18064,29
4,12	21,51	0,19	22,10	19093,93
4,13	21,31	0,19	22,91	19598,42
4,15	21,53	0,18	23,99	20675,12
4,17	21,66	0,18	23,99	20681,64
4,18	21,95	0,18	27,77	20681,64
4,20	21,95	0,18	38,38	20267,26
4,22	21,79	0,18	49,12	21016,07
4,23	21,88	0,18	60,45	20239,87
4,25	21,98	0,19	75,02	20134,51
4,27	22,01	0,19	75,02	20182,66
4,28	21,37	0,19	89,39	20527,31
4,30	21,58	0,18	97,64	21475,88
4,32	21,35	0,18	108,61	21771,87
4,33	21,43	0,18	120,16	20486,25
4,35	21,43	0,18	120,16	21076,62
4,37	21,42	0,18	128,44	21076,62
4,38	21,53	0,18	135,39	22147,00
4,40	21,69	0,18	122,66	18623,58
4,42	21,83	0,17	131,43	22622,26
4,43	21,83	0,17	131,43	22112,85
4,45	22,41	0,16	126,61	22115,05
4,47	22,30	0,15	119,32	21068,55
4,48	22,22	0,14	110,34	18186,50
4,50	22,73	0,14	101,94	18468,35
4,52	23,69	0,13	92,60	15781,66
4,53	23,92	0,12	92,60	15745,95
4,55	24,59	0,10	83,36	14357,30
4,57	24,67	0,09	72,55	12599,03
4,58	24,67	0,09	58,67	9874,72
4,60	24,43	0,07	45,19	7653,80
4,62	24,43	0,05	45,19	5258,99
4,63	24,73	0,04	32,40	5258,99
4,65	26,63	0,02	20,26	2889,38
4,67	26,63	0,02	8,75	755,37
4,68	26,63	0,01	5,39	730,46

4,70	26,63	0,01	5,39	628,91
4,72	26,63	0,00	4,98	633,33
4,73	26,63	0,00	4,69	555,07
4,75	26,61	0,00	4,44	495,47
4,77	26,61	0,00	4,21	449,32
4,78	26,59	0,00	4,06	410,18
4,80	26,59	0,00	4,06	410,38
4,82	26,59	0,00	3,85	378,28
4,83	26,58	0,00	3,71	351,19
4,85	26,59	0,00	3,58	328,61
4,87	26,59	0,00	3,50	307,84
4,88	26,59	0,00	3,50	291,18
4,90	26,59	0,00	3,40	291,18
4,92	26,59	0,00	3,30	270,61
4,93	26,59	0,00	3,22	260,48
4,95	26,59	0,00	3,12	247,64
4,97	26,59	0,00	3,12	236,10
4,98	26,59	0,00	3,03	236,30

Grane oil experiments (from section 4.2.2)

69% oil fraction:

Time [min]	Temperature [C]	Mass flow [kg/s]	dP Pipe [mBar/m]	dP Pump [mBar]
9,05	29,03	0,27	31,42	5673,68
9,07	28,98	0,27	31,23	5610,97
9,08	29,03	0,28	31,55	5632,04
9,10	29,03	0,28	31,45	5631,64
9,12	29,08	0,27	31,34	5687,73
9,13	29,04	0,27	31,34	5680,20
9,15	29,04	0,27	31,14	5680,20
9,17	29,08	0,27	31,15	5566,42
9,18	29,04	0,27	31,29	5661,34
9,20	29,06	0,27	30,58	5664,75
9,22	29,08	0,27	30,58	5661,54
9,23	29,08	0,27	31,16	5663,34
9,25	29,03	0,27	31,21	5678,39
9,27	29,09	0,27	31,40	5680,60
9,28	29,12	0,27	32,05	5761,37
9,30	29,14	0,27	32,22	5745,92
9,32	29,19	0,27	32,22	5744,31
9,33	29,19	0,27	31,93	5757,86
9,35	29,14	0,27	31,73	5840,53
9,37	29,14	0,27	31,64	5894,62
9,38	29,14	0,27	31,87	5978,60
9,40	29,14	0,27	31,87	5977,49
9,42	29,12	0,27	31,82	5977,49
9,43	29,16	0,27	32,42	5956,42
9,45	29,12	0,27	32,37	6002,78
9,47	29,14	0,27	32,52	5862,52
9,48	29,16	0,27	32,52	5971,28
9,50	29,14	0,27	33,39	5973,89
9,52	29,14	0,27	33,33	6038,60
9,53	29,20	0,27	33,18	6055,86
9,55	29,16	0,27	33,38	5958,13
9,57	29,16	0,27	33,44	5928,44
9,58	29,14	0,27	33,44	5927,63

9,60	29,20	0,27	33,00	5977,79
9,62	29,17	0,27	32,83	5903,15
9,63	29,19	0,27	32,49	5841,74
9,65	29,17	0,27	32,29	5889,70
9,67	29,17	0,27	32,29	5811,24
9,68	29,16	0,27	32,86	5811,24
9,70	29,20	0,27	32,75	5845,05
9,72	29,17	0,27	32,83	5926,63
9,73	29,24	0,27	32,78	5947,79
9,75	29,24	0,27	32,78	6037,90
9,77	29,22	0,27	32,64	6038,70
9,78	29,24	0,27	33,03	6048,73
9,80	29,22	0,27	33,06	5990,94
9,82	29,22	0,27	32,99	6002,78
9,83	29,25	0,27	33,46	6010,11
9,85	29,25	0,27	33,46	6008,90
9,87	29,19	0,27	33,82	5982,31
9,88	29,16	0,27	34,42	5938,46
9,90	29,30	0,27	34,65	5959,53
9,92	29,32	0,27	35,22	6009,81
9,93	29,30	0,27	35,22	6054,95
9,95	29,28	0,27	35,60	6054,95
9,97	29,22	0,27	35,30	6231,54
9,98	29,30	0,27	34,81	6183,19
10,00	29,27	0,27	33,96	6259,24
10,02	29,30	0,27	33,96	6217,90
10,03	29,32	0,27	34,00	6219,70
10,05	29,32	0,27	34,46	6300,97
10,07	29,33	0,27	34,78	6396,50
10,08	29,37	0,27	35,50	6359,98
10,10	29,32	0,27	36,06	6518,71
10,12	29,30	0,27	36,06	6538,27
10,13	29,32	0,27	36,21	6538,27
10,15	29,32	0,27	36,46	6503,05
10,17	29,37	0,27	36,30	6485,49
10,18	29,40	0,27	36,06	6531,15
10,20	29,40	0,27	36,06	6453,89
10,22	29,43	0,27	36,71	6455,10

10,23	29,35	0,27	37,58	6414,46
10,25	29,40	0,27	38,76	6303,79
10,27	29,45	0,27	39,60	6209,98
10,28	29,45	0,27	40,12	6442,35
10,30	29,41	0,27	40,12	6443,75
10,32	29,37	0,27	41,10	6501,95
10,33	29,37	0,27	41,59	6576,50
10,35	29,45	0,27	41,72	6669,21
10,37	29,41	0,27	40,94	6735,13
10,38	29,46	0,27	40,94	6631,88
10,40	29,41	0,27	39,86	6631,88
10,42	29,45	0,27	39,31	6640,81
10,43	29,48	0,27	39,33	6540,57
10,45	29,49	0,27	40,40	6738,83
10,47	29,51	0,27	40,40	6813,58
10,48	29,48	0,27	41,83	6811,58
10,50	29,56	0,27	42,93	6890,35
10,52	29,56	0,27	43,86	7093,63
10,53	29,54	0,27	43,92	7195,27
10,55	29,56	0,27	43,46	7271,12
10,57	29,43	0,26	43,46	7273,12
10,58	29,54	0,26	42,63	7451,22
10,60	29,53	0,26	42,45	7284,27
10,62	29,59	0,26	42,88	7244,23
10,63	29,56	0,26	44,30	7142,69
10,65	29,56	0,26	44,30	7083,79
10,67	29,61	0,27	45,58	7083,79
10,68	29,61	0,27	47,02	6973,92
10,70	29,62	0,27	48,38	7083,99
10,72	29,57	0,27	49,62	7102,26
10,73	29,59	0,27	49,62	7052,69
10,75	29,61	0,27	50,85	7053,69
10,77	29,61	0,26	52,40	7230,28
10,78	29,65	0,26	52,26	7348,38
10,80	29,64	0,26	52,50	7411,49
10,82	29,65	0,26	52,72	7217,74
10,83	29,62	0,27	52,72	7220,75
10,85	29,70	0,26	53,48	7231,79

10,87	29,67	0,26	53,71	7376,16
10,88	29,67	0,26	55,56	7436,47
10,90	29,67	0,27	58,98	7343,45
10,92	29,69	0,27	58,98	7450,51
10,93	29,72	0,26	59,76	7450,51
10,95	29,72	0,26	60,40	7605,33
10,97	29,69	0,26	60,91	7619,78
10,98	29,69	0,26	62,19	7681,99
11,00	29,69	0,26	62,19	7895,90
11,02	29,70	0,26	62,40	7898,31
11,03	29,72	0,26	63,81	8314,71
11,05	29,56	0,24	61,42	11705,06
11,07	29,53	0,24	62,79	10610,49
11,08	29,69	0,25	65,14	9603,92
11,10	29,49	0,26	65,14	9580,85
11,12	28,47	0,23	61,74	13095,12
11,13	28,16	0,21	56,36	17324,29
11,15	28,29	0,21	62,81	16764,71
11,17	28,15	0,22	71,94	17505,39
11,18	27,89	0,21	71,94	18515,68
11,20	27,79	0,21	81,93	18522,50
11,22	27,89	0,21	94,22	18289,72
11,23	27,89	0,21	100,68	19252,14
11,25	27,78	0,21	107,06	19384,98
11,27	27,68	0,21	110,07	19941,34
11,28	27,46	0,21	110,07	19950,97
11,30	27,55	0,21	111,84	20553,99
11,32	27,47	0,21	111,86	20207,63
11,33	27,41	0,21	111,09	20149,53
11,35	27,60	0,21	111,38	19314,52
11,37	27,76	0,21	111,38	17479,96
11,38	28,23	0,20	106,36	17479,96
11,40	28,08	0,20	102,02	16940,74
11,42	28,50	0,20	101,81	15819,88
11,43	28,04	0,20	98,13	18910,82
11,45	28,63	0,18	98,13	16600,29
11,47	28,61	0,18	94,02	16574,81
11,48	28,61	0,16	88,26	18264,47

11,50	28,82	0,15	81,28	17231,42
11,52	29,30	0,15	74,77	15047,32
11,53	29,48	0,14	68,60	12410,39
11,55	29,93	0,12	68,60	12380,10
11,57	29,94	0,10	61,07	11283,93
11,58	29,83	0,09	52,60	9340,64
11,60	29,99	0,09	42,88	6869,37
11,62	29,93	0,07	33,89	5141,60
11,63	30,07	0,05	33,89	3171,42
11,65	31,94	0,03	24,30	3171,42
11,67	31,94	0,02	16,52	1168,34
11,68	31,94	0,02	9,07	734,98
11,70	31,94	0,01	7,31	651,90
11,72	31,94	0,01	7,31	572,02
11,73	31,93	0,00	6,61	572,02
11,75	31,94	0,00	5,94	507,31
11,77	31,94	0,00	5,49	456,14
11,78	31,93	0,00	5,12	415,00
11,80	31,91	0,00	4,73	380,08
11,82	31,90	0,00	4,73	380,08
11,83	31,91	0,00	4,36	351,99
11,85	31,91	0,00	4,04	326,40
11,87	31,88	0,00	3,83	304,83
11,88	31,88	0,00	3,49	286,27
11,90	31,88	0,00	3,49	269,21
11,92	31,86	0,00	3,33	269,21
11,93	31,85	0,00	3,14	255,16
11,95	31,85	0,00	2,91	241,62
11,97	31,86	0,00	2,74	229,38
11,98	31,86	0,00	2,74	218,84
12,00	31,85	0,00	2,62	218,44
12,02	31,85	0,00	2,45	208,91
12,03	31,85	0,00	2,37	199,88
12,05	31,85	0,00	2,23	192,25
12,07	31,83	0,00	2,10	185,33
12,08	31,82	0,00	2,10	185,33
12,10	31,83	0,00	2,04	179,31

62.5 % oil fraction:

Time [min]	Temperature [C]	Mass flow [kg/s]	dP Pipe [mBar/m]	dP Pump [mBar]
18,22	27,89	0,25	19,83	5674,99
18,23	27,91	0,25	19,97	4983,96
18,25	27,89	0,26	19,97	4514,28
18,27	27,88	0,27	21,59	4514,28
18,28	27,89	0,28	24,73	4426,08
18,30	27,89	0,27	27,86	4863,55
18,32	27,92	0,27	31,03	5432,06
18,33	27,92	0,27	32,66	6270,17
18,35	27,86	0,27	32,66	6255,93
18,37	27,91	0,26	30,53	7187,05
18,38	27,91	0,23	24,88	9259,09
18,40	27,88	0,23	7,07	11114,12
18,42	27,92	0,16	8,20	10203,16
18,43	27,88	0,12	8,20	9096,76
18,45	27,96	0,11	7,47	9096,76
18,47	27,94	0,12	8,24	8064,00
18,48	27,86	0,12	11,75	6810,30
18,50	27,91	0,15	19,57	4683,97
18,52	27,94	0,21	19,57	4736,03
18,53	27,94	0,26	25,74	4738,64
18,55	27,89	0,26	27,05	4573,58
18,57	27,92	0,26	33,87	5296,01
18,58	27,94	0,26	49,16	5616,68
18,60	27,96	0,27	81,55	5809,02
18,62	27,92	0,27	81,55	5792,37
18,63	27,96	0,27	89,82	6200,74
18,65	27,92	0,27	70,69	7426,95
18,67	27,81	0,27	48,83	12066,99
18,68	27,60	0,23	25,75	14108,84
18,70	27,84	0,19	25,75	11033,74
18,72	27,92	0,16	22,31	11033,74
18,73	27,97	0,14	14,48	8701,52
18,75	27,96	0,14	14,94	7441,98
18,77	27,96	0,14	24,85	5768,75

18,78	27,97	0,17	24,85	6526,68
18,80	27,97	0,19	30,34	6558,58
18,82	27,94	0,23	35,60	6580,66
18,83	27,97	0,24	46,58	4591,60
18,85	27,96	0,24	48,27	5456,40
18,87	27,92	0,25	50,54	6234,33
18,88	27,94	0,25	50,54	6198,63
18,90	27,46	0,24	62,62	10877,80
18,92	26,55	0,19	68,22	18584,72
18,93	26,69	0,19	63,48	18748,27
18,95	26,91	0,17	58,84	17176,00
18,97	26,87	0,17	58,84	16664,18
18,98	26,63	0,17	51,58	16664,18
19,00	26,63	0,18	39,44	16572,77
19,02	26,45	0,18	31,90	17344,95
19,03	26,82	0,18	25,42	17641,02
19,05	26,43	0,17	25,42	18881,86
19,07	26,22	0,16	20,46	18936,02
19,08	26,71	0,16	26,23	18183,51
19,10	27,19	0,15	40,09	16862,07
19,12	28,02	0,15	37,82	12170,27
19,13	28,13	0,11	49,80	11598,17
19,15	27,09	0,10	49,80	11718,94
19,17	26,64	0,15	91,86	18754,00
19,18	26,93	0,18	140,63	19534,09
19,20	27,57	0,18	159,12	17271,33
19,22	27,43	0,19	147,48	17074,07
19,23	27,67	0,18	147,48	13567,63
19,25	27,67	0,16	143,71	13567,63
19,27	27,67	0,14	129,12	14839,40
19,28	27,83	0,14	108,88	14396,52
19,30	27,89	0,12	93,83	14672,25
19,32	28,10	0,10	93,83	11655,37
19,33	28,20	0,08	79,57	11628,28
19,35	28,10	0,07	70,22	10121,23
19,37	27,94	0,06	60,04	8746,84
19,38	28,08	0,06	47,37	5866,11
19,40	28,10	0,04	33,90	4155,30

19,42	30,09	0,03	33,90	4050,58
19,43	30,05	0,01	21,52	1472,44
19,45	30,07	0,01	11,97	702,37
19,47	30,05	0,01	8,56	646,98
19,48	30,05	0,00	7,50	581,66
19,50	30,07	0,00	7,50	527,07
19,52	30,05	0,00	6,87	527,47
19,53	30,07	0,00	6,42	482,32
19,55	30,07	0,00	6,04	444,60
19,57	30,05	0,00	5,67	411,69
19,58	30,07	0,00	5,32	355,20
19,60	30,07	0,00	5,32	361,22

50% oil fraction:

Time [min]	Temperature [C]	Mass flow [kg/s]	dP Pipe [mBar/m]	dP Pump [mBar]
62,53	26,85	0,28	22,28	4728,71
62,55	26,85	0,28	22,72	5131,97
62,57	26,80	0,28	21,69	5571,53
62,58	26,82	0,27	21,69	5418,12
62,60	26,82	0,27	20,28	5418,12
62,62	26,85	0,27	19,47	5066,04
62,63	26,90	0,27	19,22	4615,84
62,65	26,80	0,27	20,35	4400,92
62,67	26,79	0,28	20,35	4183,29
62,68	26,82	0,28	21,82	4178,07
62,70	26,82	0,28	23,65	4374,22
62,72	26,83	0,28	24,73	4744,77
62,73	26,85	0,28	24,23	4954,87
62,75	26,85	0,27	22,70	5060,93
62,77	26,80	0,27	22,70	5066,75
62,78	26,82	0,27	20,20	4826,95
62,80	26,87	0,27	19,06	4537,88
62,82	26,82	0,27	19,01	4382,55
62,83	26,82	0,28	19,88	4294,85
62,85	26,83	0,28	19,88	4408,04
62,87	26,83	0,28	21,16	4408,04
62,88	26,91	0,28	22,01	4997,11
62,90	26,85	0,27	22,61	5403,57
62,92	26,91	0,27	21,64	5761,97
62,93	26,82	0,27	20,76	5703,58
62,95	26,87	0,27	20,76	5705,79
62,97	26,83	0,27	18,92	5075,18
62,98	26,85	0,27	18,67	4664,40
63,00	26,85	0,27	20,48	4373,72
63,02	26,87	0,28	21,28	4231,84
63,03	26,87	0,28	21,28	4385,86
63,05	26,80	0,28	22,82	4385,86
63,07	26,83	0,28	23,96	4648,34
63,08	26,83	0,28	23,62	4951,16

63,10	26,88	0,28	22,20	5039,95
63,12	26,85	0,27	22,20	4907,41
63,13	26,95	0,27	20,37	4906,01
63,15	26,80	0,27	19,27	4618,55
63,17	26,87	0,28	18,80	4382,65
63,18	26,88	0,28	19,76	4218,51
63,20	26,90	0,28	20,42	4425,50
63,22	26,85	0,28	20,42	4426,90
63,23	26,91	0,28	21,33	4846,80
63,25	26,91	0,28	22,32	5317,39
63,27	26,83	0,28	22,16	5481,34
63,28	26,87	0,28	20,89	5493,07
63,30	26,83	0,27	20,89	5395,25
63,32	26,83	0,27	18,71	5395,25
63,33	26,91	0,27	18,73	5314,87
63,35	26,88	0,27	19,84	4825,03
63,37	26,83	0,28	21,44	4595,76
63,38	26,88	0,28	21,44	4537,97
63,40	26,88	0,28	22,04	4533,96
63,42	26,88	0,28	22,96	4569,58
63,43	26,85	0,28	23,14	4922,06
63,45	26,85	0,28	21,96	5431,26
63,47	26,93	0,27	20,08	5354,01
63,48	26,90	0,26	20,08	5359,23
63,50	26,85	0,27	19,22	5045,68
63,52	26,83	0,28	19,75	4583,13
63,53	26,87	0,28	19,55	4304,89
63,55	26,87	0,28	19,64	4411,85
63,57	26,85	0,28	19,64	4793,13
63,58	26,90	0,28	20,49	4793,13
63,60	26,87	0,28	21,23	5186,34
63,62	26,87	0,28	21,81	5235,01
63,63	26,83	0,28	21,52	5074,97
63,65	26,82	0,28	21,52	5317,78
63,67	26,85	0,28	20,04	5306,15
63,68	26,83	0,27	18,57	5800,31
63,70	26,91	0,27	19,04	5894,52
63,72	26,83	0,27	20,76	5616,69

63,73	26,88	0,28	21,58	5226,08
63,75	26,87	0,28	21,58	5227,08
63,77	26,85	0,28	21,82	5063,53
63,78	26,90	0,28	22,13	5019,48
63,80	26,90	0,28	22,55	4941,22
63,82	26,85	0,28	21,98	5117,81
63,83	26,95	0,27	21,98	5141,70
63,85	26,82	0,27	21,76	5141,70
63,87	26,90	0,28	21,69	4889,95
63,88	26,87	0,28	21,01	4713,87
63,90	26,85	0,28	20,35	4711,96
63,92	26,87	0,28	20,35	4972,83
63,93	26,87	0,28	19,47	4969,83
63,95	26,88	0,27	18,90	5261,30
63,97	26,83	0,28	19,44	5290,19
63,98	26,87	0,28	20,42	5012,06
64,00	26,88	0,28	20,34	4672,22
64,02	26,90	0,28	20,34	4667,41
64,03	26,90	0,28	20,04	4797,85
64,05	26,87	0,28	19,71	5318,49
64,07	26,88	0,28	19,91	5952,61
64,08	26,90	0,27	20,06	6320,04
64,10	26,91	0,27	20,06	6288,83
64,12	26,90	0,27	19,92	6287,43
64,13	26,91	0,28	20,85	5840,44
64,15	26,83	0,28	20,57	5481,13
64,17	26,90	0,28	20,15	5465,38
64,18	26,82	0,28	21,13	5553,98
64,20	26,88	0,28	21,13	5549,57
64,22	26,87	0,28	22,17	5538,53
64,23	26,91	0,27	22,62	5385,61
64,25	26,87	0,27	23,31	5077,18
64,27	26,87	0,28	22,39	4846,71
64,28	26,83	0,28	22,39	5025,11
64,30	26,87	0,28	21,08	5025,11
64,32	26,91	0,28	19,94	5284,97
64,33	26,87	0,28	19,33	5403,76
64,35	26,88	0,28	19,21	5308,24

64,37	26,88	0,28	19,21	5031,71
64,38	26,90	0,28	19,67	5042,94
64,40	26,85	0,28	18,98	4909,49
64,42	26,88	0,28	18,98	4999,10
64,43	26,90	0,28	18,82	5318,66
64,45	26,87	0,28	19,32	5822,25
64,47	26,87	0,27	19,32	5795,17
64,48	26,88	0,27	19,23	6567,26
64,50	26,88	0,27	19,09	7329,42
64,52	26,85	0,27	19,10	7714,20
64,53	26,88	0,27	18,89	7839,23
64,55	26,90	0,27	18,89	8172,74
64,57	26,90	0,27	18,62	8172,74
64,58	26,91	0,27	19,37	7338,96
64,60	26,85	0,27	18,65	7272,73
64,62	26,91	0,26	20,33	7085,51
64,63	26,93	0,27	20,33	7039,45
64,65	26,93	0,27	21,13	7041,05
64,67	26,87	0,28	27,37	5694,54
64,68	26,91	0,28	27,58	5558,49
64,70	26,93	0,28	35,94	5542,23
64,72	26,95	0,28	34,83	5981,81
64,73	26,93	0,28	34,83	6011,70
64,75	26,93	0,28	30,98	6010,70
64,77	26,91	0,28	28,23	5864,69
64,78	26,85	0,28	26,09	5784,39
64,80	26,95	0,27	22,10	5808,85
64,82	27,01	0,26	22,10	5722,73
64,83	26,99	0,24	18,06	5722,73
64,85	26,87	0,23	17,14	5842,11
64,87	26,85	0,23	15,07	4960,43
64,88	26,91	0,21	11,92	3388,95
64,90	26,82	0,17	11,92	2380,49
64,92	26,85	0,13	6,71	2364,04
64,93	26,82	0,11	9,65	2199,99
64,95	26,80	0,11	7,36	2278,57
64,97	26,91	0,11	8,83	3062,69
64,98	26,91	0,17	9,80	2762,52

65,00	26,91	0,44	9,80	2660,20
65,02	26,93	0,50	7,16	4176,78
65,03	26,74	0,40	10,07	5617,44
65,05	26,55	0,40	12,73	5075,94
65,07	27,17	0,50	15,57	3967,05
65,08	26,74	0,38	15,57	2706,96
65,10	28,74	0,52	13,56	2706,96
65,12	28,74	0,26	9,22	805,35
65,13	28,74	0,26	6,83	855,57
65,15	28,72	0,08	5,30	817,25
65,17	28,72	0,02	4,64	773,19
65,18	28,74	0,01	4,64	775,00
65,20	28,74	0,00	4,01	733,87
65,22	28,74	0,00	3,91	697,04
65,23	28,74	0,00	3,87	663,43
65,25	28,74	0,00	3,67	633,33
65,27	28,74	0,00	3,67	605,93
65,28	28,74	0,00	3,68	605,93
65,30	28,74	0,00	3,74	579,35
65,32	28,74	0,00	3,59	556,07
65,33	28,74	0,00	3,29	534,70
65,35	28,76	0,00	3,29	515,13
65,37	28,74	0,00	3,13	515,13
65,38	28,74	0,00	3,18	498,07
65,40	28,74	0,00	3,14	476,30
65,42	28,76	0,00	3,09	461,25
65,43	28,74	0,00	3,01	444,39
65,45	28,74	0,00	3,01	444,19
65,47	28,74	0,00	3,01	430,65
65,48	28,72	0,00	2,93	418,11
65,50	28,74	0,00	2,93	408,07
65,52	28,76	0,00	2,82	397,24
65,53	28,72	0,00	2,82	387,00
65,55	28,74	0,00	2,58	387,00
65,57	28,74	0,00	2,40	376,97
65,58	28,74	0,00	2,29	368,74
65,60	28,76	0,00	2,17	357,90
65,62	28,74	0,00	2,17	350,68

65,63	28,74	0,00	2,05	350,68
65,65	28,76	0,00	2,02	344,16
65,67	28,76	0,00	1,96	336,63
65,68	28,76	0,00	1,86	330,11
65,70	28,76	0,00	1,70	324,09
65,72	28,76	0,00	1,70	324,09
65,73	28,76	0,00	1,62	318,57
65,75	28,76	0,00	1,57	313,05
65,77	28,76	0,00	1,54	307,34
65,78	28,76	0,00	1,51	303,32
65,80	28,76	0,00	1,51	296,40
65,82	28,76	0,00	1,42	296,40
65,83	26,51	0,00	1,40	292,39
65,85	26,79	0,00	1,34	587,55
65,87	26,98	0,00	1,91	1679,88
65,88	26,83	0,01	1,91	6696,66
65,90	27,09	0,03	1,41	6662,35
65,92	27,01	0,05	18,74	12552,58
65,93	27,01	0,05	44,65	12591,82
65,95	26,98	0,05	60,22	11241,10
65,97	26,91	0,05	61,96	8246,18
65,98	26,79	0,04	61,96	8172,56
66,00	27,15	0,02	49,75	6102,12
66,02	28,72	0,01	38,22	2742,99
66,03	28,71	0,01	25,43	768,30
66,05	28,71	0,00	15,29	789,65
66,07	28,69	0,00	15,29	759,05
66,08	28,66	0,00	10,46	759,05
66,10	28,68	0,00	7,95	717,31
66,12	28,68	0,00	6,34	677,88
66,13	28,64	0,00	5,34	643,17
66,15	28,64	0,00	5,34	610,96
66,17	28,64	0,00	4,60	597,92
66,18	28,64	0,00	4,14	568,32
66,20	28,64	0,00	3,69	548,05
66,22	28,64	0,00	3,25	524,36
66,23	28,64	0,00	2,80	500,69

Apendix B – Chord length readings

Appendix B presents the recorded chord length data for the four experiments where phase inversion occurred. Only readings from around the phase inversion are shown.

Primol 352 experiments (from section 4.2.1.1)

69% oil fraction with 4 g/L of surfactant (Arlacel P135):

Relative Time	Time [min]	Median, No Wt	Mean, Sqr Wt	Counts/sec, No Wt, <10	counts/sec, No Wt, 10-50	counts/sec, No Wt, 50-150	counts/sec, No Wt, 150-300	counts/sec, No Wt, 300-1000	counts/sec, No Wt, >1000
00:00:04	1,57	8,77	173,01	388,77	279,69	46,83	3,82	0,56	0
00:00:13	1,72	8,11	172,10	3710,84	2373,33	441,54	53,24	8,16	0
00:00:23	1,88	9,25	124,66	3066,55	2335,17	439,40	36,42	2,47	0
00:00:33	2,05	8,08	189,09	3532,21	2254,86	437,17	47,95	7,26	0
00:00:43	2,22	9,02	240,30	3233,62	2380,42	434,29	50,51	8,50	0
00:00:53	2,38	8,77	177,85	3269,82	2317,00	442,47	49,36	8,90	0
00:01:03	2,55	8,34	171,92	3644,42	2429,28	469,64	49,17	7,71	0
00:01:13	2,72	9,25	175,49	3185,67	2355,03	488,44	65,88	9,75	0
00:01:23	2,88	8,19	191,62	3716,47	2431,85	497,88	55,63	12,06	0
00:01:33	3,05	8,83	191,96	3556,90	2552,03	500,98	50,17	9,82	0
00:01:43	3,22	8,64	192,67	3675,83	2535,98	543,46	55,47	13,14	0
00:01:53	3,38	8,60	146,72	4089,28	2913,34	483,90	38,03	5,78	0
00:02:03	3,55	8,03	146,10	4074,67	2605,22	526,69	45,62	6,92	0
00:02:13	3,72	9,77	330,28	6629,07	4905,94	1187,07	217,69	139,34	0
00:02:23	3,88	9,20	394,05	11876,10	9002,75	1374,93	158,74	94,99	0
00:02:33	4,05	10,71	343,03	12236,50	11242,80	1851,49	185,37	96,56	0
00:02:43	4,22	9,67	496,17	5878,14	4325,42	952,57	136,00	224,32	0
00:02:53	4,38	6,85	618,63	3473,93	1554,84	386,01	61,09	181,58	0
00:03:03	4,55	7,15	642,18	3674,19	1583,40	481,84	68,33	178,47	0
00:03:13	4,72	7,20	476,30	4038,72	1886,99	542,24	104,17	164,77	0
00:03:23	4,88	7,84	796,44	3512,42	1789,94	496,61	91,43	228,93	0
00:03:33	5,05	8,50	583,86	3448,79	1895,23	617,73	169,28	193,86	0
00:03:43	5,22	8,58	671,06	2813,86	1550,56	517,59	135,92	232,30	0
00:03:53	5,38	9,40	623,63	2475,17	1473,68	503,25	149,73	190,74	0

Grane oil experiments (from section 4.2.2)

69% oil fraction:

Relative Time	Time [min]	Median, No Wt	Mean, Sqr Wt	Counts/sec, No Wt, <10	counts/sec, No Wt, 10-50	counts/sec, No Wt, 50-150	counts/sec, No Wt, 150-300	counts/sec, No Wt, 300-1000	counts/sec, No Wt, >1000
00:00:04	0,07	4,57	25,18	237,78	20,56	0,00	0,00	0,00	0
00:00:13	0,22	4,65	25,66	2067,94	200,18	1,76	0,00	0,00	0
00:00:23	0,38	4,77	30,13	1967,00	182,21	13,90	0,00	0,00	0
00:00:33	0,55	4,69	37,87	1924,30	127,46	36,02	0,00	0,00	0
00:00:43	0,72	4,62	38,68	1894,92	136,55	28,64	0,00	0,00	0
00:00:53	0,88	4,70	38,91	1815,28	176,16	25,12	0,00	0,00	0
00:01:03	1,05	4,65	38,07	1785,94	200,98	20,97	0,00	0,00	0
00:01:13	1,22	5,05	34,24	5735,38	1342,99	50,07	0,00	0,00	0
00:01:23	1,38	4,93	588,64	27235,00	6010,10	265,00	62,06	46,89	0
00:01:33	1,55	7,94	299,30	7556,26	4971,40	384,16	72,76	41,20	0
00:01:43	1,72	8,86	340,69	4654,74	3044,19	843,41	99,15	48,62	0
00:01:53	1,88	5,68	288,06	6138,01	2228,99	374,89	64,67	25,88	0
00:02:03	2,05	6,92	156,90	11088,20	5769,46	693,12	127,25	13,90	0
00:02:13	2,22	8,34	192,94	5861,71	3818,04	696,95	122,00	20,53	0
00:02:23	2,38	7,48	155,27	6836,05	3993,86	618,73	104,61	12,21	0
00:02:33	2,55	8,25	139,27	6617,01	4451,65	587,06	60,30	7,32	0
00:02:43	2,72	6,09	97,31	9273,60	3809,96	425,03	30,68	1,29	0
00:02:53	2,88	6,15	126,03	12393,00	4956,81	685,16	67,00	5,17	0
00:03:03	3,05	6,39	112,42	12388,30	5532,36	702,75	54,80	4,19	0
00:03:13	3,22	7,17	150,32	8430,06	4586,93	389,21	73,89	4,14	0
00:03:23	3,38	8,03	163,58	6888,02	4535,46	415,67	50,45	8,62	0
00:03:33	3,55	6,77	104,00	6843,78	3598,02	343,06	26,07	2,17	0
00:03:43	3,72	7,27	125,94	5896,23	3267,49	410,37	44,31	4,04	0
00:03:53	3,88	6,75	125,77	6978,20	3697,37	312,89	33,36	5,51	0
00:04:03	4,05	7,33	107,59	6454,89	3739,25	419,31	37,30	2,24	0
00:04:13	4,22	7,29	109,29	6304,17	3518,25	429,51	22,96	2,22	0
00:04:23	4,38	7,03	97,42	7041,75	3730,68	537,22	28,13	1,56	0
00:04:33	4,55	7,40	109,89	6749,25	3861,47	540,82	38,62	2,29	0
00:04:43	4,72	7,26	104,90	6280,33	3425,49	440,69	28,79	2,81	0
00:04:53	4,88	6,56	100,47	6014,47	3020,39	382,98	27,21	1,40	0
00:05:03	5,05	5,94	77,77	7082,42	3174,46	336,92	13,44	0,54	0
00:05:13	5,22	6,01	80,58	6864,10	3105,35	369,27	15,41	0,65	0
00:05:23	5,38	6,56	86,14	6675,76	3419,27	377,73	17,23	0,78	0
00:05:33	5,55	6,64	84,99	6565,77	3191,98	498,51	22,97	0,44	0

00:05:43	5,72	6,28	88,65	6312,24	2771,16	443,67	24,52	0,42	0
00:05:53	5,88	5,50	79,88	7225,05	2660,64	469,18	13,65	0,37	0
00:06:03	6,05	5,11	87,01	7486,63	2230,19	386,25	10,77	1,27	0
00:06:13	6,22	5,56	125,27	6272,32	2477,93	413,75	27,42	3,81	0
00:06:23	6,38	5,33	88,77	6534,74	2412,42	435,23	13,45	1,16	0
00:06:33	6,55	5,56	82,50	6714,42	2732,25	420,87	16,38	0,74	0
00:06:43	6,72	5,32	110,53	6750,65	2293,33	421,32	10,70	2,44	0
00:06:53	6,88	5,44	140,95	7306,26	2565,26	419,31	33,93	5,23	0
00:07:03	7,05	5,06	77,52	7104,34	2226,50	386,88	11,75	0,54	0
00:07:13	7,22	5,08	107,33	7106,43	2201,26	383,74	18,13	1,56	0
00:07:23	7,38	5,02	113,65	7811,43	2552,38	382,45	18,92	3,26	0
00:07:33	7,55	5,41	97,73	8253,67	2939,15	420,80	19,07	1,88	0
00:07:43	7,72	5,62	80,99	8375,96	3065,36	450,66	16,93	0,76	0
00:07:53	7,88	5,49	110,60	7216,66	2545,85	452,87	24,55	2,28	0
00:08:03	8,05	5,77	107,92	7036,12	2675,26	481,16	41,65	1,70	0
00:08:13	8,22	5,91	118,79	6646,35	2725,91	454,54	37,24	2,96	0
00:08:23	8,38	5,99	151,10	6273,52	2743,73	470,85	37,54	5,47	0
00:08:33	8,55	5,60	99,27	6546,22	2557,90	468,95	26,18	1,43	0
00:08:43	8,72	5,57	131,51	6559,22	2445,72	492,04	44,20	5,04	0
00:08:53	8,88	5,64	112,07	6776,75	2588,13	532,61	33,95	1,45	0
00:09:03	9,05	5,54	96,23	6450,04	2508,62	494,85	30,12	0,92	0
00:09:13	9,22	5,27	128,01	7216,26	2492,72	524,85	41,61	4,67	0
00:09:23	9,38	5,25	153,94	7353,28	2403,72	515,02	54,99	8,99	0
00:09:33	9,55	4,96	173,14	7988,27	2360,56	514,73	50,27	9,28	0
00:09:43	9,72	5,09	168,74	7260,44	2321,40	498,05	46,86	9,47	0
00:09:53	9,88	5,50	163,98	6401,75	2433,46	520,02	52,82	10,06	0
00:10:03	10,05	5,09	185,63	7119,51	2312,72	532,32	60,80	12,32	0
00:10:13	10,22	4,91	181,54	7990,85	2348,10	504,46	48,93	10,21	0
00:10:23	10,38	4,81	193,59	8612,68	2262,57	470,07	47,50	13,07	0
00:10:33	10,55	4,93	169,90	8449,72	2291,25	503,72	50,50	9,49	0
00:10:43	10,72	4,76	197,46	8789,83	2257,14	441,93	49,65	12,68	0
00:10:53	10,88	4,81	162,70	9046,19	2308,12	478,36	50,55	8,68	0
00:11:03	11,05	4,54	163,67	10277,40	2265,57	435,68	31,68	8,14	0
00:11:13	11,22	4,36	112,74	10832,70	2172,29	389,95	19,77	2,37	0
00:11:23	11,38	4,49	107,10	9866,59	2293,60	425,12	27,62	1,96	0
00:11:33	11,55	4,33	76,77	11295,40	2207,95	364,39	9,14	0,21	0
00:11:43	11,72	4,34	81,54	11436,50	2222,72	359,94	14,72	0,00	0
00:11:53	11,88	4,37	90,06	11582,30	2252,49	387,08	20,39	0,11	0
00:12:03	12,05	6,04	111,40	7275,94	2785,99	1057,00	59,22	0,85	0
00:12:13	12,22	6,71	173,06	7381,39	3202,99	1155,45	111,85	21,10	0
00:12:23	12,38	6,11	179,30	7100,28	2747,09	1003,61	203,68	14,89	0
00:12:33	12,55	6,82	271,16	6980,42	3140,13	859,28	203,48	42,92	0

62.5% oil fraction:

Relative Time	Time [min]	Median, No Wt	Mean, Sqr Wt	Counts/sec, No Wt, <10	counts/sec, No Wt, 10-50	counts/sec, No Wt, 50-150	counts/sec, No Wt, 150-300	counts/sec, No Wt, 300-1000	counts/sec, No Wt, >1000
00:15:07	15,12	4,97	121,49	9139,08	2467,50	556,31	22,67	5,44	0
00:15:09	15,15	4,72	77,61	10908,10	2346,76	569,51	17,63	0,00	0
00:15:12	15,20	4,82	100,07	8960,95	2228,20	481,70	26,72	1,44	0
00:15:14	15,23	4,85	276,99	9939,32	2431,47	483,16	27,42	30,63	0
00:15:16	15,27	4,90	67,39	10964,30	2520,22	610,50	14,94	0,00	0
00:15:18	15,30	4,73	80,42	11238,90	2357,68	682,84	24,63	0,00	0
00:15:19	15,32	4,68	99,24	10047,50	2155,48	666,70	20,93	3,44	0
00:15:22	15,37	4,77	77,72	11470,30	2527,82	562,76	14,10	0,00	0
00:15:23	15,38	4,86	143,60	9338,67	2255,73	661,96	32,20	13,44	0
00:15:25	15,42	4,88	80,61	9857,33	2506,08	687,70	17,89	0,00	0
00:15:27	15,45	4,70	98,07	10367,80	2205,91	527,14	32,17	0,00	0
00:15:29	15,48	4,70	108,84	9178,24	2097,18	479,89	27,69	2,00	0
00:15:31	15,52	4,80	113,85	9710,30	2289,51	621,41	35,90	2,88	0
00:15:33	15,55	4,93	64,42	9887,72	2691,33	565,26	7,69	0,00	0
00:15:35	15,58	4,92	98,67	9985,92	2552,46	614,15	23,47	4,00	0
00:15:38	15,63	4,82	118,89	10049,60	2376,86	748,17	41,36	2,00	0
00:15:40	15,67	4,73	91,96	10782,30	2378,07	753,02	28,58	0,00	0
00:15:42	15,70	4,78	109,96	9750,62	2223,38	624,00	47,99	1,00	0
00:15:44	15,73	4,74	75,24	10701,40	2420,92	711,09	7,58	1,00	0
00:15:46	15,77	4,76	119,36	9611,86	2205,70	606,56	58,89	3,00	0
00:15:48	15,80	4,88	177,25	10043,70	2234,98	624,75	63,65	13,88	0
00:15:50	15,83	4,86	84,72	9853,06	2373,60	808,86	17,49	1,00	0
00:15:51	15,85	4,67	110,80	10932,70	2245,12	633,68	46,21	0,26	0
00:15:53	15,88	4,72	88,47	10996,40	2139,39	700,42	25,40	0,44	0
00:15:55	15,92	4,62	147,19	11032,60	2203,71	685,68	69,57	11,44	0
00:15:57	15,95	4,85	282,16	10065,00	2134,79	821,09	38,16	18,00	0
00:15:59	15,98	4,68	192,52	10951,80	2407,23	675,60	40,92	14,44	0
00:16:01	16,02	4,62	100,09	10009,90	2189,15	572,83	14,90	1,26	0
00:16:04	16,07	4,60	78,82	11195,50	2216,15	653,81	19,54	0,00	0
00:16:06	16,10	4,55	118,47	11665,30	2217,24	623,84	32,37	4,26	0
00:16:08	16,13	4,74	170,64	11199,40	2337,95	740,85	67,85	14,98	0
00:16:10	16,17	4,84	240,40	9299,71	2458,28	704,44	98,38	40,19	0
00:16:12	16,20	4,68	76,46	11972,70	2415,10	735,06	8,16	1,00	0
00:16:13	16,22	4,69	70,33	12403,00	2606,80	606,78	15,43	0,00	0
00:16:16	16,27	4,79	68,21	8645,35	2500,89	576,60	10,16	0,00	0
00:16:17	16,28	4,52	111,05	11613,40	2041,90	654,33	21,54	3,88	0

00:16:19	16,32	4,63	152,26	11845,20	2512,31	739,83	41,79	10,88	0
00:16:21	16,35	4,62	99,80	11351,80	2332,58	720,64	47,94	0,00	0
00:16:23	16,38	4,61	92,67	10859,50	2400,01	759,68	38,83	0,00	0
00:16:25	16,42	4,75	81,95	10957,00	2468,22	638,44	16,36	1,00	0
00:16:27	16,45	4,59	161,96	12369,20	2260,49	705,73	43,18	16,45	0
00:16:30	16,50	4,70	215,25	11119,70	2294,10	754,33	59,72	21,19	0
00:16:32	16,53	4,73	169,39	10380,60	2305,47	777,22	29,23	12,44	0
00:16:34	16,57	4,87	99,69	9324,10	2459,61	741,56	46,72	0,00	0
00:16:36	16,60	4,74	131,71	11654,90	2519,33	697,31	34,72	6,70	0
00:16:38	16,63	4,69	96,41	10345,90	2259,27	574,33	27,03	1,44	0
00:16:40	16,67	4,74	142,51	12460,80	2245,74	768,55	41,01	8,88	0
00:16:41	16,68	4,80	148,17	10582,40	2229,05	780,84	73,24	11,44	0
00:16:43	16,72	4,96	82,28	10137,10	2401,72	815,97	14,17	0,00	0
00:16:45	16,75	4,81	108,91	10469,00	2242,40	722,27	27,36	3,00	0
00:16:47	16,78	4,94	215,43	8805,54	2298,80	629,14	77,32	42,20	0
00:16:49	16,82	4,79	170,15	10264,40	2342,83	655,00	48,42	18,31	0
00:16:52	16,87	4,77	109,42	11743,90	2423,36	835,80	27,52	4,42	0
00:16:54	16,90	4,67	79,26	12074,50	2398,99	618,06	17,98	0,44	0
00:16:56	16,93	4,69	384,61	12017,50	2337,17	764,48	25,40	36,44	0
00:16:58	16,97	4,74	112,43	12162,90	2443,03	826,74	25,31	3,00	0
00:17:00	17,00	4,59	92,56	13569,50	2300,45	700,30	27,79	0,00	0
00:17:02	17,03	4,52	146,39	13910,30	2135,70	659,09	11,51	9,44	0
00:17:03	17,05	4,58	163,11	12742,50	2200,87	644,77	40,99	8,88	0
00:17:05	17,08	4,66	123,68	13275,40	2457,65	694,04	26,01	6,88	0
00:17:07	17,12	4,68	292,55	11587,30	2098,64	579,20	59,59	62,25	0
00:17:09	17,15	4,72	122,44	12840,70	2332,94	678,85	55,08	2,44	0
00:17:11	17,18	4,62	68,14	12627,20	2163,07	707,82	3,94	0,00	0
00:17:13	17,22	4,66	140,95	12626,30	2112,85	695,96	57,19	6,75	0
00:17:15	17,25	4,71	104,56	12093,60	2358,39	635,84	42,76	0,44	0
00:17:18	17,30	4,85	113,83	12067,80	2426,84	801,77	29,33	5,31	0
00:17:20	17,33	4,64	75,07	12373,10	2232,07	677,79	13,05	0,00	0
00:17:22	17,37	4,77	61,70	11749,40	2410,65	600,98	3,00	0,00	0
00:17:24	17,40	4,78	124,32	11764,10	2327,22	640,29	41,10	6,31	0
00:17:26	17,43	4,71	91,77	12791,50	2203,07	847,91	30,52	0,00	0
00:17:27	17,45	4,70	128,44	12988,10	2369,24	733,65	36,31	6,75	0
00:17:29	17,48	4,66	136,45	12218,10	2177,60	766,75	61,21	5,31	0
00:17:31	17,52	4,80	77,91	13176,40	2585,37	807,31	15,51	1,44	0
00:17:33	17,55	4,72	101,52	11154,90	2361,34	640,14	40,57	2,00	0
00:17:35	17,58	4,55	83,06	14457,80	2208,20	656,79	17,22	1,00	0
00:17:37	17,62	4,54	182,58	14241,20	2015,25	617,06	29,41	17,06	0
00:17:39	17,65	4,67	127,17	13307,80	2132,39	741,13	48,23	4,44	0
00:17:41	17,68	4,66	86,51	13733,30	2218,77	715,50	27,47	0,00	0
00:17:44	17,73	4,66	143,24	12275,60	2171,46	657,75	82,19	5,00	0

00:17:46	17,77	4,60	137,84	13082,70	2052,53	689,58	65,17	5,00	0
00:17:48	17,80	4,76	183,25	12138,90	2162,02	646,53	56,38	23,16	0
00:17:50	17,83	4,67	99,06	13148,20	2444,72	626,59	26,03	1,44	0
00:17:52	17,87	4,68	115,70	13401,70	2073,35	742,70	56,96	1,31	0
00:17:54	17,90	4,63	96,10	14146,50	2036,50	711,71	35,87	0,44	0
00:17:55	17,92	4,59	124,81	14906,20	2133,37	719,36	31,48	6,63	0
00:17:57	17,95	4,58	93,28	14604,80	1878,62	654,05	12,58	2,00	0
00:17:59	17,98	4,63	137,00	14907,60	1948,15	649,17	39,63	9,42	0
00:18:01	18,02	4,75	327,37	12899,30	2012,86	598,60	68,08	56,12	0
00:18:03	18,05	4,76	113,30	14531,60	2105,42	631,46	38,08	2,44	0
00:18:05	18,08	4,67	81,86	14523,60	2112,53	629,91	11,94	0,00	0
00:18:08	18,13	4,97	108,66	12560,10	2194,98	776,83	29,18	2,88	0
00:18:10	18,17	4,91	131,56	12184,40	2009,76	682,02	55,79	5,98	0
00:18:12	18,20	4,80	138,95	14102,10	2209,97	645,42	27,90	6,57	0
00:18:14	18,23	4,83	156,11	13471,90	2206,99	750,23	47,42	16,44	0
00:18:16	18,27	4,75	104,77	14388,50	1999,82	763,35	38,31	1,00	0
00:18:17	18,28	4,70	233,11	13558,00	1816,39	540,56	51,07	18,94	0
00:18:20	18,33	4,76	142,20	14809,70	2152,14	647,63	34,29	8,19	0
00:18:21	18,35	5,07	113,59	10824,90	2083,15	648,65	30,61	4,70	0
00:18:23	18,38	4,93	74,77	13844,70	2383,01	693,45	13,89	0,00	0
00:18:25	18,42	5,01	87,03	12769,00	2384,18	627,29	29,52	1,00	0
00:18:27	18,45	4,95	114,93	12960,00	2448,37	562,34	36,37	4,88	0
00:18:29	18,48	4,90	108,85	13574,00	2274,60	759,07	15,38	5,00	0
00:18:31	18,52	5,00	266,27	12655,70	2310,32	768,41	38,65	23,88	0
00:18:34	18,57	5,02	159,69	13364,70	2384,23	809,12	43,45	17,50	0
00:18:36	18,60	4,76	92,80	15094,20	1947,81	681,19	12,40	2,44	0
00:18:38	18,63	4,92	107,30	14228,20	2010,99	667,29	36,48	1,00	0
00:18:40	18,67	4,89	173,27	13791,60	1971,87	637,17	33,93	14,44	0
00:18:42	18,70	4,97	93,93	14897,30	2369,69	771,01	22,73	1,26	0
00:18:44	18,73	4,90	79,37	14312,10	2233,02	770,46	12,39	1,00	0
00:18:45	18,75	4,79	115,00	15120,20	2030,76	698,67	27,49	4,88	0
00:18:47	18,78	4,89	179,88	13611,70	2035,57	671,46	48,45	19,86	0
00:18:49	18,82	4,80	200,47	14577,70	2056,24	575,95	35,97	37,17	0
00:18:51	18,85	5,14	99,88	13673,90	2603,50	846,75	41,45	0,44	0
00:18:53	18,88	5,04	99,75	14397,70	2478,37	840,15	47,74	0,00	0
00:18:55	18,92	4,82	74,69	15368,40	1996,21	700,94	8,47	0,00	0
00:18:57	18,95	4,95	113,10	13808,40	1986,81	775,52	63,31	0,00	0
00:19:00	19,00	4,71	117,12	15215,70	1785,75	521,34	23,17	5,00	0
00:19:02	19,03	5,02	93,60	13353,10	2267,29	734,65	15,96	3,00	0
00:19:04	19,07	5,08	86,77	11996,20	2195,59	458,06	12,28	1,88	0
00:19:06	19,10	4,80	74,72	15169,20	2032,76	531,61	11,42	0,00	0
00:19:07	19,12	4,75	96,62	14349,40	1619,99	568,71	39,89	0,00	0
00:19:09	19,15	4,72	100,03	14583,30	1666,15	509,17	32,41	0,00	0

00:19:12	19,20	4,81	137,79	14938,30	1862,05	482,26	40,23	5,19	0
00:19:13	19,22	4,84	135,39	13769,10	1983,09	579,54	31,87	5,44	0
00:19:15	19,25	4,87	100,39	12517,00	2043,12	481,10	21,78	2,00	0
00:19:17	19,28	5,02	121,96	12658,40	2299,74	631,18	14,99	4,70	0
00:19:19	19,32	4,88	94,07	13470,40	2209,95	678,03	16,21	2,44	0
00:19:21	19,35	4,81	86,65	15095,80	2103,71	545,49	30,00	0,00	0
00:19:23	19,38	4,58	64,84	15871,70	1755,46	440,89	2,94	0,00	0
00:19:26	19,43	4,68	76,89	15590,40	1854,79	554,19	8,58	0,00	0
00:19:28	19,47	4,67	80,57	15557,10	1772,26	505,95	11,64	0,00	0
00:19:30	19,50	4,68	207,70	14610,10	1547,80	376,58	57,78	17,75	0
00:19:32	19,53	4,66	108,92	15545,30	1723,40	378,40	36,87	0,00	0
00:19:34	19,57	4,88	132,02	11243,00	1538,03	678,61	106,31	0,00	0
00:19:36	19,60	4,76	78,71	15253,60	1785,64	523,65	12,10	0,00	0
00:19:37	19,62	4,71	96,78	15545,70	1930,16	491,96	23,16	0,00	0
00:19:39	19,65	4,76	102,40	16060,00	1952,93	485,94	39,11	0,00	0
00:19:41	19,68	4,88	94,54	14103,10	2038,81	611,16	29,95	0,00	0
00:19:43	19,72	5,16	94,00	14245,80	2085,94	785,29	42,01	0,00	0
00:19:46	19,77	5,00	77,90	12174,00	1740,28	730,31	10,36	0,00	0
00:19:48	19,80	5,03	68,06	10694,70	1700,81	492,03	0,47	0,00	0
00:19:50	19,83	5,01	69,28	10553,60	1847,58	546,85	0,00	0,00	0
00:19:52	19,87	5,01	89,56	11325,60	1711,11	607,33	38,95	0,00	0
00:19:54	19,90	5,06	82,96	12430,10	1839,54	613,34	15,06	0,00	0
00:19:56	19,93	5,25	101,85	10463,20	2077,29	829,11	44,36	0,00	0
00:19:57	19,95	5,38	133,34	11949,90	2120,23	943,86	216,99	0,00	0
00:19:59	19,98	5,20	130,69	11802,50	1709,15	733,48	186,87	0,00	0
00:20:01	20,02	5,12	100,28	13497,10	2165,57	940,33	54,04	0,00	0
00:20:03	20,05	5,09	157,53	11716,70	1800,68	698,60	221,33	5,70	0
00:20:05	20,08	5,32	133,85	12705,20	2333,84	695,11	110,84	0,00	0
00:20:07	20,12	5,29	107,24	13820,10	2632,18	903,53	62,22	0,00	0
00:20:10	20,17	5,49	269,32	12465,60	2921,52	764,71	196,33	50,88	0
00:20:12	20,20	5,83	154,86	10418,10	2651,34	1162,90	319,63	0,00	0
00:20:14	20,23	5,29	179,99	11811,70	2136,94	797,18	152,31	23,85	0
00:20:16	20,27	5,44	177,40	13046,50	2546,85	772,12	165,22	19,28	0
00:20:18	20,30	5,40	127,84	12535,70	3096,02	1021,82	172,47	0,00	0
00:20:20	20,33	6,05	149,59	9511,69	2847,66	1337,35	244,91	6,39	0
00:20:21	20,35	5,61	130,41	12026,70	3232,55	1212,55	116,93	0,26	0
00:20:23	20,38	5,65	136,44	10464,50	2989,24	775,30	140,99	0,00	0
00:20:25	20,42	5,73	153,70	10910,10	2692,76	938,16	346,54	0,44	0
00:20:27	20,45	5,91	145,64	10683,70	3246,96	924,37	305,99	0,00	0
00:20:29	20,48	5,84	172,21	10115,20	2730,69	904,47	285,16	24,45	0
00:20:31	20,52	5,94	133,48	12188,90	3011,64	888,44	185,05	0,00	0
00:20:34	20,57	5,85	234,45	9664,13	2520,66	683,86	260,09	36,26	0
00:20:36	20,60	5,64	170,52	10605,10	2236,80	637,53	435,60	0,00	0

00:20:38	20,63	5,77	158,22	8901,53	2305,70	853,59	364,29	2,89	0
00:20:40	20,67	5,90	163,81	9312,79	2626,11	729,00	375,09	0,00	0
00:20:42	20,70	6,42	175,90	9894,09	3304,41	854,41	383,97	9,12	0
00:20:44	20,73	6,39	148,35	10499,90	3488,66	796,42	324,84	8,17	0
00:20:45	20,75	6,01	168,57	9124,96	2277,47	711,02	393,48	3,06	0
00:20:47	20,78	6,12	193,92	9224,83	2626,19	663,53	429,17	14,28	0
00:20:49	20,82	6,63	157,51	8487,29	2999,67	1148,52	326,45	7,06	0
00:20:51	20,85	5,86	133,28	9864,88	3019,92	919,69	296,51	0,00	0
00:20:53	20,88	6,24	157,15	8822,72	2829,33	1041,70	382,49	6,76	0
00:20:55	20,92	6,10	139,89	9066,57	2488,96	927,56	296,91	0,00	0
00:20:57	20,95	6,24	117,46	9801,32	3158,94	1195,88	139,87	0,00	0
00:21:00	21,00	6,63	135,82	8060,58	3013,79	1099,19	220,44	0,00	0
00:21:02	21,03	6,45	138,14	9091,08	3226,81	1090,09	272,02	0,00	0

50% oil fraction:

Relative Time	Time [min]	Median, No Wt	Mean, Sqr Wt	Counts/sec, No Wt, <10	counts/sec, No Wt, 10-50	counts/sec, No Wt, 50-150	counts/sec, No Wt, 150-300	counts/sec, No Wt, 300-1000	counts/sec, No Wt, >1000
00:58:04	58,07	6,78	90,68	9345,76	4082,13	1576,82	69,94	0,36	0
00:58:09	58,15	6,31	99,56	9529,64	3666,37	1452,99	74,46	1,54	0
00:58:14	58,23	6,30	85,43	10448,10	4054,95	1362,86	38,62	0,46	0
00:58:19	58,32	6,83	164,68	6991,26	2860,42	1290,19	130,07	23,56	0
00:58:24	58,40	6,61	159,13	6844,26	2895,54	1040,14	113,35	16,96	0
00:58:29	58,48	6,16	156,92	7657,85	3021,66	1095,50	77,60	20,14	0
00:58:34	58,57	6,55	143,90	6911,43	3149,01	844,68	117,83	5,29	0
00:58:39	58,65	6,29	160,17	8303,01	3594,84	1233,22	60,39	15,04	0
00:58:44	58,73	5,91	168,75	8372,24	3242,80	1000,60	82,55	20,31	0
00:58:49	58,82	5,64	139,83	9220,22	3213,53	1204,17	100,62	5,46	0
00:58:54	58,90	5,49	200,19	8618,47	2910,20	974,72	118,54	29,56	0
00:58:59	58,98	5,80	119,72	9644,13	3624,64	1145,73	63,18	5,33	0
00:59:04	59,07	6,00	111,52	8559,74	3284,41	1137,88	59,17	2,80	0
00:59:09	59,15	5,84	129,51	9085,03	3295,55	1112,23	82,64	6,05	0
00:59:14	59,23	5,74	124,78	8952,20	3172,36	1179,20	99,52	5,22	0
00:59:19	59,32	5,56	170,35	9678,42	3413,80	918,91	80,27	12,35	0
00:59:24	59,40	5,81	121,67	9194,33	3185,59	1189,87	97,73	3,97	0
00:59:29	59,48	5,81	169,37	8541,15	3190,63	881,43	86,77	12,27	0
00:59:34	59,57	6,22	201,23	7857,86	3043,08	1130,95	109,69	29,16	0
00:59:39	59,65	5,48	144,76	9541,25	3174,77	1086,64	65,84	10,26	0
00:59:44	59,73	5,33	120,50	9810,37	2899,14	1221,12	87,86	3,77	0
00:59:49	59,82	5,05	166,32	10100,50	2855,50	1050,27	81,68	10,33	0
00:59:54	59,90	5,18	156,44	9954,95	2943,54	1092,69	90,61	17,21	0
00:59:59	59,98	5,60	158,49	8705,93	2902,35	1090,74	142,17	12,31	0
01:00:04	60,07	5,24	204,04	9159,43	2783,90	1089,21	88,70	23,52	0
01:00:09	60,15	5,24	162,83	9266,29	2798,45	1133,97	108,01	17,78	0
01:00:14	60,23	5,16	145,75	9283,97	2677,25	1203,90	86,99	10,39	0
01:00:19	60,32	4,94	126,20	10097,80	2686,28	1133,63	119,82	2,72	0
01:00:24	60,40	5,20	143,31	10054,50	2941,00	1017,18	77,31	11,49	0
01:00:29	60,48	5,06	314,26	10091,90	2697,11	1044,82	85,47	29,43	0
01:00:34	60,57	5,26	178,50	9264,58	2749,32	1052,05	106,80	22,25	0
01:00:39	60,65	5,15	155,00	10124,80	2743,23	1178,43	112,64	13,15	0
01:00:44	60,73	5,03	137,93	10538,60	2890,37	1020,20	78,81	7,23	0
01:00:49	60,82	5,48	141,48	9485,02	2844,43	1118,13	110,67	6,25	0
01:00:54	60,90	5,30	148,49	10128,10	3013,97	1134,98	70,27	14,14	0
01:00:59	60,98	5,25	227,99	10120,40	2707,64	1021,19	100,89	31,91	0

01:01:04	61,07	5,30	123,26	10662,00	3092,74	1084,74	56,38	5,63	0
01:01:09	61,15	5,06	121,57	11265,80	2847,42	1052,02	84,20	4,57	0
01:01:14	61,23	5,51	152,88	10135,80	3047,21	1121,85	70,05	14,29	0
01:01:19	61,32	5,44	110,81	10033,40	2987,42	1186,73	66,84	3,11	0
01:01:24	61,40	5,24	164,02	10542,30	2981,69	1027,18	79,09	10,20	0
01:01:29	61,48	5,43	153,83	10040,70	2960,23	1050,12	98,23	9,27	0
01:01:34	61,57	5,20	121,80	11034,10	2961,71	1050,77	84,99	6,65	0
01:01:39	61,65	5,16	157,82	10249,70	2789,13	1089,27	85,31	11,58	0
01:01:44	61,73	5,22	218,09	10334,00	2743,45	1124,40	99,10	10,34	0
01:01:49	61,82	4,93	176,80	11175,50	2667,21	1011,00	81,40	20,67	0
01:01:54	61,90	5,07	173,89	10349,10	2715,14	978,35	98,02	24,42	0
01:01:59	61,98	5,10	173,92	10836,80	2712,38	1054,78	90,54	12,77	0
01:02:04	62,07	5,01	200,85	10515,10	2526,07	1030,48	102,07	31,77	0
01:02:09	62,15	4,86	171,93	11488,10	2561,59	1064,66	104,59	21,05	0
01:02:14	62,23	4,75	144,49	12490,20	2421,57	1012,93	105,64	7,91	0
01:02:19	62,32	4,78	131,50	12718,10	2511,21	1029,97	83,58	6,91	0
01:02:24	62,40	4,94	168,88	11944,70	2532,93	1011,18	94,31	11,14	0
01:02:29	62,48	4,95	121,05	12057,10	2600,49	1045,49	90,11	3,01	0
01:02:34	62,57	4,72	158,65	12962,60	2468,61	1065,26	59,56	13,00	0
01:02:39	62,65	5,00	145,16	11303,80	2374,23	993,37	119,26	6,55	0
01:02:44	62,73	4,88	118,78	12741,20	2559,30	1094,76	63,93	3,30	0
01:02:49	62,82	4,94	125,14	12680,00	2496,67	1018,93	73,83	4,56	0
01:02:54	62,90	5,07	162,26	12241,40	2558,12	1072,14	79,18	10,13	0
01:02:59	62,98	4,92	126,68	13158,60	2745,18	1060,93	41,20	8,83	0
01:03:04	63,07	4,93	216,13	12336,40	2679,50	1009,85	77,04	20,42	0
01:03:09	63,15	5,02	202,34	11562,50	2627,99	952,13	104,92	17,52	0
01:03:14	63,23	5,04	158,08	11862,40	2800,16	1068,29	96,35	14,81	0
01:03:19	63,32	5,04	131,88	11825,10	2861,98	1145,80	78,87	4,25	0
01:03:24	63,40	4,84	129,02	12959,80	2780,97	1024,41	87,10	6,02	0
01:03:29	63,48	4,88	128,17	12639,40	2800,19	1115,34	72,44	6,13	0
01:03:34	63,57	4,91	133,04	12291,00	2796,55	1071,06	92,28	8,14	0
01:03:39	63,65	4,96	153,54	12074,50	2883,24	1089,40	82,00	5,86	0
01:03:44	63,73	5,04	125,44	12199,90	3049,16	1142,55	74,46	3,47	0
01:03:49	63,82	4,95	162,62	12250,10	2829,33	1067,49	78,37	20,97	0
01:03:54	63,90	4,85	160,34	12608,30	2757,65	1048,00	100,95	14,34	0
01:03:59	63,98	5,05	136,33	11765,40	2895,85	1080,05	109,04	5,66	0
01:04:04	64,07	4,98	157,19	12316,40	2827,02	1163,15	76,96	10,97	0
01:04:09	64,15	5,03	119,96	12249,90	2839,85	1168,62	87,26	2,09	0
01:04:14	64,23	5,05	123,02	12538,80	2850,09	1178,22	91,46	4,14	0
01:04:19	64,32	5,08	210,69	12139,40	2829,83	1137,08	83,81	30,91	0
01:04:24	64,40	5,11	138,39	12715,00	2885,38	1111,77	89,71	5,84	0
01:04:29	64,48	5,27	134,90	12289,30	3013,58	1184,20	73,18	6,00	0
01:04:34	64,57	5,09	133,73	12832,20	2790,62	1010,75	72,98	8,22	0

01:04:39	64,65	5,13	143,52	12761,60	2810,85	1000,01	78,98	11,05	0
01:04:44	64,73	5,26	139,89	12144,40	2995,02	1134,35	97,08	7,41	0
01:04:49	64,82	5,38	140,54	11632,40	3165,35	1109,92	98,34	6,73	0
01:04:54	64,90	5,55	144,80	11246,10	3249,61	1193,76	94,07	9,44	0
01:04:59	64,98	5,19	125,25	11876,60	2975,70	1223,02	74,19	5,77	0
01:05:04	65,07	5,04	127,44	12742,40	3002,98	1085,26	81,57	7,27	0
01:05:09	65,15	5,17	177,26	12359,90	3038,61	1064,25	104,76	8,48	0
01:05:14	65,23	5,81	184,40	10483,10	3380,98	1108,05	115,64	21,94	0
01:05:19	65,32	4,66	223,64	14489,50	2955,99	835,02	84,03	19,97	0
01:05:24	65,40	4,56	140,14	15444,10	2836,62	922,08	66,59	9,89	0
01:05:29	65,48	4,59	103,59	15334,20	2784,28	1195,92	61,54	1,04	0
01:05:34	65,57	4,54	91,33	16981,90	2771,12	1231,05	35,45	0,22	0
01:05:39	65,65	4,57	232,25	15981,20	2622,38	1048,60	85,46	28,66	0
01:05:44	65,73	4,74	274,69	13915,00	2580,49	1106,32	83,33	56,91	0
01:05:49	65,82	4,88	140,80	14153,60	2708,75	1271,27	82,06	16,59	0
01:05:54	65,90	5,05	166,51	13614,50	2740,26	1269,27	178,11	24,66	0
01:05:59	65,98	5,19	164,34	12369,20	2800,20	1426,56	138,69	25,37	0
01:06:04	66,07	5,09	191,71	11910,20	2573,06	1368,22	195,20	38,83	0
01:06:09	66,15	5,43	182,81	12345,70	3135,67	1581,61	191,06	35,43	0
01:06:14	66,23	5,98	203,66	10405,60	2927,23	1334,85	364,63	41,48	0
01:06:19	66,32	5,76	171,43	11274,70	3045,31	1308,12	296,75	34,67	0
01:06:24	66,40	5,81	205,11	10486,40	3058,07	1030,34	257,36	61,04	0
01:06:29	66,48	5,49	234,36	10856,20	2878,60	853,94	235,54	57,48	0
01:06:34	66,57	6,56	290,28	8181,00	2852,42	925,08	251,14	138,10	0
01:06:39	66,65	6,61	254,55	7684,84	3038,26	759,48	461,07	99,10	0
01:06:44	66,73	7,49	231,38	6627,28	3092,21	1031,46	370,43	82,38	0
01:06:49	66,82	7,12	311,94	6989,46	3049,78	738,01	229,04	94,45	0
01:06:54	66,90	6,87	243,25	7867,73	3362,56	925,63	361,31	99,02	0
01:06:59	66,98	6,89	171,93	8420,91	3537,95	1058,18	375,91	15,80	0
01:07:04	67,07	7,35	201,11	7609,08	3213,32	1212,73	358,35	57,27	0
01:07:09	67,15	8,03	257,34	7961,79	3998,18	1226,80	350,16	87,06	0
01:07:14	67,23	8,67	279,53	6297,53	3530,74	1159,57	269,75	85,91	0
01:07:19	67,32	8,72	336,74	6561,70	3678,78	1284,87	365,46	92,94	0
01:07:24	67,40	8,61	286,09	6363,31	3349,45	1181,41	365,03	113,80	0
01:07:29	67,48	7,41	567,50	6444,48	2826,63	890,16	320,78	127,20	0
01:07:34	67,57	7,83	199,54	6547,47	2929,57	1101,17	411,82	42,96	0
01:07:39	67,65	7,65	267,37	5465,18	2466,89	883,62	311,36	81,44	0
01:07:44	67,73	7,29	193,55	6891,42	3000,70	719,67	618,84	35,63	0
01:07:49	67,82	7,57	196,64	7512,85	3168,87	1190,70	516,01	39,57	0
01:07:54	67,90	7,39	214,51	6260,41	2587,37	865,17	554,52	30,78	0
01:07:59	67,98	7,51	203,99	6863,49	3038,90	1039,64	384,40	38,57	0
01:08:04	68,07	7,54	197,65	6875,17	2961,47	927,58	545,68	33,10	0
01:08:09	68,15	8,26	206,55	6023,57	3050,65	1247,78	588,61	59,14	0

01:08:14	68,23	7,94	207,48	6277,59	2674,94	1253,23	649,14	63,85	0
01:08:19	68,32	7,84	221,49	4983,58	2120,33	872,74	275,13	84,98	0
01:08:24	68,40	8,17	180,58	5455,46	2560,88	952,70	483,45	21,01	0
01:08:29	68,48	7,90	267,93	6435,62	3212,32	1069,54	459,13	88,40	0
01:08:34	68,57	8,43	258,83	5422,11	2776,09	911,98	341,53	127,80	0
01:08:39	68,65	7,58	227,95	5988,87	2703,96	910,04	424,29	81,10	0
01:08:44	68,73	7,81	191,82	5287,02	2553,77	895,30	357,38	12,53	0
01:08:49	68,82	7,93	217,22	5360,55	2333,07	823,72	538,31	39,59	0
01:08:54	68,90	7,70	230,12	6748,91	2844,43	835,38	530,46	81,32	0
01:08:59	68,98	7,89	200,46	7259,07	3317,03	1177,95	457,26	33,93	0
01:09:04	69,07	7,79	232,87	5391,31	2415,46	906,66	452,09	53,73	0
01:09:09	69,15	7,61	227,56	6887,86	2891,45	831,32	428,67	61,71	0
01:09:14	69,23	7,97	222,73	6364,35	3095,10	899,26	574,99	60,30	0
01:09:19	69,32	8,22	268,11	5189,48	2642,97	692,13	487,20	149,96	0
01:09:24	69,40	7,95	195,63	5291,65	2419,34	1066,86	387,94	48,71	0
01:09:29	69,48	7,90	236,56	5464,37	2367,72	857,68	489,44	137,53	0
01:09:34	69,57	8,17	169,09	6816,90	3161,93	1357,74	404,41	3,53	0
01:09:39	69,65	8,35	200,37	5653,90	2861,93	945,71	453,57	32,13	0
01:09:44	69,73	8,12	207,51	5683,16	2861,39	895,92	361,90	32,63	0
01:09:49	69,82	8,30	217,80	6094,04	3056,34	837,06	470,61	48,44	0
01:09:54	69,90	8,13	197,53	5827,95	2537,61	1083,28	463,47	46,70	0
01:09:59	69,98	8,34	248,58	5783,87	2632,61	1240,95	302,69	123,38	0
01:10:04	70,07	8,66	283,02	5317,79	2795,45	842,76	365,87	140,13	0
01:10:09	70,15	8,68	243,55	4963,65	2681,33	693,96	520,78	52,03	0
01:10:14	70,23	8,59	227,95	5276,30	2580,05	935,68	456,06	70,66	0
01:10:19	70,32	8,38	203,44	6025,57	2854,08	1067,58	572,53	52,99	0
01:10:24	70,40	8,50	212,92	4606,88	2448,39	870,06	415,70	56,22	0
01:10:29	70,48	8,76	219,52	4124,78	2226,19	998,32	310,51	87,45	0
01:10:34	70,57	8,29	259,17	5409,38	2757,00	708,32	491,36	170,69	0
01:10:39	70,65	8,71	181,65	5341,13	2798,96	1033,95	638,34	10,12	0
01:10:44	70,73	8,33	215,75	5328,92	2527,13	926,30	459,35	83,57	0
01:10:49	70,82	8,57	226,52	5129,97	2592,92	872,29	447,25	68,57	0
01:10:54	70,90	8,29	247,21	5169,37	2573,86	750,06	498,91	85,80	0
01:10:59	70,98	8,32	192,20	4602,10	2478,99	925,37	409,90	21,90	0
01:11:04	71,07	8,31	210,35	5968,07	2894,21	914,59	531,18	45,45	0
01:11:09	71,15	8,09	288,97	5927,93	3026,58	837,41	207,63	151,20	0
01:11:14	71,23	8,56	210,42	5722,87	2864,14	1180,03	401,97	78,23	0
01:11:19	71,32	8,64	167,84	5664,62	2845,77	1174,01	463,33	11,28	0
01:11:24	71,40	8,68	189,35	5348,74	2706,32	1133,77	505,63	37,79	0
01:11:29	71,48	8,37	237,42	5612,78	2936,65	1036,15	391,52	92,90	0
01:11:34	71,57	8,16	245,85	5845,54	2604,80	936,26	510,26	105,14	0
01:11:39	71,65	7,99	225,95	6812,38	3057,10	1197,59	396,32	114,11	0
01:11:44	71,73	8,10	232,45	6242,01	2839,44	895,70	526,34	129,25	0

01:11:49	71,82	8,04	204,80	5233,62	2342,16	928,34	384,34	57,04	0
01:11:54	71,90	7,94	214,81	5827,46	2715,17	1312,09	468,08	86,96	0
01:11:59	71,98	8,39	197,76	6408,14	3026,30	1607,16	483,94	45,21	0
01:12:04	72,07	7,91	226,32	5597,61	2650,07	849,42	375,05	89,85	0
01:12:09	72,15	8,31	216,66	5032,29	2303,64	910,24	554,23	76,86	0
01:12:14	72,23	8,06	236,17	5404,89	2315,66	982,66	552,33	88,46	0
01:12:19	72,32	8,18	239,21	5357,87	2409,67	1000,99	464,74	91,23	0
01:12:24	72,40	7,80	251,81	6153,10	2590,50	918,72	400,46	140,97	0
01:12:29	72,48	8,17	211,78	5931,98	2745,80	1225,51	507,56	65,15	0
01:12:34	72,57	7,77	274,59	5674,35	2364,18	962,23	557,99	117,76	0